The distribution of extracellular matrix in the human uterus

by

VASILIKI METAXA-MARIATOU B.Sc. (Hons).

Thesis submitted for the degree of Master of Science to the University of Glasgow.

Department of Obstetrics and Gynaecology, University of Glasgow.

ProQuest LLC.
789 East Eisenhower Parkway
P.O. Box 1346
Ann Arbor, MI 48106 – 1346

Summary

Several lines of evidence suggest that there may be a distinction between the inner and outer myometrium. Magnetic resonance imaging has shown that the uterus of women of reproductive age consists of three layers. In addition, transvaginal ultrasound has revealed that peristaltic waves, during the course of the normal menstrual cycle, emanate only from the inner myometrial muscle. Finally histological findings have suggested that there is a three-fold increase in the nuclear density of the inner compared to the outer myometrium. In addition, trophoblast invasion is restricted to the inner third of the myometrium.

Based on these lines of evidence it was postulated that there could be a difference in extracellular matrix between inner and outer myometrial smooth muscle. To test this hypothesis, the distribution of different laminin chains, collagen IV and elastin were examined in the human uterus. In addition observations were made to determine whether there was tissue specificity of laminin type expression.

Forty-four hysterectomy specimens were collected, from women undergoing hysterectomy for benign conditions, representing all phases of the menstrual cycle. These also included specimens from patients who had been treated with intrauterine levonorgestrel (Mirena®). Cryo- and paraffin embedded sections were prepared. Immunocytochemistry was carried out using monoclonal antibodies directed to the α2, β1, β2, and γ1 laminin chains, collagen IV, elastin, CD31 and the 68kD neurofilament protein. Digital imaging, by microscopy and scanning, was undertaken and novel image analysis methods were developed to examine the myometrial distribution of extracellular matrix proteins. Elastin detection was confirmed by orcein staining.

As predicted collagen IV and the γ1 laminin chain were present in the basement membranes of the vascular smooth muscle, myometrial smooth muscle, vascular endothelium and endometrial epithelium. Qualitative observation revealed that the β2 laminin chain was much less widely distributed in the inner part of the smooth muscle. Reverse-transcriptase polymerase reaction was used to confirm the expression of the β2 and γ1 laminin chains. Quantitative comparison of the β2 laminin chain and collagen IV distribution within the myometrium demonstrated the existence of layers of laminin type. A measurement of sectional thickness of this layering was devised. The sectional thickness of the inner layer was highly variable between individuals (7mm median, 2-15mm range). These results confirmed the existence of layering within the human myometrium.

The β2 laminin chain was also present in the vascular smooth muscle but variably expressed in the endometrial endothelium. The β1 laminin chain was uniformly distributed throughout the smooth muscle. It was also present in the endometrial vascular smooth muscle but absent from the myometrial vascular smooth muscle. The endothelial basement of the endometrium and myometrium contained the β1 laminin chain. The α2 laminin chain was present in the myometrial smooth muscle but absent from the myometrial vascular smooth muscle and endothelium. These observations provided evidence that the vascular endothelium and smooth muscle of the endometrium are structurally different from their counterparts within the myometrium.

After exposure to intrauterine levonorgestrel no differences were observed in the myometrial distribution of the different laminin chains and collagen IV. By contrast in the highly decidualised areas of the endometrium, extensive peri-cellular staining of laminin chains was observed.

It was hypothesised that layering of the muscle may also involve a variation in elasticity. As expected, immunoreactivity was observed in the internal elastic laminae and walls of the large myometrial arteries. Elastin was also present in the peri-vascular tissue particularly near the large vessels. The walls of the myometrial arterioles also contained elastin. In addition, elastin was present within the outer myometrial smooth muscle but was less abundant, or in some cases, absent from the inner smooth muscle. More extra-vascular elastin was present in the outer myometrium in all cases. Quantitative analysis demonstrated a linear gradient in the myometrial distribution of elastin. However, these distributions did not correspond to the more distinct myometrial layering pattern of the β2 laminin chain.

Although others have described an absence of elastin within the human endometrium, it was shown that elastin was restricted to the basal portion of the endometrial arterioles. Traces of elastin were also observed in 78% of cross-sections of lymphoid aggregates.

The results presented in this thesis suggest that there are important structural differences between the inner and outer myometrial smooth muscle. The anatomy of the human myometrium therefore appears to be more complex than previously reported. As a consequence of these findings it is postulated that the outer myometrium is more elastic than the inner and that the variation in basement membranes composition may influence the contractile properties of the muscle.

CONTENTS

CHAPTER.3: RESULTS

List of Figures

List of Tables

List of Plates

List of Plates (cont.)

List of Diagrams

List of Appendices

Acknowledgements

I would like to thank my supervisor Dr. Steven Campbell for his advice and direction throughout this research study. I would also like to acknowledge Ms Anne Young, for teaching immunocytochemistry and for all her help in the lab. Many thanks must go to Ms Fiona Jordan for guiding me through RT-PCR and RNA isolation. I would like to thank, Mr Mark Smith for scanning the 35mm slides, Mr Iain Macmillan for carrying out the orcein staining and Miss Catherine Robertson for the CD31 staining. The staff of the Pathology Department were very helpful in processing the fixed tissue sections and Dr Colin Stewart for his expertise in identifying at which stage of the menstrual cycle the specimen were collected and any tissue abnormalities.

A big thank you must go to Dr Jay McGavigan for her help in tissue collection and for her clinical advice but above all for being a true friend.

Dedication

This thesis is dedicated to my parents Elias and Helen for all their love, support and help throughout the whole time I have been away from home.

To my sister Denia, for all her love and emotional support and for reminding me that I come first!

And to Michael for all his love, support and endless patience!!

Declaration

I declare that I have contributed to the experimental work described in this thesis, with help from Mrs Anne Young with immunocytochemistry and Fiona Jordan with RNA isolation and RT-PCR, under the supervision of Dr Steven Campbell, in the Department of Obstetrics and Gynaecology at the University of Glasgow.
The work presented here is original research and had not been previously submitted for a higher degree. I am the author of the thesis and have consulted all the references cited.

Signed _____

Vasiliki Metaxa-Mariatou

I certify that the experimental work reported in this thesis was performed by Miss Vasiliki Metaxa-Mariatou at the University of Glasgow and that during the period of the study she has fulfilled the conditions of the relevant regulations governing the degree of Master of Science (MSc)

Signed _____

Dr Steven Campbell

Abbreviations

Å : Armstrong

1°A : Primary antibody

2°A : Secondary Antibody

BL : Basal lamina

BM : Basement membrane

BSA : Bovine Serum Albumin

bp : base pairs

°C : degrees of Celsius

cm : centimeters

C-terminal : carboxy terminal

DAB : Diaminobenzedine

DH_2O : Distilled water

DDH_2O : Distilled deionised water

DEPC : Diethylpyrocarbonate

DNA : Deoxyribonucleic acid

d NTP: Deoxynucleotide tri-phosphate

dpi : dots per inch

ECM : Extracellular matrix

EDS : Ehlers-Danlos syndrome

EDTA : Ethylenediaminetetra-acetic-acid disodium salt

EGF : Epidermal growth factor

EHS : Engelbreth-Holm-Swarm

ER :Estrogen Receptor

ET_A: Endothelin receptor A

g : Grams

GAGs : Glycosaminoglycans

GBM : Renal glomerular

HRT : Hormone Replacement Therapy

IgG1 : Immunoglobulin class I

IUS : Intrauterine system

JZ : Junctional zone

kDa : kilodalton

L : Liter

LAMC1 : laminin γ1 gene

LE motif :

LNG-IUS : Levonorgestrel intrauterine system

M : Molarity

MAPG : Microfibril-associated glycoprotein

$MgCl_2$: Magnesium Chloride

mg : milligram

mg/ml : milligram per milliliter

mm : millimeter

ml : milliliter

mM: millimolar

mins : minutes

mRNA : messenger RNA

µl : micro-liter

µm : micro-meter

MOPS : 3-N-Morpholinopropane-sulphonic acid

MR : Magnetic Resonance

MRI : Magnetic Resonance Imaging

N/A : Not available

ND: Neutral Density

N-terminal : amino terminal

nm : nanometers

P70 : Power

PBS : Phosphate Buffer Solution

PR : Progesterone Receptor

RGB: Red Green Blue

RNA: Ribonucleic Acid

rpm : rounds per minute

R.T : Room temperature

RT-PCR : Reverse transciptase polymerase chain reaction

sec: seconds

SMC : Smooth muscle cells

TBE : Tris Borate Buffer

V: Volts

% : percentage

Chapter.1 Introduction

1.1 The human uterus

The uterus is a "pear shaped" organ with its rounded end directed upwards comprising the fundus and body of the uterus while its lower end forms the cervix. The uterus fits rather loosely into the bony pelvis where it is maintained in place by several ligaments. The uterus varies in size from 2.5-3.5cm in length in the pre-pubertal child to 6-8cm in the nulliparous adult to 9-10cm in the multiparous women. Uterine weight also changes from 50-70g in nulliparae to 80g or over in multiparae and at term it can achieve 500 to 1000 times greater capacity than in the nulliparous state, reflecting a weight increase up to 1100g. The two distinct parts of the uterus are the body or corpus and the cervix. The wall consists of three layers, an outer covering, the serosa; a middle muscular layer, the myometrium and a glandular tissue, the endometrium (Ramsey, 1994).

1.1.1 *Organization of the myometrium*

The myometrium is the thickest of the layers composing the uterine wall with the greatest concentration of muscle in the fundus. The protective and expulsive functions of the myometrium are accomplished first by the sheer bulk of smooth muscle composing it and then by the pattern of arrangement of the muscle. The myometrium consists of muscle cells, fibroblasts, blood and lymphatic vessels, immune cells and connective tissue (Garfield &Yallampalli, 1994).

The uterine wall of rats and rabbits is composed of an innermost layer, the endometrium, an inner circular layer and an outer longitudinal muscle layer. The outer longitudinal muscle layer of the myometrium consists of a network of bundles of smooth muscle cells that are generally orientated in the long axis of the uterus. The bundles interconnect and form a network over the surface of the uterus, with each bundle consisting of smooth muscle cells arranged in the long axis of the bundle (Garfield & Yallampalli, 1994). The muscle cells in the circular layer are arranged more diffusely and the bundle arrangement, when present, is not as apparent as that of the longitudinal layer. According to structural and functional studies the longitudinal layer is continuous with the circular layer (Osa & Katase, 1975).

During mammalian pregnancy the uterus increases tremendously in size, accounted for by an increase in the number of cells (hyperplasia) and then increases in muscle cell size (hypertrophy) (Garfield & Yallampalli, 1994). However, in the human uterus there is no distinct muscle organization like that seen in the rodent uterus.

1.1.2 *The muscle cell*

Smooth muscle cells (SMC) of the myometrium are generally thought to be long, spindle-shaped cells, ranging in size from 5 to 10μm in diameter in the centre of the cell and from 300 to 600μm in length (Csapo, 1962). The size of smooth muscle cells varies considerably between species. The plasma membrane of the smooth muscle cells, besides being a barrier between the intracellular compartment and the extracellular environment, also forms cell-to-cell contacts known as gap junctions. Uterine smooth muscle cells have an extensive system of sarcoplasmic reticulum, the major functions of which are those of a storage site of activator calcium (smooth endoplasmic reticulum) and a site for protein synthesis (rough endoplasmic reticulum) (Garfield & Yallampalli, 1994).

The major function of smooth muscle cells is contraction through the interaction of myosin and actin filaments (Somlyo, 1980). There are three groups of filaments classified on the basis of size, shape, location and composition. By far the largest number of filaments are the thin filaments (50-80Å in diameter) containing actin and tropomyosin. The second type of filaments are the thick filaments (120-180Å in diameter) composed of myosin and the last type of filaments are the intermediate filaments (100Å in diameter) containing vimentin or desmin (Chamley-Campbell *et al.*, 1979).

The notion that a smooth muscle cell is capable of synthesis of extracellular matrix (ECM) was originally proposed on the basis that it is the only cell type present in the media of mammalian arteries and therefore must be responsible for connective tissue elements, such as elastin collagen and glycosaminoglycans (Thyberg *et al.*, 1990). In human adult arteries, SMC have a highly differentiated contractile phenotype whereas in the embryo SMC are in a synthetic phenotype (Thyberg *et al.,* 1990). In the synthetic state, SMC have a fibroblast-like appearance with an extensive rough ER, a prominent Golgi complex and a few myofilaments (Nakamura, 1988). They proliferate and secrete ECM components like collagen and elastin (Ross & Klebanoff, 1967). In adults, the arterial media is made up of highly differentiated SMC arranged in concentric layers, with each cell encircled by a BM composed of collagen type IV, laminin, nidogen and heparan sulfate proteoglycans (Timpl, 1989).

As the vessels mature the synthetic organelles decrease in size and myofilaments occupy larger parts of the cytoplasm (Nakamura, 1988). Smooth muscle cells, in adult life, are able to return from a contractile to a synthetic phenotype (Thyberg *et al.,* 1990), where the cells lose their contractility and gain the ability to secrete ECM components and divide, which is an important early event in atherogenesis.

1.1.3 *Myometrial contractions*

The uterus contracts autonomously, rhymically and unceasingly throughout the menstrual cycle. The first studies of the contractions of the nonpregnant uterus were carried out in 1889 by Heinricius. In the past decades uterine activity was mainly studied by invasive catheter techniques. The major disadvantage of the intrauterine sensors used to record uterine activity was their profound impact on the uterine muscle (Mosler, 1968). This prompted a search for noninvasive techniques, such as magnetic resonance imaging (MRI) and ultrasound, for recording uterine contractility without direct contact with the organ. Trans-vaginal ultrasound proved to be the method of choice for analysis of myometrial peristalsis in women (Chalubinski *et al.*, 1993).

Several groups, using ultrasonic techniques, have reported that in the non-gravid uterus myometrial peristalsis emanates from the inner myometrium at an amplitude and frequency of the contraction that correlates with the phase of the menstrual cycle. The direction of propagation of the subendometrial myometrial contractions became progressively more consistent from menstruation to the periovulatory period, thereafter declining in the luteal phase. In the periovulatory period the predominant direction was from cervix towards the fundus. It must be noted that the characteristics of the subendometrial myometrial contractions are very different from the contractions of the entire myometrium, which are markedly diminished during the periovulatory period (Lyons *et al.*, 1991). The amplitude and frequency of the subendometrial contractions in the follicular and periovulatory phases increase towards ovulation. Short, asymmetrical myometrial waves are present during the luteal phase, but during menstruation propagated fundo-cervical subendometrial contractions waves were noted (de Vries *et al.*, 1990; Lyons *et al.*, 1991; Chalubinski *et al.*, 1993; Kunz *et al.*, 1996).

The mechanisms that govern the contractions of the inner myometrium are not understood. It appears likely that the symmetrical, high amplitude propagated contraction waves in the late follicular phase require electrical and mechanical coupling of myocytes in the inner myometrium (Brosens *et al.*, 1998).

Although gap junctions expression is likely to be essential, mere expression is not sufficient to trigger co-ordinated contractions. Several cytokines have been identified which might modulate myometrial contractions. For example, epidermal growth factor, is not only a potent mitogen for myometrial smooth muscle cells but it can also induce uterine contractions (Gardner & Stancel 1989).

Kunz *et al.* (1996) demonstrated, by means of vaginal sonography of uterine peristalsis and hysterosalpingoscintigraphy, that subendometrial cervico-fundal contraction waves could be

responsible for the rapid sperm transport through the female genital tract in the pre-ovulatory phase. Others have postulated that the asymmetrical myometrial peristalsis during the luteal phase serves to maintain the developing blastocyst within the uterine fundus. The role of fundo-cervical contractions during menstruation has not yet been elucidated, but one report noted hyperperistalsis in a woman suffering from excessive menstrual blood loss (Chalubinski *et al.,* 1993).

In vitro studies have also confirmed the functional polarity of the myometrium (Daels, 1974). In contrast to the in vivo observation, myometrial strips taken from the outer myometrium show spontaneous strong regular contractions which can be amplified by adrenaline or, to a lesser extent, by oxytocin (Brosens *et al.,* 1998).

Contractions of the pre-term uterus (37 weeks) are local and synchronous whereas contractions at term (40 weeks) become increasingly more frequent, synchronous and intense while producing powerful propulsive contractions that propel the fetus through the birth canal (Garfield *et al.,* 1988).

The ability of myometrial cells to contract depends upon the ionic distribution across their plasma membrane. Sodium and calcium ions are higher outside the cell than inside, whereas potassium ions are higher within the cells (Kao, 1989). The sequence of contraction and relaxation of the myometrium results from the cyclic depolarization and repolarization of the muscle cells in the form of action potentials (Garfield &Yallampalli, 1994). The frequency and intensity of contractions are directly proportional to the regularity and duration of action potentials in each muscle cell and total number of cells that are active (Marshall, 1962).

The driving force for myometrial contractility is thought to be provided by propagated action potentials that arise from pacemaker regions (Marshall, 1962). However such pacemaker regions have not been experimentally identified. The electrical activity that arises from the pacemaker areas then excites surrounding non-pacemaker regions. Pacemaker cells are autonomously active smooth muscle cells in which the resting membrane potential varies as compared with non-pacemaker cells (Lodge & Sproat, 1981). It has been proposed that any muscle cell can act as a pacemaker cell (Marshall, 1962).

1.1.4 *Gap junctions as sites of propagation of action potentials*

Since the myometrium is composed of billions of small muscle cells, a specialized mechanism of conduction must be present between the cells to coordinate their activity (Csapo, 1981). After the elimination of possible reasons for the propagation of action potentials, such as the innervation of the uterus, the effects of stimulants on contractility and the absence of a specific conduction pathway (comparable to the Purkinje fibre system in the heart) present in the myometrium, it was

concluded that electrical activity must propagate from cell-to-cell (Csapo, 1981) and that gap junctions serve as sites of propagation, at least in the mouse.

Gap junctions are intercellular channels that link neighbor cells and allow the passage of inorganic ions and small molecules (Garfield & Yallampalli, 1994). They consist of channels composed of proteins termed connexins that span the plasma membrane to form a pore (Saez *et al.,* 1993). Each gap junction consists of a few hundred to thousands of channels each constructed from six connexin proteins (connexons) (Alberts *et al.,* 1994). Two connexons join across the intercellular gap to form a continuous aqueous channel connecting the two cells (Alberts *et al.,* 1994). In the myometrium a 43kD protein termed connexin 43 is thought to be the major component of the gap junction (Beyer *et al.,* 1989).

Garfield *et al.* (1988) suggested that the changes in steroid hormones and prostaglandins that precede or accompany labour, regulate the presence of gap junctions. Progesterone appears to inhibit whereas oestrogen promotes gap junction synthesis in the myometrium (MacKenzie & Garfield, 1985). Prostaglandin synthesis inhibitors such as indomethacin and meclofenamate are known to alter the area of gap junction in the myometrium (Garfield & Yallampalli, 1994).

1.1.5 *Vascular anatomy of the human uterus*

The uterine arteries and one or more branches of the ovarian arteries penetrate the lateral margins of the uterine wall at an oblique angle and proceed directly to the middle layer of the myometrium where they ramify into an arcuate wreath (Okkels & Engle, 1938).

Blood supply to the endometrium arrives through the radial arteries, which arise from the arcuate arteries within the myometrium. The radial arteries, after passing through the myometrial-endometrial junction, split to form the smaller basal arteries and spiral arteries that supply the basal portion and the functional layer of the endometrium respectively (Rogers, 1998). The stroma and peri-glandular networks are supplied by capillaries that branch from the spiral arteries. Just below the endometrial surface the spiral arterioles break up into the prominent sub-epithelial capillary plexus, which drains into a number of venules that pass down through the endometrium collecting blood from other capillaries on the way (Rogers, 1998).

Following menstruation, the long precapillary channels grow from the remaining segments of spiral arterial coils deep in the basalis. The growth of the artery involves the formation of a media and adventitia around these precapillaries, thus converting them into arteries (Ramsey, 1967).

All endometrial vessels are lined by a continuous single layer of endothelial cells arranged on a vascular BM. The wall of most blood vessels consists of three layers: tunica intima, tunica media and tunica adventitia (Zhang, 1999).

The spiral arteries, the most striking structural feature of the endometrial vasculature, have a distinct coiled appearance that becomes more pronounced during the secretory phase of the menstrual cycle (Rogers, 1998). These vessels also play a major role in placentation. The conversion of spiral arteries into utero-placental arteries depends upon two waves of endovascular invasion by trophoblast in the first two trimesters of pregnancy (Pijnenbourg *et al.*, 1990). At term the trophoblastic cells are characteristically buried in the vessel walls and wrapped in fibrinoid material (Pijnenbourg *et al.*, 1981). These changes are an essential part of placentation and the establishment of an adequate choriodecidual blood flow in normal pregnancy (Pijnenbourg *et al.*, 1990).

1.1.6 *Innervation of the human uterus*

The female reproductive organs have an extensive autonomic innervation. The sympathetic nerves to the smooth muscle coats of the Fallopian tubes, uterus and vagina comprise a mixture of short adrenergic nerves from the utero-vaginal ganglion formations and fibres in the inferior mesenteric ganglion (Stjernquist & Sjöberg, 1994). The adrenergic nerves are sensitive to the action of ovarian sex steroids (Thorbert, 1978). Oestrogen for example increases neurotransmitter (NA) content of individual adrenergic fibres, whereas progesterone causes a reduction (Falck *et al.*, 1975). Due to steroid effects and additional mechanical effects exerted by the growing conceptus the uterus during pregnancy is said to undergo a complete and entirely physiological adrenergic denervation (Stjernquist & Sjöberg, 1994). A slow and incomplete restitution takes place post-partum. These changes may be functionally associated with the maintenance of pregnancy, initiation of labour and expulsion of the fetus during parturition (Stjernquist & Sjöberg, 1994).

1.1.7 *Myometrial zonal anatomy*

Myometrial zonal anatomy was first described with magnetic resonance imaging (MRI) (Hricak *et al.*, 1983). In the uterus of women of reproductive age, three distinct layers can be seen on T2-weigthed images: a high-signal-intensity endometrial stripe, a medium-signal-intensity outer myometrium and in-between a low-signal-intensity junctional zone (JZ).

Various hypotheses have been put forward concerning the nature of the JZ. Hricak *et al.* (1983), suggested that the low-signal-intensity band seen on T2-weighted images represented the stratum basale of the endometrium, as vascular or physiological phenomenon at the myometrial-endometrial junction. A suggestion which was dismissed by Lee *et al.* (1985) and McCarthy *et al.* (1989) because the histological locations did not match. Haematoxylin and Eosin staining failed to reveal any significant differences in the light microscopic appearances between the junctional zone and the outer myometrium.

Lee *et al.* (1985) suggested that the JZ represented a physiological phenomenon such as blood flow, since it was indistinct or not visible ex vivo. Both Hriack *et al.* (1983) and Lee *et al.* (1985) agreed that the JZ was not part of the endometrium, since thickness measurements of the high-signal-intensity layer accounted for the entire endometrium (stratum functionale and basale).

Worthington *et al.* (1985) proposed that the JZ represents a layer of compact myometrium a proposal which was later supported by the findings of McCarthy *et al.* (1989), Scoutt *et al.* (1991) and Brown *et al.*, (1991).

In 1989 McCarthy and colleagues showed, by means of multiple cycles of uterine desiccation in an oven until there was no further reduction in the weight of the specimens, that the water content of the junctional zone was significantly lower than that of the endometrium and myometrium, the reason for which still remains unclear.

Although detailed studies (Farrer-Brown, *et al.*,1970 a,b) on the arterial vasculature of the uterus have demonstrated that all parts of the myometrium are well vascularised, an abrupt change occurs in the density of the arterial pattern. It has been claimed that the arterial density is greater in the subjacent myometrium than in the endometrium (McCarthy *et al.*, 1989).

Scoutt *et al.* (1991) reported that there was no difference in the distribution of components of the ECM such as, collagen (III, IV, V), laminin and fibronectin, between the JZ and the outer myometrium. However the antibodies used had no known chain specificity. Therefore the possibility of laminin type variation was not examined. The same study revealed that there is a three-fold difference in the percentage of nuclear area in the JZ compared with the outer myometrium, reflecting an increase in both size and number of nuclei. The reason for this remains unclear.

1.1.8 *Structural myometrial zonal differentiation in response to ovarian sex steroids*

Demas *et al.*, (1985); McCarthy *et al.*, (1986); Andreyko *et al.*, (1988), reported that zonal dedifferentiation depends on gonadal hormones. In both premenarchal girls and postmenopausal women, the zonal anatomy is often indistinct, with a comparatively low-signal-intensity myometrial zone. Ovarian suppression with gonadotrophin-releasing hormone analogues leads to an MR appearance of the uterus mimicking that of postmenopausal women (Demas *et al.*, 1985). Hormone replacement therapy (HRT) in postmenopausal women results in a re-appearance of the myometrial zonal anatomy.

Changes in the myometrial zonal anatomy can also be observed during pregnancy. Focal disruption of the JZ occurs in early pregnancy (Turnbull *et al.*, 1995). In general, the JZ signal intensity increases and the zonal differences become indistinct (Willms *et al.*, 1995), with the normal zonal anatomy gradually reappearing within 6 months of delivery.

1.1.9 *Mechanisms controlling myometrial structure and polarity*

In non-pregnant myometrial cells, oestrogen receptor (ER) expression is maximal in the late proliferative phase and declines sharply in the early secretory phase. An increase in ER immunoreactivity has been reported in the late secretory phase. Following an initial rise in progesterone receptor (PR) immunoreactivity in the proliferative phase, there is, by contrast, no significant change in the PR expression (Snijder *et al.,* 1992).

No zonal differences in steroid receptor expression in the myometrium were reported (Brosens *et al.,* 1995) however Richards *et al.* (1995) demonstrated, using immunocytochemistry and radioimmunoassay techniques, that the subendometrial myometrium expresses significantly higher numbers of ER than the outer myometrium.

The mechanisms underlying elevated ER expression in the JZ are not well understood and remain to be determined (Richards *et al.,* 1995). There is, however, increasing evidence for a complex interaction between gonadal steroids and locally expressed cytokines in the myometrium (Brosens *et al.,* 1998).

1.1.10 *Junctional zone disease*

Adenomyosis is a disease characterized by disruption of the endometrial-myometrial interface with loss of normal uterine polarity, with smooth muscle proliferation and an altered local immune micro-environment (Brosens & Brosens, 1998). Although the definition of adenomyosis appears straightforward, the precise histopathological criteria have been the subject of considerable controversy (Brosens & Brosens, 1998). The common approach is to use a minimum depth of myometrial invasion to define the condition. Current criteria range widely from the presence of glands and stroma 1mm below the endometrial-myometrial junction to as deep as one third of the total myometrial thickness (Azziz, 1989).

Despite the diversity of diagnostic criteria applied, adenomyosis is thought to be a disease typical of multiparous women in the late reproductive years and the perimenopause. JZ distortion can also be found in young nulliparous women with heavy periods (Brosens, *et al.*, 1998).

In recent years, ultrasound has been increasingly used to diagnose adenomyosis. Although adenomyotic uteri tend to be larger with asymmetrical thickening of the anterior and posterior walls, uterine morphometry alone is insufficient for the diagnosis (Brosens, *et al.*, 1995). In comparison with ultrasound, MRI has proved to be a useful non-invasive technique for the diagnosis of adenomyosis (Hricak *et al.*, 1983).

The two cardinal symptoms of adenomyosis are excessive menstrual loss and dysmenorrhoea. Symptomatic relief can be achieved with conventional treatment such as mefenamic acid. As yet there is no evidence that any form of medical therapy is specifically effective, as the diagnostic

elusiveness of adenomyosis has precluded controlled clinical trials (Brosens & Brosens, 1998). At present, the most common treatment for patients unresponsive to medical treatment is hysterectomy.

1.2 Morphological changes of the human endometrium during the menstrual cycle

The morphology of the female genital tract is not static but during the years from the menarche to the menopause undergoes repetitive cyclical changes, controlled by the action of the ovarian hormones which are themselves under the control of the pituitary (Noyes *et al.*,1950). These cyclical changes are most apparent in the endometrium, which is a tissue derived from the Müllerian ducts and consists of two layers, the functionalis located under the surface epithelium and the basalis underneath the functionalis (Ramsey, 1994).

In the peri-natal and pre-pubertal periods the glands and their supporting stroma proliferate and gradually mature (Ramsey, 1994). At menarche, menstruation is initiated and recurrent cycles commence, due to a coordinate and effective pituitary and ovarian stimulation. Each cycle consists of three phases, the follicular or proliferative phase, the luteal or secretory phase and finally menstrual shedding (Shearman, 1985).

1.2.1 *The proliferative phase*

Throughout the proliferative phase, the endometrial changes show a rather constant pattern and accurate dating of the endometrium is difficult (Russell & Fraser, 1998). Under the influence of oestradiol, various cells of the functional layer such as glandular, stromal and vascular endothelial cells, proliferate thus producing a measurable thickening of the uterine mucosa (Noyes *et al.*, 1950).

Mitotic figures are seen throughout the proliferative phase, both in glands and the stroma (Noyes et al., 1950). The stroma which is originally compact becomes somewhat oedematous towards the middle of the phase. The oedema then regresses and the stroma becomes compact again towards the end of the proliferative phase (Noyes et al., 1950).

The surface and glandular cells acquire numerous cilia and cytoplasmic extensions such as microvilli that will increase the overall cell surface and thus enhance excretory, secretory and absorptive functions (Russell & Fraser, 1998).

1.2.2 *The secretory phase*

In contrast to the proliferative phase, the oestradiol-primed endometrium during the secretory phase under the influence of progesterone undergoes rapid architectural and cellular changes sufficiently distinct to permit accurate dating (Hendrickson & Kempson, 1980). During the first 36-48 hours after ovulation no appreciable changes occur within the endometrium (Noyes *et al.*,

1950). The secretory phase is characterised by the twin processes of glandular secretion and stromal differentiation.

On the 16th day of the cycle, sub-nuclear vacuolation of the glandular epithelium becomes prominent (Noyes *et al.*, 1950). By the 17th day of the cycle the basal vacuoles are enlarged pushing the nuclei towards the apical end of the cell where they form an almost uniform row around the lumen. A few mitoses are seen since the epithelial cells generally lose their ability to divide with the onset of this specific differentiation brought by progesterone (Dallenbach & Hellweg, 1981). On the 18th day of the cycle, some nuclei return to the base of the cell (Noyes *et al.*, 1950) and on the 19th-20th days of the cycle, apical glycoprotein-rich and mucopolysacharide-rich cytoplasmic fragments are expelled into the glandular lumen by protrusion and eventual detachment with consequent loss of vacuolization of the supranuclear cytoplasm (Dallenbach & Hellweg, 1981).

Seif *et al.* (1989) in an immunohistochemical study reported the presence of a cycle-dependent sialoglycoprotein in the endometrium. The glycoprotein was absent in the proliferative phase but was present at maximal levels in the early secretory phase and persisted in slowly diminishing amounts throughout the secretory phase of the cycle (Seif *et al.*, 1989).

In another immunohistochemical study the presence of a large cell type surface glycoprotein called mucin-1 (MUC-1) in the endometrial epithelium was reported (Hey *et al.*, 1994). Low levels of MUC-1 mRNA and protein were detected in the proliferative phase whereas the levels of both MUC-1 mRNA and protein increased in the early secretory phase.

A glycosaminoglycan (GAG) known as keratan sulphate was reported to be present in association with the glandular epithelium in the normal endometrium. Secretion appears to occur throughout the normal cycle with a highly significant increase in glandular biosynthetic activity from the proliferative to the early secretory phase, resembling the pathway documented previously for the cycle-dependent sialoglycan protein (Seif et al., 1989).

Until this point there is little obvious morphological changes in the endometrial stroma compared to the changes that take place in the glandular epithelium but approximately on the 21st day of the cycle, stromal oedema develops again reaching its maximum on the 22nd day of the cycle, when secretion of oestrogen is also at its highest (Noyes *et al.*, 1950).

As the oedema subsides on the ninth day after ovulation (23day of a 28days cycle) groups of spiral arterioles become prominent due to enlargement of nuclei and increase of cytoplasm of the periarteriolar stromal cells. The first stromal cells to undergo differentiation to become decidual cells are the periarteriolar stromal cells and capillaries of the functionalis (Russell & Fraser, 1998). Later, predecidual changes are seen in cells around the glands and below the surface

epithelium and towards the latter part of the late secretory phase, the stroma consists of sheets of decidualised stromal cells which are infiltrated by granulated lymphocytes, especially uterine natural killer (NK) cells (Noyes, 1950).

If pregnancy fails to take place the corpus luteum begins to regress. As a result of the fall in both progesterone and oestrogen, the endometrium contracts, the glands collapse, assuming a saw-toothed appearance and the decidual stroma becomes vary dense (thirteenth day after ovulation) (Dallenbach & Hellweg, 1981).

1.2.3 *Menstruation*

Menstruation normally lasts 3-5days during which time the endometrium rapidly fragments and degenerates with most of the surface shedding occurring within the first 24-48 hours (Ludwig *et al.*, 1990). On the 28th day through to the second day of the following cycle the functionalis is characterised by degenerate, pseudo-decidual cells which rapidly lose their eosinophilic cytoplasm (Russell & Fraser, 1998). Lysosomal and other proteinase autodigestion are thought to destroy grandular and stromal cells and also vascular endothelium. During menstruation regressive changes begin in parts of the endometrium not shed that enable the glandular and stromal cells to survive and restore themselves in order to participate in the physiological buildup of the next cycle (Dallenbach & Hellweg, 1981).

Immediately after menstrual shedding ceases and before proliferation begins, a regenerative phase takes place, lasting 1-2days (Dallenbach & Hellweg, 1981). During the regenerative phase the denuded endometrium becomes epithelialised. Re-epithelization is completed by the 5day of the cycle. The onset progress and duration of re-epithelisation vary from patient to patient (Dallenbach & Hellweg, 1981).

1.3 Levonorgestrel Intrauterine Releasing System (LNG-IUS)

One of the aims of this study was to examine the effect of a high dose exogenous intrauterine progesterone on the distribution of ECM in the human myometrium and endometrium. The levonorgestrel-releasing intrauterine system (IUS) (LNG-IUS), which is the most extensively tested and most widely used IUS, has the frame of a Nova-T device on which a silastic capsule has been attached to the vertical arm, releasing 20μg per 24h from a total 52mg of levonorgestrel. The LNG-IUS was developed during the late 1970s and the 1980s, and it was first marketed in Finland in 1990 (Odlind, 1997). It is licensed for use as a contraceptive, for women suffering from menorrhagia and dysmenorrhoea.

1.3.1 *Mechanism of action*

The LNG-IUS is a highly effective, long-term, safe and reversible method of contraception. It is thought to exert its contraceptive effect by causing the cervical mucus to become thicker, thus

impermeable to sperm, and by making the endometrium thin and inactive. (Nilsson *et al.*, 1978). In addition the LNG-IUS is known to elicit a local foreign body reaction, comparable to that produced by sterile particles or objects with low biocompatability placed elsewhere in the body. (Ortiz *et al.*, 1996).

1.3.2 *Non-contraceptive beneficial effects*

Excessive menstrual bleeding affects 10% to 15% of women in Western Europe. In Europe and other developed countries it is the most common cause of anaemia in fertile women (Sturridge & Guillebound, 1997). The LNG-IUS can help to improve both heavy and painful menses and increase haemoglobulin concentrations, by rendering the endometrium inactive and insensitive to the proliferative effects of oestradiol (Luukkainen *et al.*, 1990). Dysmenorrhoea is also generally improved (Bounds *et al.*, 1993).

1.3.3 *Side effects*

Hormonal effects including mood changes, headache, mastalgia, nausea, acne, and hirsutism have been reported in a minority of women maximally at three months of use by most studies. These effects were reduced with time (Andersson *et al.*, 1994; Luukkainen *et al.*, 1990).

In the first few months after insertion of the LNG-IUS, there is often a period of frequent, irregular bleeding or spotting (McGavigan & Cameron, in press 2000). During this period of time the number of bleeding "spotting" is usually increased, but the total volume of blood lost is nevertheless reduced as compared to the woman's normal menstruation (Allonen, 1994). This irregular bleeding pattern could be an unwanted side effect, by many women. With prolonged use, menstrual blood loss is dramatically reduced and many women develop amenorrhoea or report extremely scanty but regular bleeds (Andersson K *et al.*, 1994; Kohnen *et al.*, 1998).

1.3.4 *Effects on the human endometrium*

The effect the LNG-IUS on the endometrium has been considered to be dose-dependent (Xiao *et al,* 1990). However, the dose-response relationship is still incompletely understood, particularly with regard to side effects such as irregular menstrual bleeding, oligomenorrhoea and amenorrhoea (Zhao *et al.,* 1995).

Several studies have shown that after exposure to LNG-IUS, the endometrial glands become atrophic, the epithelial cells inactive and the stroma decidualised. Locally released levonorgestrel causes atrophy of the glandular epithelium, the glands become scarce and the stroma shows pseudodecidual features (Silverberg *et al.,* 1986). These effects on the endometrium are noticed as soon as 1 month after insertion and are maintained for at least 7 years.

Zhao and colleagues (1995) reported that the capillaries of the endometrium were dilated, occasionally accompanied by local thrombosis and the stromal inflammatory reaction included infiltration of polymorphonuclear leukocytes, lymphocytes and plasma cells.

It has also been reported that intrauterine administration of progesterone reduces the number of oestrogen receptors in the endometrium (Janne & Ylostalo, 1980). However, Lu *et al.,* 1991, reported that the oestrogen receptors are not completely downregulated, at least on women maintaining scanty regular bleeding, while exposed to the LNG-IUS.

Kohnen and colleagues (1998) demonstrated an up-regulation of the endothelin receptor ET_B in areas of abundant stromal basement membrane deposition after treatment with the intrauterine levonorgestrel, using ligand autoradiography. The same group also reported that there was variability in the pattern of endothelin receptor ET_A.

1.4 The extracellular matrix and basement membranes

The extracellular matrix (ECM) is an intricate network of macromolecules composed of a variety of versatile proteins and polysaccharides that are secreted locally and assembled into an organized meshwork in close association with the surface of the cells that produce it. Two main classes of extracellular macromolecules make up the matrix, the glycosaminoglycans (GAGs) and the fibrous proteins. The later are of two functional types; the mainly functional, including collagen and elastin and the mainly adhesive such as fibronectin and laminin (Alberts *et al.,* 1994).

Until recently the ECM of vertebrates was thought to serve only as a relatively inert scaffolding to stabilize the physical structure of tissue. However, it is now well known that the matrix plays a far more active and complex role in regulating the behaviour of the cells that contact it by influencing their development, proliferation, migration, shape, function, gene expression and programmed cell death (Adams & Watt, 1993). There are at least three mechanisms by which the ECM can regulate cell behaviour. The first mechanism is through the composition of the ECM. The second mechamism is through synergistic interactions between growth factors and matrix molecules and the third mechanism is through the cell surface receptors that mediate adhesion to ECM components (Adams & Watt, 1993).

At the interface between an epithelial layer and connective tissue, the matrix is organized into a thin but tough mat that plays an important role in controlling cell behavior and is know as the basal lamina (Alberts *et al.,* 1994). Basal laminae (BL), as revealed by electron microscopy, are thin (50-100nm), flexible sheet-like structures with an amorphous appearance (Timpl & Brown, 1996). They can be found underlying epithelial or endothelial cells or sheets as well as surrounding individual muscle cells, fat cells and Schwann cells (Alberts *et al.,* 1994).

The basal lamina is synthesized by the cells that rest on it and is composed of laminin, type IV collagen, entactin/nidogen, perlecan, fibronectin and agrin. Also associated with basal laminae is a group of basement membrane proteins including BM-40, SPARC and fibulins. (Yurchenko, *et al.,* 1994).

With the transmission electron microscope, the basal lamina can be seen to consist of three parts. Two of the parts are constant, the lamina lucida adjacent to the basal plasma membrane of the cells resting on the lamina, and the lamina densa attached to the lamina lucida (Alberts *et al.* 1994). The third part, the lamina fibroreticularis is frequently missing but when present, is composed of collagen fibrils connecting the basal lamina to the underlying connective tissue (Chan *et al.* 1993). Some authors use the term basement membrane (BM) to describe all three layers while others use the terms basal lamina and basement membrane interchangeably.

The lamina lucida is an electron-lucent layer crossed by irregular filamentous strands that end on the cell plasmalemma (Chan *et al.*, 1993) while the lamina densa is composed of a dense three-dimensional network of filamentous strands similar to and continuous with those of the lamina lucida (Inove & Leblond, 1988).

The two layers were initially thought to have distinct properties and different components. It has been stated that the lamina densa is mainly composed of type IV collagen (Yaoita *et al.* 1978) whereas the lamina lucida includes laminin, fibronectin and heparan sulfate proteoglycan (Chan & Wong, 1989). However, Laurie *et al* (1984) reported that both layers contain all the above substances, localised to a cord network, but in greater amount in the lamina densa than in the lamina lucida, a view that has been accepted in reviews by Abrahamson (1986) and Yurchenko & Schittny (1990).

Although this appearance (lamina densa, lamina lucida) has been considered a hallmark of basement membrane cross-sectional structure, according to Goldberg and Esgaig-Haye (1986), the layering may be an artifactual fixation-induced phase separation, as it is not observed in freeze-substituted vitreous specimens. In conventionally processed specimens that were fixed in gluteraldehyde-formaldehyde and dehydrated at room temperature, the basement membranes were composed of a lamina lucida and lamina densa consisting of muscle fibres and pre-ameloblasts, (Goldberg & Escaig-Haye, 1986). However, after slam freezing and dehydration by freeze substitution the basement membrane consisted of a lamina densa without a lamina lucida (Goldberg & Escaig-Haye, 1986).

In another study which examined the glomerular basement membrane, it was reported that after conventional processing a lamina lucida was present on both sides of the lamina densa but after fixation in gluteraldehyde-formaldehyde followed by freezing and freeze substitution no lamina

lucida was observed on either side of the lamina densa (Reale & Luciano, 1990). Thus the authors were drawn to the same conclusion of Goldberg & Escaig-Haye, that the lamina lucida was an artefact due to fixation.

In 1993 Chan *et al.*, working with mouse tissues, reported that the occurrence of the lamina lucida is due to rapid dehydration and not due to fixation. Hence the basement membranes are simply composed of a lamina densa that closely follows the plasmollema of the associated cells (Chan *et al.,* 1993).

Basement membranes have several biological roles. Firstly, they supply mechanical support for cell layers, secondly they form barriers between tissue compartments that impede the transmigration of cells and passively regulate the exchange of macromolecules, and thirdly serve as interactive surfaces for cells, providing adhesion, cells shape and migration signals. They also help in communicating information for the regeneration and differentiation of cells (Yurchenko, 1994).

The evidence so far largely supports macromolecule self-assembly as the mechanism for the formations of BM. Protomers interact to form an organized superstructure. The architecture of the superstructural axis is a direct consequence of interacting binding sites present on collagen, glycoproteins and proteoglycans. (Yurchenko *et al.,* 1994). How the ECM macromolecules interact with each other in order to form basement membranes will be discussed in greater detail.

1.5 The laminin family

Purification and characterization of a laminin molecule began in 1979 with the observation that the stroma of a tumor transplantable to the mouse, the Engelbreth-Holm-Swarm (EHS) tumor contained large amounts of basement membrane-like material (Aumailley & Smyth, 1998). Besides the presence of collagen IV, a noncollagenous component was present in substantial quantities, which was purified and identified as a large glycoprotein and named laminin (Timpl *et al.,* 1979). Initially this was the only known laminin type but it was in fact the first member of a large family of laminin trimers.

Laminins are a family of multifunctional macromolecules with a specific localization in the basement membranes. They are heterotrimers, consisting of 3 different gene products, the α, β and γ chains (Burgeson *et al.,* 1994), with a molecular mass of 140-400kD. So far, 5α (α1-5), 3β (β1-3) and 2γ (γ1-2) chains have been cloned and sequenced. These assemble into at least eleven isomeric forms of laminin, namely: laminin-1 (α1, β1, γ1); laminin-2 (α2, β1, γ1); laminin-3 (α1, β2, γ1); laminin-4 (α2, β2, γ1); laminin-5 (α3, β3, γ2); laminin-6 (α1, β3, γ1); laminin-7 (α3, β2, γ1); laminin-8 (α4, β1, γ1); laminin-9 (α4, β2, γ1); laminin-10 (α5, β1, γ1) and laminin-11 (α5, β2, γ1) (Aumailley & Smyth, 1998). An old nomenclature exists which rather

confusingly uses the terms A and B to refer to laminin chains. For example laminin γ1 is known as laminin B2 with the old nomenclature.

In mammals, laminins play at least three essential roles. Firstly, they are major structural components of basal laminae, forming one of two self-assembling networks. The other network is formed by collagen IV, to which other glycoproteins and proteoglycans of the BL attach. Secondly, laminins interact with cell surface components such as dystroglycan to attach cells to the extracellular matrix (ECM). Thirdly, they are signaling molecules that interact with cellular receptors such as integrins to convey morphogenetically important information to the cell's interior (Miner *et al.*, 1997).

1.5.1 *Laminin structure*

All chains show a homologous domain structure, with an N-terminal region and a C-terminal region. The amino-terminal region consists of two domain types; a cysteine-rich 60 amino acid domain (LE motifs) which occurs repeatedly and another cysteine rare area named domain VI (***Figure.1***). These LE motifs, according to the nomenclature adopted by the SWISS-PROT data Bank, are homologous to the epidermal growth factor (EGF) with the exception of the presence of 6 cysteine residues in the EGF instead of 8 residues in the equivalent laminin motif. These motifs, in turn, are arranged in rows and form domains III and V, which are either interspaced by or contain inserted laminin-specific cysteine-poor regions, known as domains IV. The presence, location and numbers of domains IV and VI, as well as the number of the LE motifs vary with the different laminin chains (Aumailley & Smyth, 1998) (***Figure.1***).

The carboxy-terminal region (domains I and II) on the other hand, is characterized by repeated heptad peptides typical of polypeptides that fold into coil-coiled dimers or trimers (Aumailley & Smyth, 1998). Unique to the β chains, is the interruption of the repetitive heptad by a stretch of amino acids at the border between domains I and II, whereas the α chains contain an additional domain. This domain is located at the carboxy-terminus, which is conserved between the chains and which in turn can be subdivided into 5 sequence repeats, G1 to G5 sub-domains (***Figure.1***)

Laminins have a cross-shaped or T-shaped structure when visualized by transmission electron microscopy and rotary shadowing. The short arms vary in size and are contributed by the N-terminal regions of individual chains. The rod of the long arm consists of a triple coiled coil formed from the α-helical domains of all three chains (Timpl & Brown, 1996). Among the many potential α/β/γ combinations between known chains, there is so far *in vivo* evidence of only 11 different heterotrimers listed previously (***Figure.1***).

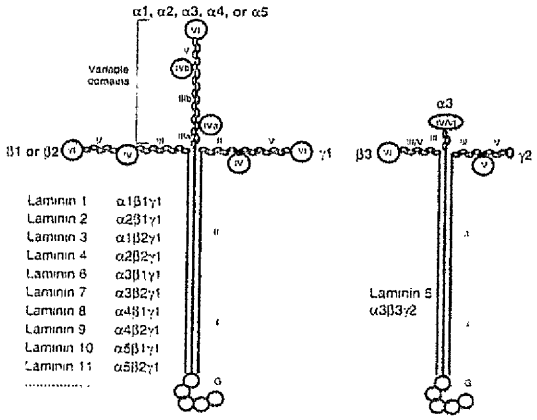

***Figure.1*:** The laminin family: Representation of laminin heterotrimers. The α/β/γ associations identified to-date are listed and the variable domains. Picture reproduced from Aumailley & Smyth, 1998.

1.5.2 *Synthesis and assembly of laminin chains*

The α/β/γ trimers are formed intracellularly through chain selection, assembly and stabilisation. The first step is the formation of the stable, disulphide-linked β/γ dimers via a 10-residue peptide localised to the C-terminal region of the laminin γ1 chain. β and γ chain dimers and other intermediates were observed during biosynthesis, but apparently secretion in vitro occurred only after addition of an α chain. The stability of the coiled-coils is thought to be determined by ionic interaction, which also control chain selection (Beck *et al.,* 1993). It was demonstrated by Sanes *et al.* (1990) that individual cells can produce several laminin isoforms simultaneously and deposit them together in the adjacent membrane.

The α chain is then incorporated, a step which could be controlled by sequences located in the amino-terminal portion of domain II. Finally the formed heterotrimer is secreted. Assembly and stabilisation by disulphide bonds are probably required for translocation of the heterotrimers from the endoplasmic reticulum to the Golgi complex for glycosylation, before transfer to the extracellular space (Cooper *et al.,* 1981).

For α1, β1, β2 or γ1 chains no extracellular processing has so far been reported, except for cleavage of the signal peptides. The terminal regions of the α2 and α3 chains are probably processed whereas the last 2G domains (G4 and G5) are cleaved off. (Ehrig *et al,* 1990; Paulsson *et al.,* 1991; Marinkovich *et al.,* 1992; Burgeson, 1996).

1.5.3 *Role of laminins in basement membrane formation*

Although collagen IV is an abundant structural component of mature basement membranes conferring stability, laminin plays an important role in basement membrane formation because of multiple interactions with itself and with other components such as nidogen, perlecan etc.

One model of laminin self interactions involves the formation of hexagonal networks (Yurchenko *et al.,* 1985; 1992) by means of interactions between the amino-terminal globular

domain VI. This assembly model was derived from studies with laminin 1 (Yurchenko & Cheng, 1993) and also applies to laminin 2 and 4 because both laminin isoforms posses three full short arms. In contrast the full sized isoforms laminin 5, a rod-like molecule whose short arms lack their domains, does not assemble in a manner similar to laminin 1(Cheng *et al.,* 1997).

It has been suggested that this assembly model does not apply to laminin isoforms containing α3, α4 or γ2 chains because they lack domain VI (Cheng *et al.,* 1997). Instead, α3 chain-containing laminins, laminins 5, 6 and 7, form dimers by establishing a disulphide bond between the amino-terminal region of laminin 5 with that of laminin 6 or 7 (Champliaud *et al.,* 1996).

Laminin binds to nidogen via a high affinity interaction between an LE motif in domain III of the laminin γ1 chain, γ1III4, and the carboxy-terminal G3 domain of nidogen (Fox *et al.,* 1991; Gerl *et al.,* 1991; Mayer *et al.,* 1993). Laminin and collagen IV interact indirectly via nidogen. Nidogen binds to collagen IV by its amino-terminal G2 domain and to laminin forming tertiary complexes thus allowing the connection of two major networks.

The one exception to laminin-nidogen interactions is laminin 5, where the γ2 chain is present instead of the γ1. Despite the high sequence identity in the γ2III4 motif, nidogen cannot bind to laminin 5 due to a replacement of a single crucial amino acid (Mayer *et al.,* 1995; Pöschl *et al.,* 1996). The integration of γ2 chain containing isoforms with the basement membrane is facilitated by other specific interactions. Laminin 5 interacts with collagen VII (Chen *et al.,* 1997) which is the major component of anchoring fibrils where laminin 5 is also localised. It is also speculated that laminin 5 interacts with collagen XVII although experimental evidence is still lacking.

Ott *et al* (1982) demonstrated, using radioimmunoassays specific for the proteolytic fragment E3 (globular shape located at G4-G5 domains) that more than 98% of the E3 fragment (***Figure.2***) binds to heparin hence it might contribute to perlecan binding to laminins, via the heparan sulphate chains located on perlecan. Perlecan is a large BM glycoprotein and has a large protein core around 480kD with a single polypeptide folded into 5-6 globular domains aligned in a 80nm long row. The 3 heparan sulphate chains are connected to the core protein at one end (Paulsson *et al.,* 1987). Laminin 1 seems to be the only laminin to bind directly to perlecan (Battanglia *et al.,* 1992) whereas laminin 2 or 4 do not indicating that the laminin α1 and α2 chains differ functionally (Brown *et al.,* 1994).

Timpl & Brown (1996) reported that ECM proteins fibulin 1 and 2 may be directly or indirectly involved in laminin interactions. Both fibulins bind to nidogen or fibronectin, fibulin 1 binds to nidogen G2 domain. On the other hand, fibulin 2 binds to nidogen G3 domain, possibly competing with laminin binding to nidogen (Sasaki *et al.,* 1995). Additional interactions are

possible with fibulin 2 interacting with domain IV of the laminin γ2 chain and to a peptide sequence of the laminin α1 chain (Utani *et al.,* 1997).

Not only integral basement membrane components but many other molecules such as proteases, serum amyloid A and P and growth factors have the propensity to bind to laminins which may affect their functions in the context of a basement membrane (Aumailley & Smyth, 1998).

1.5.4 *Expression of laminin chains*

The earliest studies on laminin chain expression showed that laminin appears at a very early developmental stage of the mouse embryo. Dziadek and Timpl (1985) reported that the β1 and γ1 chains are detected within the 2-4 cell embryo. Two years earlier, in 1983 Cooper and MacQueen reported the presence of laminin containing the α1, β1 and γ1 chains extracellularly at the 16-cell stage, whereas synthesis of collagen IV chain does not start before the blastula stage.

The importance of laminin in early development has recently been confirmed by deletion of the laminin γ1 (LAMC1) gene. The absence of laminin γ1 chain precludes the formation of laminin trimers and of a local lamina, leading to early embryonic lethality in both the mouse and drosophila. Early studies have failed to detect all of the 3 chains (in particular α1 chain), in some basement membranes of laminin expressing cell, in later developmental stages and in adult tissues. This finding initially suggested the possibility of laminin dimers lacking an α chain. The possibility of laminin dimers has now been excluded by the identification of new α laminin chains and by the use of better characterised chain-specific reagents, leading us to a more comprehensive picture of laminin chain expression and distribution (Aumailley & Smyth, 1998). Nevertheless, an exhaustive picture of cell and time specific deposition of laminin isoforms is at the moment not available, restricting our knowledge to the chains for which precisely characterised reagents have been developed (Aumailley & Smyth, 1998).

The laminin α1 chain is expressed by newly forming embryonic epithelial cells. Ekblom *et al.* (1991), showed that during kidney development the α1 chain is present in proximal renal tubules and in the glomerular mesangium but it is not present in the glomerular or vascular basement membrane.

On the contrary, the α2 laminin chain is predominantly synthesised by mesodermal derived cells, including mesanglial and myogenic cells (Schuler & Sorokin 1995; Sorokin *et al.,* 1997a). α2 chain-containing isoforms are typically present in the basal lamina of muscle and motor neuron synapses (Engvall *et al.,* 1990; Sanes *et al.,* 1990).

The laminin α3 and/or α5 chains are expressed by epithelial cells (Ryan *et al.,* 1994; Sorokin *et al.,* 1990) whereas α4 chain synthesis might be restricted to endothelial cells (Sorokin *et al.,* 1994). Isoforms of the α3 are present in the basal lamina of mature epithelium chain whereas isoforms of the α5 are present in the kidney, heart, muscle and lungs.

1.5.5 ***Laminins and cellular interactions***

Soon after discovery, EHS laminin (laminin 1) was shown to have cell adhesion-promoting activity (Terranova *et al.,* 1980). It is now well established that laminins are endowed with the property of controlling directly or indirectly cellular activities such as adhesion and migration, differentiation and apoptosis and gene expression (Aumailley & Smyth, 1998).

The first cell adhesion site described on laminin 1 corresponds to a 200kD pepsin-resistant fragment named P1 (Ott *et al.,* 1982, Timpl *et al.,* 1983). This fragment is the target for several promiscuous RGD-binding integrins such as αvβ1 or αvβ3 (Aumailley *et al.,* 1990b) (***Figure.2***). In the mouse laminin α1 chain an RGB sequence located on one LE motif of domain IIIα is responsible for the activity of P1 (Aumailley *et al.,* 1990α). In native laminin 1 the RGB sequence is cryptic and becomes accessible, in vitro, to cells only after proteolytic degradation of the adjacent domain IVα (Nurcombe *et al.,* 1989; Aumailley *et al.,* 1990b). However, in the human α1 laminin chain the equivalent sequence, RAD, has not been proven to be active.

The proteolytic fragment E8 (240 kD) (Figure.2) consisting of the carboxy terminal part of the triple-stranded helix formed by the α1, β1 and γ1 chains and by the G1 to G3 domains of the α1 chains, is the major cell binding domain of laminin 1 (Aumailley *et al.,* 1987; Goodman *et al.,* 1987). It has been shown that unfolding of the fragment E8 coiled-coil conformation or proteolytic cleavage between the rod and the G domains leads to partial or complete loss of the cell adhesion activity respectively, without cell spreading (Deutzmann *et al.,* 1990).

The activity of recombinant G domains also did not reproduce that of native laminin. Reactivity similar to that of the authentic molecule was restored only after reconstruction of a coiled-coil fold (Sung *et al.,* 1993). Other investigated laminin isoforms, such as laminins 2,4 and 5 show a helical conformation-dependency for cell binding activity.

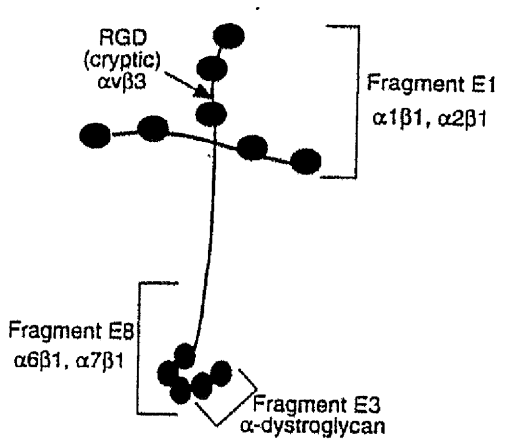

***Figure.2*:** Mapping of cell binding sites on laminin 1. The laminin proteolytic fragments with biological activity as well as the corresponding receptors are indicated. Picture reproduced from Aumailley & Smyth, 1998.

Most cells use the α6β1 integrin to recognize the long arm of laminin1 (Aumailley *et al.,* 1990 a,b) while certain cells such myoblasts or melanoma cells use the α7β1 integrin (Kramer *et al.,* 1991) (***Figure. 2***). Integrin α3β1 was initially thought to be a promiscuous receptor for several ECM proteins such as laminin, fibronectin and collagen (Takada *et al.,* 1991; Hynes *et al.,* 1992). Later studies though indicated a specificity restricted to laminin isoforms with the exception of laminin 1 (Carter *et al.,* 1991). Another integrin potentially involved in cell anchorage to laminins is integrin α6β4, (De Luca *et al.,* 1990) although most in vitro studies have failed to demonstrate a distinct binding of this integrin to laminins (Sonnenberg *et al.,* 1990) possibly because the affinity between α6β4 integrin and laminin may be too low to be seen in vitro.

Integrin α3β1 may play a role in matrix assembly as chain deficient mice show a disorganization of the kidney and skin basal lamina (Kreidberg *et al.,* 1996). Integrin α6β4 is thought to mediate stable anchorage of cells to laminins (Carter *et al.,* 1994) since keratinocytes lacking the β4 integrin chain have an increased mobility (Niessen *et al.,* 1996).

However, integrins are not the only molecules mediating cellular interactions with laminins. Laminin 1 has a minor cell binding site assigned to the heparin binding fragment E3 (Sonnenberg *et al.,* 1992). Its interaction with cells is integrin-independent and is perturbed by heparin (Sorokin *et al.,* 1992), an interaction probably mediated by α-dystroglycan, a component of the dystrophin-glycoprotein complex (Henry & Cambpell, 1996). The dystroglycan-laminin interactions are important for branching epithelial morphogenesis such as kidney, lung, or salivary gland (Sorokin *et al.,* 1992) (***Figure.2***).

Furthermore, several galectins, cytosolic proteins involved in cell-adhesion and cell-signaling, (Barondes *et al.,* 1994) interact with laminins and may control the spreading and migration of cells on specific domains of laminins (Hall *et al.,* 1997), but the exact mechanisms of these effects together with the ligand binding sites are unclear. Several synthetic peptides from the

laminin α1, β1, β2 or γ1 chains also affect cellular interactions with laminin (Nomizu *et al.*, 1997). However, whether they merely perturb the cell surface receptor or really mimic the activity of the authentic laminin molecule still remains to be shown (Brandenberger *et al.*, 1996).

1.5.6 *Laminin expression in the human uterus*

Scoutt *et al.* (1991) undertook an MRI and histological examination of hysterectomy specimens and demonstrated a normal distribution of laminin throughout the myometrium, with no significant difference in the distribution between the junctional zone and outer myometrium.

An immunohistochemical study revealed that the interstitial matrix around stromal cells of the proliferative phase of the normal menstrual cycle, was unreactive with a monoclonal antibody against human laminin (Faber *et al.*, 1986). However, in the secretory phase the stromal cells accumulated distinct cytoplasmic and pericellular laminin–immunoreactive material with the maximal amount of stromal cell-associated laminin observed around the stromal decidual cells of the late secretory phase. The same group observed that the epithelial basement membranes of the endometrial glands, vessels and smooth muscles contained laminin. They also claimed that in cystic and adenomatous hyperplasia the epithelial basement membrane could be visualized by laminin staining as a continuous band around the glands but no qualitative evidence was shown. By contrast, in atypical adenomatous hyperplasia the staining of basement membranes was often discontinuous (Faber *et al.*, 1986).

Later, Aplin *et al.* (1988) in a immunofluorescence study of selected basement membrane and interstitial matrix components of human endometrium, reported that in the proliferative phase endometrium the only laminin immunoreactive structures were the walls of the blood vessels and the glandular basement membrane. However, in the mid and late secretory phase endometrium laminin staining was visible in the endometrial stroma as streaks and spots around the periphery of the cells (Aplin *et al.*, 1988) in agreement with the results of Faber *et al.* (1986). It was also reported that decidualising stromal cells produce laminin and other basement membrane components (Aplin *et al.*, 1988).

In a study using the indirect immunofluoresence method, it was shown that laminin was localised exclusively in the basement membrane of endometrial glands and in the walls of blood vessels during the proliferative and secretory phases of the normal menstrual cycle (Iwahashi *et al.*, 1996). However, the results on the secretory phase reported by Iwahashi and colleagues (1996) do not agree with the findings of Faber *et al.* (1986) and Aplin *et al.* (1988). Strong staining was only recognized in the pericellular region of endometrial stromal cells in the decidua (Iwahashi *et al.*, 1996).

Stromal cell BM contain subunits α2, β1, β2, γ1 and low levels of α1 as was shown by immunofluoresence by Church and colleagues (1996). The glandular and vascular basement membranes of decidua tissue were reported to contain subunits α1, β1 and γ1 (Church *et al.,* 1996). By using Western blots, of decidual tissue, the presence of high molecular complexes containing α2, β1, β2, and γ1 were detected, indicating that laminins 2 and 4 are coexpressed by decidual cells (Church *et al.,* 1996). In the non-pregnant cycle, α2 could not be detected in the proliferative phase but present in the late secretory in the perivascular areas where predecidual differentiation occurs. However, RT-PCR showed that α2 mRNA is present throughout the non-pregnant cycle (Church *et al.,* 1996).

1.6 Elastin

The elastic properties of many tissues such as the lung, dermis and large blood vessels are due to the presence of elastic fibers in the extracellular matrix (Rosenbloom *et al.*, 1993). Elastic fibres have morphologically distinct structures specific to the organ or tissue. In elastic filaments, elastic fibres form interwoven rope-like filaments that branch and rejoin in a three-dimensional network, whereas in the aorta they are organized as concentric sheets or lamellae. In elastic cartilage, large anastomosing fibres form a three-dimensional honeycomb-like pattern (Mecham & Davis, 1994).

Biochemical and ultrastructural analysis have shown that elastic fibres are comprised of two distinct components, an abundant amorphous component and a microfibrillar component (Rosenblomm, 1984). The amorphous component is a chemically-inert, insoluble and extremely hydrophobic protein called elastin that endows the fibre with the characteristic property of elastic recoil. The microfibrillar component consists of 10 to 12nm fibrils which are located primarily around the periphery of the amorphous component, but also to some extent interspersed within it (Rosenbloom *et al.*, 1993). Because of their insolubility and their association with other extracellular matrix components, the composition of microfibrils has proven difficult to determine. Two glycoproteins appear to be true constituents of microfibrils. The first is fibrillin, a 350kD glycoprotein and the second is a 31kD glycoprotein called microfibrils-associated glycoprotein (MAPG). Other proteins such as fibronectin, amyloid P component, vitronectin, lysyl oxidase and other components of reductive guanidine hydrochloride extracts also appear to be associated with microfibrils (Mecham & Davis, 1994).

1.6.1 *Elastic fibre assembly*

Relatively little is known concerning the detailed mechanism involved in fibre assembly. Elastin fibrillogenesis takes place at unique sites close to the cell membrane, generally in infoldings of the cell surface (Mecham & Davis, 1994). Microfibrils are the first visible components of elastic

fibres and are found grouped in small bundles near the plasma membrane (Rosenbloom *et al.*, 1993). It has been demonstrated, by Jaques and Serafini-Francassini (1985), that newly synthesized elastin appears unevenly distributed on the surface of the elastic fibres, often forming continuous strips of variable width arranged in a helical pattern around the fibre. This observation supports the possibility that the cell might control the orientation of the elastic fibre by secreting elastin over a specific cell surface. However these observations are not consistent with a noncontrolled passive process of elastic fibre assembly. Thus a special dynamic relationship between the elastin producing cells and the elastic fibre has been proposed (Mecham & Davis, 1994). It has been suggested that microfibrils may be necessary only in the initial stages of elastic fibre assembly and that they are not required during the subsequent maturation of the fibre (Daga-Gordini *et al.,* 1987).

Little in known about the intracellular trafficking of tropoelastin. Although the evidence to date (Damiano *et al.,* 1984; Daga-Gordini *et al.,* 1989) suggest that tropoelastin appears to follow the classical pathway of protein synthesis and secretion, few electron-dense vesicles or immunolabelled vesicles are observed in elastogenic cells (Mecham & Davis, 1994).

Examination of the cell-free translation product of elastin mRNA shows the polypeptide to contain a signal sequence of 24-26 residues (Karr & Foster, 1981) that is cleaved during translocation. The processed tropoelastin polypeptide chain enters the endoplasmic reticulum (ER) (Grosso & Mecham, 1988).

It has been shown that helper or chaperone proteins direct tropoelastin secretion and facilitate elastin assembly at the cell surface (Hinek *et al.,* 1988). Evidence so far, suggests that a nonintegrin cell surface receptor complex consisting of three subunits mediates elastic fibre assembly (Hinek *et al.,* 1988). Two of the subunits are integral membrane proteins. The third one is a 67-kD cell surface protein which binds via three separate sites to a hydrophobic sequence of elastin (VGVAPG), to the integral membrane subunits and to beta-galactosugars (Hinek *et al.,* 1993). The intracellular motor that transports the tropoelastin-67kD complex appears to be intracellular actin (Mecham et al., 1991), which may be directed to membrane sites by cell-matrix receptors that interact with microfibrillar proteins.

The cytoskeleton of the elastin-producing cell may play a role in directing elastic fibre components to the appropriate membrane sites for secretion and assembly (Mecham & Davis, 1994). Evidence come from electron microscopy, which revealed the presence of microfilament bundles in the cytoplasm adjacent to regions of association between the developing elastic fibres and the surface of the elastin-producing cell (Mecham & Davis, 1994). Furthermore, Mecham *et*

al. (1991), showed that both the distribution of the receptor on the cell surface and the affinity of the receptor for elastin were influenced by the underlying cytoskeleton.

At the plasma membrane, tropoelastin remains bound to the 67-kD protein until an interaction with the microfibril induces the transfer of tropoelastin to the growing fibre (Rosenbloom et al., 1993). The domain on tropoelastin that mediates interactions with microfibrils is unknown, although the carboxy-terminal end of the protein has been suggested to serve such a function (Brown et al., 1992). In this part of the molecule, the only two cysteine residues in elastin are found where they form a disulfide bond that stabilizes a positively charged pocket suitable for binding acid microfibrils (Brown et al., 1992). Furthermore, experiments conducted to study the synthesis and secretion of tropoelastin by chick embryo artery walls, have provided biochemical evidence suggesting that tropoelastin may follow a secretory pathway from the rough ER to the plasma membrane (Saunders & Grant, 1985). Since tropoelastin appears to undergo little, if any, post-translational modification and no glycosylation, the necessity of the newly synthesized tropoelastin to follow a Golgi-dependent pathway is brought into question (Mecham & Davis, 1994).

1.6.2 *Elastin expression in the human uterus*

When the elastic tissues of the non-pregnant human uterus are viewed by scanning electron microscopy, they resemble the structure of a sponge (Leppert & Yu, 1991). Elastin within the uterus is thought to provide the dynamic function of the tissue and play a significant role in pregnancy, labour and postpartum period (Woessner & Brewer, 1963). The uterine elastic membranes consist of continuous sheets with a smooth surface on which small fibrils are attached (Leppert & Yu, 1991). Thin flat sheets of elastic membranes (0.1-0.4μm in thickness) with a relatively smooth surface are observed in the myometrial uterine wall. No specific pillars are seen between the lamellae whereas fibrous pillars are seen to connect the elastic lamellae of the aorta (Leppert & Yu, 1991).

According to Gunja-Smith (1985), during pregnancy the elastin content of the human uterus increases four to fivefold from the nulliparous to the multiparous uterus. An early MR study of water content and relaxation properties of the uterine junctional zone, also using immunocytochemistry for the localization of elastin claimed that both the content and nature of elastin did not differ between the junctional zone and the adjacent myometrium (McCarthy *et al.* 1989).

In an immunohistochemical study, examining the localization of fibrillin-1 and elastin in human endometrium and decidua during the menstrual cycle and pregnancy, elastin was claimed to be

absent from all tissues whereas fibrillin was present throughout the menstrual cycle (Fleming & Bell, 1997).

Malak & Bell (1994), failed to demonstrate the presence of elastin in fetal membranes, using histochemical, immunohistochemical, immunofluoresence and electron microscopy techniques. Fibrillin-containing microfibrils were detected as longitudinal bundles that were primarily found in the fibroblast and reticular layers. Based on the above results they proposed that the fibrillin-containing microfibrils provided the required elasticity to the fetal membranes. Nevertheless, Hieber *et al.* (1997), in a biochemical and histopathologic study, demonstrated that human fetal membranes synthesize and deposit elastic fibre, concluding that an elastic system, consisting of elastic and fibrillin-containing microfibrils provides a probable molecular basis for the elastic properties of the human fetal membranes.

1.7 The collagen family

The collagens are a large, diverse family of proteins which account for about one third of the total protein mass in vertebrates. To date, nineteen different vertebrate collagens referred to, as types I-XIX have been identified (Timpl & Brown, 1995). The triple helix, a special secondary structure formed from three polypeptide segments aligned in parallel, is the common structural hallmark of collagens (Piez, 1984). A further characteristic, is their exclusive localization in extracellular matrices where they perform various structural functions, since they differ in their modular structure, supramolecular organization and function (Timpl & Brown, 1995).

The basic subunits of the collagens are the α chains, which vary in size (from 600 to 3000 amino acid residues) and contain one or more polypeptide segments with multiple Gly-Xaa-Yaa sequence repeats that form the triple helix (Timpl & Brown, 1995). The presence of several non-triple-helical protein molecules in the α chains of collagens, not only gives them a greater module diversity than any other protein family known so far but it also makes it difficult to classify them into distinct subfamilies (Timpl & Brown, 1995). The major collagens are types I, II, III found in bone, skin and cartilage tissue. Type IV is present in the BM whereas type V forms heterotypic fibrils with type I or types I and III collagens in bone, tendon and blood vessels. Type VI collagen is present in most connective tissue, type VII collagen in the major component of anchoring filaments whereas type VIII collagen is the major component of Descemet's membrane (one of the five layers of the cornea). Finally type IX collagen is the prototype of a sub-family of collagens called FACIT collagens that include types XII, XIV, XVI and XIX. They are found in cartilage, invertebral disc and vitreous humour (Timpl & Brown 1995).

So far, three groups of collagens are known; the fibrillar collagens, the non-fibrillar and the novel collagens. As this study involved examination of collagen IV, it is the only type of collagen discussed in further detail.

1.7.1 *Collagen IV structure*

Collagen type IV, of the chain composition $[\alpha1(IV)]_2\alpha2(IV)$, is the principal collagenous constituent of basement membranes (Timpl & Brown, 1995) and is considered to be responsible for the mechanical stability of BM (Hudson *et al.,* 1993). Each monomer is thought to consist of two α1 chains (185kD) and one α2 chain (170kD). Unlike the interstitial collagens, each triple-helical chain is longer and more flexible (Dölz *et al.,* 1988) and is interrupted by variably sized breaks in the Gly-X-Y sequence characteristic to collagens (Yurchenko, 1994).

Variant type IV collagen α3, α4 and α5 chains have been identified (Hostikka, 1990). Both the α3 and α4 chains are found in lower amounts relative to the α1 and α2 chains, in the renal glomerular (GBM) and pulmonary alveolar BM. The α5 chain is also present in the GBM (Yurchenko, 1994).

In ultrastructural studies, the isolated $[\alpha1(IV)]_2\alpha2(IV)$ molecule appears as a 300-nm-long flexible thread (Kühn, 1994). At the C terminus, a ~10-nm-long globular domain (NC1) is derived from all three chains (two α1 chains and one α2 chain) that is not processed (Yurchenko, 1994). Each subglobule possesses six cysteines divided among pairs of homologous disulfide-stabilized loop-like repeats (Siebold *et al.,* 1988). The N terminal region (7S domain) is 28-nm-long, rich in cysteines and lysines, representing another major structural site in BM collagen (Timpl *et al.*, 1981).

The sequence of the α5 chain is particularly homologous to the α1 chain, with preservation of the 7S domain, interruptions in the triple helix and the cysteine structure of the C terminal globular domain (Hostikka *et al.,* 1990). The recently described α6 chain (Zhou *et al.,* 1993) of collagen IV has been found to be the triple helical partner of the α5 chain. A further collagen, type VII consists of three α1(VII) chains with different domain structure to collagen IV and is a constituent of anchoring filaments (Timpl & Brown, 1995).

1.7.2 *Collagen IV assembly*

Collagen IV, of the composition $[\alpha1(IV)]_2\alpha2(IV)$, is a network-forming collagen and a ubiquitous component of BM. A network model for the organization of collagen IV monomers is based on at least two different interaction sites involving assembly via the N and C termini. The initial step, in the assembly via the N terminus, is an antiparallel 25-nm overlap of two molecules, controlled by hydrophobic interactions, so that two intermolecular crosslinks, a disulfide bond and a non-reducible lysine-derived aldimine bond can be formed (Kühn, 1994). In

a following step, the dimers aggregate to tetramers again stabilized by intermolecular covalent bonds (Siebold *et al.,* 1987).

During end-to-end aggregation of two molecules, via their C terminus, a hexameric complex is formed which stabilizes the hydrophobic interactions between the NC1 domain and leads to a stable and highly ordered arrangement (Siebold *et al.,* 1988).

A third interaction, the process of which is not clear yet, has been proposed as part of collagen assembly. It is thought that the third interaction occurs after formation of the tetramers. Triple–helical domains interact laterally, preferentially with the C-terminal half of the molecule, whereby superhelices are formed (Kühn, 1994). The end result of this process is that it brings the C terminus of two molecules in the correct position relative to each other, so that disulfide exchange between NC1 domains can occur and hexamers can be formed (Kühn, 1994).

Discriminatory molecular interactions must operate during the assembly of the superstructure, including formation of triple helical monomers, end-to-end associations of monomers and supercoiling (Hudson *et al.,* 1993). The specificity for assembly of triple helical monomers (chain selection) as well as for end-to-end associations at the C terminus, appear to reside within the NC1 domain (Mariyama *et al.,* 1992). The specificity for end-to-end associations at the amino terminus that govern assembly of tetramers and supercoiling is unknown (Hudson *et al.,* 1993).

1.7.3 *Collagen IV interaction with cells*

Collagen IV plays an important role in the interaction of basement membranes with cells. The cell binding site of the human $[\alpha1(IV)]_2\alpha2(IV)$ molecule is located about 100 nm away from the N terminus (Kühn, 1994). This area not only contains the recognition site for the two integrin receptors $\alpha1\beta1$ and $\alpha2\beta1$ (Vanderberg *et al.,* 1991) but also is the area in which the triple-helical domain is stabilized by intramolecular disulfide bonds (Kühn, 1994). Both integrins $\alpha1\beta1$ and $\alpha2\beta1$ bind to other collagen types (I, II, III) indicating the versatility of these receptors (Timpl & Brown, 1995).

According to Eble *et al.* (1991), the essential amino acids of the $\alpha1\beta1$ integrin recognition site are Arg461 of the $\alpha2$(IV) chain and Asp461 of the two $\alpha1$(IV) chains. For the $\alpha2\beta1$ recognition site Arg and Asp are again the essential residues. Both chains of collagen IV are also involved in the interaction with $\alpha2\beta1$ (Kühn, 1994).

The part of the N terminus where the binding sites are located, according to Kühn (1994) is more exposed and less protected than the C terminal half of the triple-helical domain, which is involved in lateral aggregation and formation of superhelical structures.

1.7.4 *Collagen IV expression in the human uterus*

In an immunohistochemical and ultrastructural study human decidual cells of the early and late pregnancy were studied (Wewer *et al.,* 1985). It was found that the most prominent cell type in decidual tissue of both early and late pregnancy were large, mature epithelioid cells with a distinct pericellular BM containing at least laminin, type IV collagen, heparan sulphate proteoglycan and fibronectin (Wewer *et al.,* 1985).

In 1988, in a immunohistochemical study of human endometrial extracellular matrix during the menstrual cycle and first trimester of pregnancy, it was reported that decidualising stroma cells produce BM components such as type IV collagen, laminin and others, which become organized into a pericellular halo (Aplin *et al.,* 1988). In the proliferative phase endometrium the only immunoreactive structures were blood vessel walls and glandular BM, but by mid and particularly late secretory phase, staining with collagen IV was visible in endometrial stroma as streaks and spots around the periphery of the cells (Aplin *et al.,* 1988). Similar observations were made on decidual stroma cells.

According to the *in situ* hybridization results of Autio-Harmainen *et al.* (1991), the stroma of large fibrotic villi and small villi stained intensely for type IV collagen whereas the stroma of the poorly vascularized villi with loose stroma stained more faintly. Decidual cells, endometrial stromal cells and cells in the wall of spiral arteries all expressed mRNA for type IV collagen (Autio-Harmainen *et al.,* 1991).

In a study using *in situ* hybridization to investigate the expression of 70kD collagenase and the α1(IV) collagen chain in cells of the early human placenta and gestational endometrium, it was found that the cells of trophoblastic columns, stromal cells of villi in cells of decidua and endometrial stroma all expressed mRNA for these proteins (Autio-Harmainen *et al.,* 1990).

Aims and Objectives

1. To expand recent preliminary findings, obtained within the Department of Obstetrics & Gynaecology, which suggested the existence of layering in the myometrial distribution of the β2 laminin chain. A subsidiary aim was to determine whether these gradients are modulated during the normal menstrual cycle and after exposure to intrauterine levonorgestrel (Mirena®).

2. To determine whether there is tissue specificity in laminin chain expression within the human uterus, by comparing the γ1 chain and collagen type IV with the α1, β1, β2 laminin chains.

3. To determine whether the extracellular matrix expression changes during the course of the menstrual cycle and after exposure to exogenous progestagen (Mirena®).

4. To examine elastin expression in the smooth muscle and vascular smooth muscle of the human endometrium and myometrium. To determine whether there is a gradient of elastin distribution in the human myometrium similar to that observed with the β2 laminin chain and if it is modulated during the normal menstrual cycle and after exposure to exogenous progestagen (Mirena®).

5. To devise quantitative methods of analysing matrix distribution within histological sections.

Chapter.2 Materials and Methods

2.1 Solutions and buffers

3% BSA (Bovine Serum Albumin)

0.3g of BSA (Sigma, A-7638 Essentially Globulin Free) was dissolved in 10ml of phosphate buffer saline (PBS).

0.1% calcium chloride

100mg of calcium chloride was dissolved in 100ml of distilled water. The solution was stored at room temperature (R.T.).

0.01% calcium chloride

1ml of 0.1% calcium chloride was dissolved in 9 ml of distilled water. The solution was stored at R.T.

Citrate buffer (pH6.0)

2.1g of anhydrous citric acid (BDH, Prod.279844E) was dissolved in 1L of distilled water (DH_20). The pH was adjusted to pH6.0 using 2M sodium hydroxide. The solution was then stored at 4-8°C.

Concentrated (10x) N-Morpholino-propane-sulphonic acid (MOPS)

41.2g MOPS was dissolved in 1600ml of 0.1M sodium acetate. The pH was adjusted to pH7 with 10N sodium hydroxide. 20ml of 0.5M Ethylenediaminetetra-acetic-acid disodium salt (EDTA) was added and the final volume was adjusted to 2L with distilled deionised water (ddH_20). The MOPS buffer solution was autoclaved and stored at 4-8°C.

Distilled Deionised Water (ddH_2O) treated with diethylpyrocarbonate (DEPC)

500µl of DEPC (Sigma, D-5758) was added to 500ml of distilled water. The solution was autoclaved and then stored at 4-8°C.

0.5M Ethylenediaminetetra-acetic-acid disodium salt (EDTA)

186g of EDTA was dissolved in 1L of ddH_20. The pH was adjusted to pH8 and the solution was autoclaved and then stored at 4-8°C

0.01N hydrochloric acid (pH2.5)

890µl of hydrochloric acid (Sigma, H-7020) was added to 1000ml of distilled water in a fume cupboard wearing a protective mask and special gloves. The solution was stored at R.T.

0.2M phosphate buffer

24g of sodium phosphate (Sigma, S-0751) was dissolved in 1L of distilled water. The solution was stored at R.T.

Pepsin solution

5mg of pepsin (Sigma, P-6887) in 60ml of 0.01N hydrochloric acid (pH2.5).

0.01% Protease solution

0.01g of protease (Sigma protease type XXIV, P-8038) in 0.01% calcium chloride

Phopshate Buffer Saline (PBS) (pH 7.5)

6.0g of monobasic sodium phosphate (Sigma, S-0751) and 45.0g of sodium chloride (BDH, Prod.10245K) were dissolved in 5L of distilled water. The pH was adjusted to pH7.5 with 10M sodium hydroxide. The solution was then aliquoted in 2.5L bottles, autoclaved and stored at 4-8°C.

0.1M Sodium acetate

27.2 g of sodium acetate (Sigma, S-8750) in 2L of water. The solution was stored at R.T.

1x Tris Borate buffer (TBE)

100ml of 5xTBE added to 400ml of distilled water and stored at 4-8°C.

5x Tris Borate buffer (TBE)

136.25g of Sigma 7-9® (Sigma, T-1378), 69.7g of Boric acid (Sigma, B-7901), 18.75g EDTA (BDH, Prod.10093) were dissolved in 5L of distilled water. The pH was adjusted to pH8.3 with 5M NaOH. The solution was stored at 4-8°C.

50mM Tris (pH7.6)

In 1L of distilled water 6.10g of Sigma 7-9® (Sigma, T-1378) was dissolved and the pH was adjusted to pH7.6 with HCl.

0.1% Triton-X

100µl of Triton (Sigma, X-100) was dissolved in 100ml of PBS.

2.2 Tissue Collection and Patient Information

Full thickness endometrial and myometrial specimens (n=44) were collected from women undergoing routine hysterectomy at the Glasgow Royal Infirmary, Western Infirmary and the Southern General Hospital. The specimens were taken from the operating theatre to the Pathology Department immediately after the removal of the organ. Initially no defined tissue collecting protocol was used and the receiving Pathologist was asked to provide a full thickness endometrial and myometrial specimen. Later in the study all specimen were collected according to a defined tissue collecting protocol (***Appendix.1***). Prior to surgery all patients gave consent to allow uterine biopsies to be used for research (***Appendix.2***) and after surgery relevant patent information was collected using a patient record form (***Appendix.3***). The stage of the cycle was recorded on the Pathology Report received from the Department of Pathology for each patient.

Additional Haematoxylin and Eosin stained sections were examined by a pathologist (Dr.Colin Stewart) to verify the stage cycle and also to look for evidence of abnormalities.

2.2.1 *Tissue processing*

Where possible tissue samples were collected for preparation of frozen and paraffin embedded sections. For frozen sections, the tissue was snap frozen in liquid nitrogen and then stored in –80 °C. For paraffin embedded sections, the tissue was placed in a plastic universal bottle containing 10% Buffered Formaldehyde Solution (Chemix UN No.2209) in the day of collection. The following day it was taken to the Department of Pathology where it was further processed.

2.2.2 *Tissue cutting*

Five micrometer thick frozen sections were cut using an OTS/AS cryostat (Bright Instrument Company Ltd. Huntingdon England) and a Leica CM 1800 cryostat (Leica UK Ltd. Bedforshire, England). For paraffin embedded sections (5μm thick) a Leica RM 2135-Rotary Microtome was used (Leica UK Ltd. Bedforshire, England).

2.3 Haematoxylin and Eosin staining (H+E staining)

Haematoxylin and Eosin staining of both frozen and paraffin embedded sections was carried out at the Department of Pathology, using an automated slide stainer (Stainette 23, Reicart Jung, England).

2.3.1 *Characteristics of antibody supplies*

When a new batch of antibody was purchased the following preliminary work was undertaken to define immunocytochemistry procedures to be used. An antibody dilution series (1-10μg of protein per ml of antibody) experiment was carried out to decide the optimum dilution at which the antibody should be used. The optimum dilution for an antibody is the highest at which specific immunoglobulin can saturate the available antigen, leaving some unbound antibody in the solution to ensure continued binding. The final dilution at which the antibody was used was decided on the basis of a clear background, absence of non-specific staining and the intensity of specific staining. The effect of quenching the endogenous peroxidase activity, before the primary antibody step or after the secondary antibody step, was also tested. Segments of tissue expression no antigen were used to determine optimum conditions of reagents. Finally, if the antibody in question was known to be reactive with paraffin embedded tissue, experiments were undertaken to determine if pre-treatment for antigen retrieval was necessary or not.

2.3.2 *Antigen retrieval in fixed tissues*

Antigen retrieval is applied to aldehyde-fixed tissues in which the antigenicity has been reduced by the formation of hydroxy-methylene bridges between components of the amino acid chains of proteins. Protease digestion, trypsin, pepsin pre-treatment and microwave heating were used.

Sections to be protease treated the were deparaffinised, rehydrated and placed in a solution of 0.01% protease (Sigma protease type XXIV, P-8038) containing 0.01% calcium chloride. The solution of calcium chloride was pre-warmed in a water bath at 37°C for at least one hour. Just before the sections were placed in the calcium chloride solution, the protease was added. The sections were incubated in the protease solution for 10mins always at 37°C. The action of the enzyme was stopped by placing the slides in running tap water for 5mins and then in PBS for a further 5mins, at R.T.

Sections to be trypsin treated were deparaffinised, rehydrated and incubated in a solution of 0.1% trypsin (Sigma, T-8253) in Tris buffer (pH.7.6) containing 0.1% calcium chloride, as above. The slides were incubated in the trypsin solution for 15mins at 37°C. The action of the enzyme was stopped by washing the slides in running tap water for 5-10mins.

Sections to be pepsin treated were deparaffinised, rehydrated and placed in a solution of 2-10mg/ml of pepsin (Sigma, P-6887) in 0.01N of hydrochloric acid (pH2.5). The solution of hydrochloric acid was pre-warmed in a water bath at 37°C for at least one hour. Pepsin was added just before the slides were placed in the hydrochloric acid solution. The slides were incubated in the pepsin solution for 30mins always at 37°C. The action of the enzyme was stopped by washing the slides gently several times in distilled water.

For specimens to be pre-treated by microwave heating, a pressure cooker containing 1L of citrate buffer (pH6.0) was placed in a microwave and brought to boil (15mins on full power). When boiling, a rack containing the section was placed in to the buffer inside the pressure cooker. The microwave was set for 8mins on full power, 3mins to reach pressure and 5mins at pressure. When the procedure was completed, the pressure cooker was carefully removed from the microwave wearing protective gloves and facemask. The cooker was depressurised and the sections were left to cool for 20mins (inside the pressure cooker). The slides washed once in distilled water and once in PBS for 5mins each time.

2.3.3 *Immunocytochemistry (ICC) for frozen sections*

Sections (5μm thick) of endometrial and myometrial tissue were fixed in acetone (BDH, Prod.100034Q) for 10 min, rinsed (1x5min) in PBS, treated with 0.5% hydrogen peroxide (Sigma, H-1009) in methanol (BDH, Prod.10158BG) for 30min and then rinsed (2x10min) in PBS. For some antibodies the latter step was carried out before the addition of the primary antibody and for others after the addition of the secondary antibody, depending on the preliminary results (***Table.1***). Non-specific binding sites were blocked by incubation in 20% goat serum plus 20% human serum (Sigma, S-7023) diluted in PBS, for 30min inside a humidified box at R.T. The sections were incubated with the appropriate monoclonal antibody (***Table.1***) at

the appropriate dilution (***Table.1***), determined in preliminary work, in 2% goat serum, overnight at 4°C inside a humidified box. A monoclonal mouse antibody (Dako, X-0931) was used as a negative control at 1:200 in 2% goat serum. Sections were rinsed (2x5min) in PBS and incubated in secondary biotinylated anti-mouse antibody (Dako) diluted at 1:200 in 2% goat serum plus 5% human serum, for 30min inside a humidified box at R.T. This was followed by further rinsing (2x5min) in PBS and incubation with peroxidase-conjugated streptavidin (Dako, P0397) for 30min inside a humidified box at R.T. The sections were rinsed (2x5min) in PBS and incubated in DAB solution, made by adding a 3-3` Diaminobenzidine tablet (Sigma, D-5905) in 15ml of Tris buffer plus 12μl of 30% (w/w) hydrogen peroxide (Sigma, H-1009), for 10 min at R.T. Then the sections were washed in PBS, (1x5min) in running tap water (1x5min) and stained with haematoxylin (Sigma, GHS-2-16) for 15sec. Finally, the sections were dehydrated through a series of ethanol solutions (70%-100%, a few seconds in each) to xylene (BDH, Prod. 102936H) (a few seconds), mounted in DPX (BDH, Prod.360294H) and viewed by bright field microscopy.

2.3.4 ***Immunocytochemistry (ICC) for paraffin embedded sections***

Sections (5μm thick) of endometrial and myometrial tissue were placed in the oven (56°C) for at least 35min, rehydrated (5min in each alcohol from 100% to 70%) and washed in PBS for 5min. The procedure used was the same as that of the frozen sections.

The paraffin embedded sections were dehydrated through a series of ethanol solutions (70%-100%, 5min in each) to xylene (BDH, Prod. 102936H) (a few seconds), mounted in DPX (BDH, Prod.360294H) and viewed by bright field microscopy.

Half way through the study another biotinylated secondary antibody (Vector) was used due to technical problems arising from the batch quality of the conjugate. This biotinylated anti-mouse secondary antibody (BA-2000) was raised in horse serum, so for all antibody dilutions as well as for blocking of the non-specific sites horse serum was used instead of goat serum. In addition an avidin/biotin kit (Vectastain ABC Elite kit, PK6100, Vector) was used in the place of the streptavidin peroxidase (Dako). For the preparation of the avidin/biotin solution in 2.5ml of PBS 1 drop of solution *A* and 1 drop of solution *B* were added. As with the streptavidin solution, the avidin/biotin solution was also prepared at least 30mins before it was used.

2.3.5 ***Histochemical staining for elastin***

Additional sections were stained with orcein according to the Modified Taenzer-Unna Orcein method (Drury & Wallington, 1967). Orcein staining is not entirely selective for the elastic fibre system, it also stains nuclei and collagen components. The resorcin-fuchsin method according to WEIGERT in combination with the picrofuchsin method according to VAN GIESON and the nuclear staining technique according to WEIGERT (Elastica kit acc. to VAN GIESON, Merck

1.15974) was also used but produced a less distinct density difference between uterine tissue and elastic components, therefore it was not pursued.

Table.1 Primary monoclonal antibodies used for ECM immunocytochemistry

Antibody	Product form	Supplier/Cat.No	IgG class	Clone	Dilution	Tissue type	Pre-treatment	Inactivation step	References
Anti-Human Merosin	MAb ascites (M chain)	Life Technologies / 12076-014	IgG1	5H2	1:900	Frozen	None	After 2°Ab	1,2
Anti-beta 1	Mouse ascites fluid	Gift from Dr. Eva Engvall, via Dr.John Aplin	IgG1	3E5	1:250	Frozen	None	Before 1°Ab	3
Anti-beta 2	Supernatant, unpurified	Developmental Studies Hybridoma Bank University of Iowa	IgG1	C4	1:500	Frozen	None	Before 1°Ab	4
Gamma 1	Mouse ascites fluid	Gift from Dr. Eva Engvall, via Dr.John Aplin	IgG1	D18	1:2000	Frozen	None	Before 1°Ab	5,6
Anti-Collagen Type IV	Mouse ascites fluid	Sigma / C-1926	IgG1	COL-94	1:1000	Frozen	None	After 2°Ab	5
Anti Elastin	Mouse ascites fluid	Sigma / E-4013	IgG1	BA-4	1:2000	Paraffin	0.01%Pepsin	Before 1°Ab	7
Neurofilament 68 kD	Mouse monoclonal	NovoCastra / NCL-NF68	IgG1	NR4	1:400	Frozen	None	Before 1°Ab	8,9,10
Neurofilament 200 kD	Mouse monoclonal	NovoCastra / NCL-NF200	IgG1	RT97	1:50	Frozen	None	Before 1°Ab	11,12

1. Engvall et al., 1990.
2. Leivo I. & Engvall E., 1988.
3. Engvall et al., 1986.
4. Hunter et al., 1989.
5. Sanes et al., 1990.
6. Green et al., 1992.
7. Wrenn et al., 1986.
8. Shaw et al., 1986.
9. Shaw et al., 1984.
10. Debus et al., 1983.
11. Weber et al., 1983.
12. Anderton et al., 1982.

Key : IgG1: Immunoglobulin class 1
1°Ab: Primary antibody
2°Ab: Secondary antibody

2.4 Photo-microscopy and digital image capture

Microscopic examination of all sections was carried out using an Olympus BX50 microscope equipped with x4, x10 and x40 lenses. 35mm photomicrographs were produce with an Olympus C-35AD-4 camera, using a 64T colour slide film (Kodak). Neutral density filters (ND25, ND6) were used to adjust exposure. The speed and exposure parameters were 64 I.S.O (International Standards Organization) and 0.1-1sec, respectively.

A second Olympus BX50 microscope equipped with x4, x10, x20, x40, x100 lenses, connected to a 3-CCD color camera (JVC) was used for digital image capture. Computer visualisation of the images was achieved with an image analysis program (Image-Pro Plus 4.0). Four neutral density filters were used the ND6, ND25 and a 0.40 Wratten ND gelatin filter to adjust the brightness of the image, while maintaining a constant colour. Images of a 10μm stage micrometer (Graticules, Ltd) were recorded at x4, x10, x20 and x40 magnification and used as spatial calibration objects. All digital images were saved in uncompressed tif format to preserve the original image data.

2.4.1 *Scanning of microscopic slides to obtain low magnification images*

Microscope slides, where the α2, β1, β2, γ1 laminin chains and collagen IV had been immunolocalised, were scanned using an Epson GT 9500 scanner. The slides were positioned on the scanner facing downwards. The images were imported to Adobe Photoshop 4.0 of 5.5 using the TWAIN 32 interface program. Constant exposure and contrast settings were used.

The slides counterstained with and without Haematoxylin were scanned as a "RedGreenBlue" (RGB) image at a resolution of 1200 dots per inch (dpi). In the case of slides without Haematoxylin staining, the gamma contrast value was increased to the maximum (value of 50) resulting in a lightened images with increased contrast.

In later studies slides where elastin had been localised without Haematoxylin staining, were scanned (Medical Illustration, Glasgow Royal Infirmary) using a 35mm slide scanner. All slides were scanned as RGB images at a resolution of 2700dpi and with uniform contrast and exposure settings. All images were saved in tif format.

Spatial calibration was undertaken using the Image Pro-Plus 4.0 program. A scanned area from a precision ruler was used as a calibrating object for the images obtained from the flatbed scanner (1200 dpi). For the low magnification scans obtained from the slide scanner (2700 dpi) a 35mm slide of the 10micron-stage micrometer was scanned (2700 dpi) and then used as a calibrating object.

2.4.2 *Line profiles*

Low magnification scanned images of microscope slides where different laminin chains (n=16 for anti-beta 2 and n=3 for gamma 1), collagen IV (n=15) and elastin (n=10) had been localised without Haematoxylin, were opened in Image-Pro Plus (Image Analysis program). The blue color channel was selected, to produce an 8 bit monochrome image with suitable density information. A rectangular area of full or partial myometrial thickness was manually selected. Two vertical lines, specifying the rectangular area to be analysed, were placed on the image (***Figure.3***). The image intensity across the calculated for each pixel row. The length and width of these lines depended on the condition of the tissue and type of examination (e.g. full thickness, transition between inner and outer myometrium). Areas with artefacts and holes were avoided.

Regions of interest were defined by placing two movable boundary markers on the line profile (***Figure.3***). The upper-limit marker represented the start point of the line profile (e.g. serosa, outer myometrium) and the lower-limit marker was used to define the transition point between the endometrium and the myometrium, the numerical value of which was reported. These lines were also used to investigate the significant features, such as peaks and troughs, throughout each data set. The calibrated spatial data was expressed in mm and the intensity values were stated in arbitrary units (0-255).

From the *Line Profile: Report* menu the *Table* option was then selected and the line profile data were also displayed in a tabular form (***Figure.4***). Both the line profile graph and the tabular data where transferred to a spreadsheet (Excel, Microsoft). The grey level data were inverted (subtracted from 255) so that the dense regions had high values. An XY Scatter chart was created. The X-axis of the chart represented the distance across the tissue and the Y-axis measured the density of the staining in arbitrary values (inverted grey levels).

The image was subsequently annotated by drawing a rectangular box over the selected areas. Additionally a thin horizontal line was drawn to delineate the endometrium/myometrium boundary (elastin sections) or the inner/outer myometrium boundary (laminin sections). The annotated image was saved in *tif* format and stored for future reference.

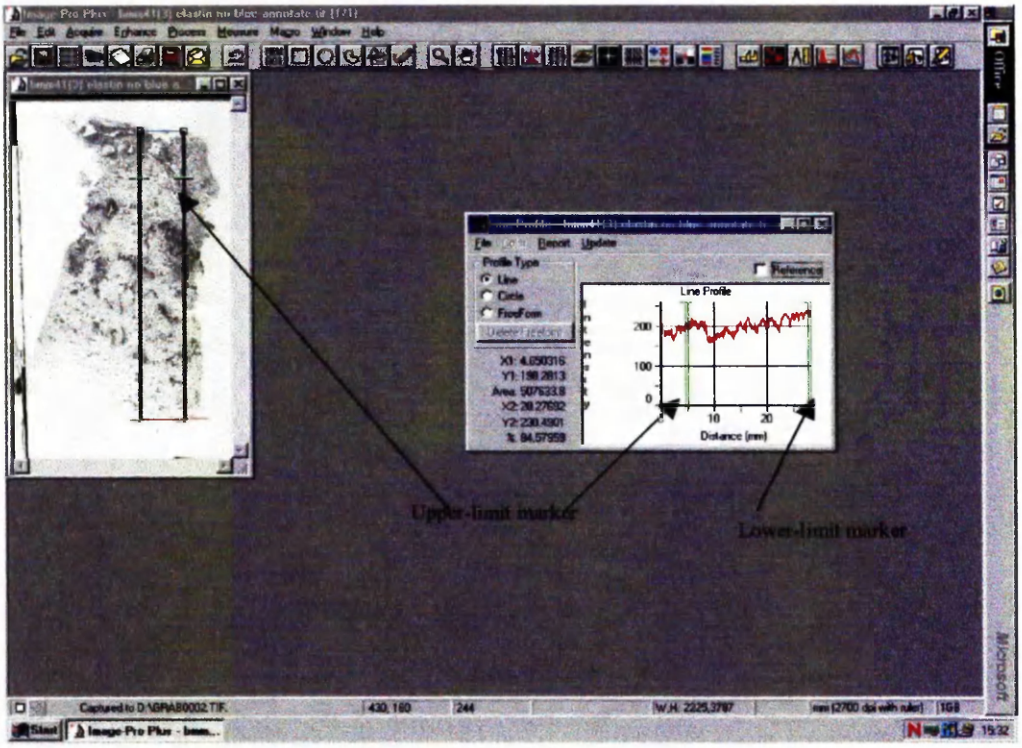

Figure.3 Captured screen image from Image Pro-Plus 4.0 program showing the line profile data in tabular form and a low-magnification image of a full thickness endometrial and myometrial section, with the vertical lines referred to in the text.

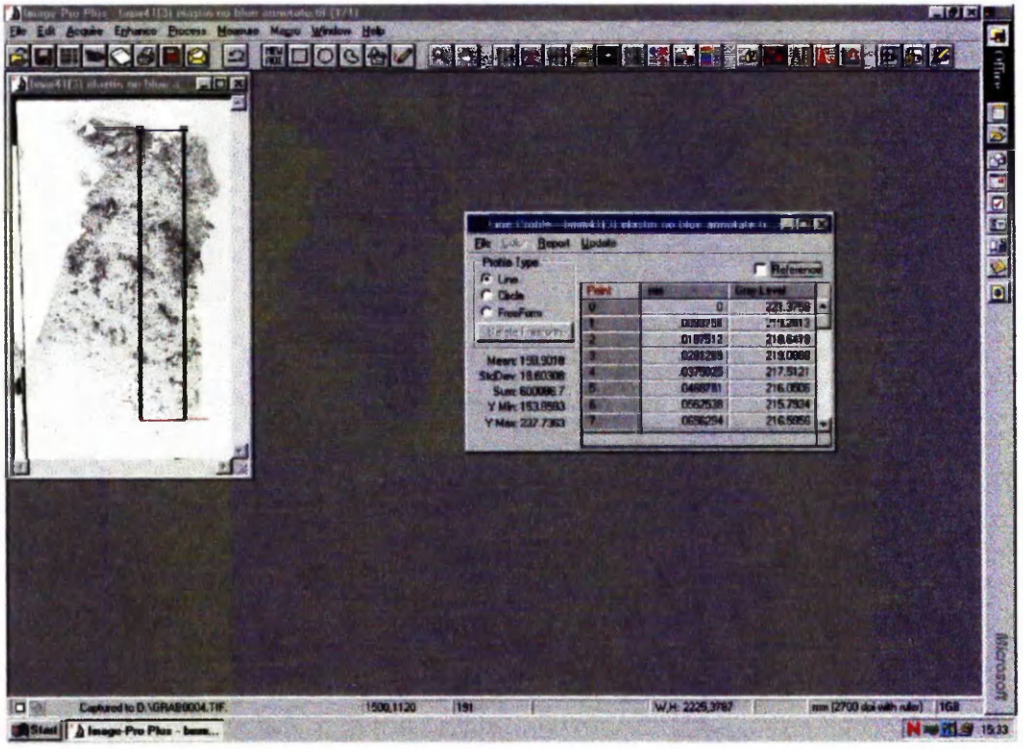

Figure.4 Captured screen image from Image Pro-Plus 4.0 program showing the line profile data in tabular form and a low-magnification image of a full thickness endometrial and myometrial section.

2.4.3 *Editing digital images*

Digital images captured at various magnifications were edited within Adobe Photoshop 4.0 or 5.0. Scanned images used for quantitative analysis were not manipulated in any way. The color balance of the images was adjusted by manually selecting a background region of the section image with no tissue, in order to produce a consistent white colour background. From the digital images of the orcein staining, monochrome images were produced by thresholding the darker areas. The images were then annotated, by adding the corresponding letter and scale bar. The annotated image was then saved in *tif* format and inserted into Microsoft's Word document where they were rescaled and a border was placed around them.

2.4.4 *Quantitative analysis of elastin distribution*

Eleven full thickness paraffin embedded myometrial sections, where elastin was immunolocalised without Haematoxylin counterstaining, were selected on the basis of tissue quality (i.e. fewer holes and artefacts present). Digital images were produced by scanning the sections at a resolution of 2700dpi with constant exposure and contrast settings. Density profiles for the intensity of elastin immunolocalisation were produced using the method described above. Because the length of the myometrial specimens (n=11) varied, two methods of combining the data sets from all sections were then applied to average the distribution of elastin throughout the myometrial length. The first method involved simple averaging of data from myometrial sections. In the first method, the data sets were aligned using the position of the outer myometrium and truncated at a length equal that of the shortest myometrial specimen (18.8mm). This method restricted the analysis to the outer myometrium. A combined horizontal average was calculated for all the tissue sections at given myometrial lengths.

In the second method the data sets were normalised by width. All myometrial sections (n=11) were arithmetically divided into an equal number of slices (n=93) within a width range of 219-300μm. The width (219-300μm) of the slices varied between the 11myometrial sections and depended on the myometrial length of the individual sections. As the calculation of the consecutive slice average involved smoothing of the data, over-smoothing of the data was avoided by selecting a width range of 219-300μm.

Patterned data sets were generated (Minitab) to label each of the 3,000 pixels with a particular slice number. The mean slice value was calculated for all patients (Minitab). The Pearson correlation coefficient was calculated and a line regression analysis was carried out (Minitab). A fitted line plot was generated displaying either the 95% confidence interval (C.I) or the 95%

prediction interval (P.I). A liner and quadratic fit were compared (Polnom, Simfit http://biomed.man.ac.uk/simfit/).

2.4.5 *Quantitative measurement of laminin β2 chain*

As it was not possible to produce full thickness myometrial frozen sections of very high quality the analytical method devised was based on the transition from inner to outer myometrium rather than the whole myometrial length.

Eight high quality frozen sections without cutting artefacts or holes were selected. In these sections the laminin β2 chain was immunolocalised without Haematoxylin counterstaining. Digital images were produced by scanning the sections at a resolution of 1200dpi with constant exposure and contrast settings.

Density profiles for the intensity of the laminin β2 chain immunolocalisation were produced using the same methods as that for elastin. An objective data averaging technique was used to define the point at which the intensity of the immuno-reaction started to decline, moving from the inner towards the outer myometrium. A region of outer myometrium at least 1.25mm from then edge of the sections and approximately 7mm in length, was selected and an average density value was calculated for the outer part of the muscle. The raw data set was then smoothed, by calculating the running average, to extract the underlying trend in the data. The running average was calculated from the outer towards the inner myometrium (Excel). The degree of smoothing used was set by comparing different smoothing widths ranging from 20-300 pixels (0.42-6.4mm). A smoothing width of 30 pixels (0.64mm) was shown to produce a reliable estimate of the transition point. The point, at which the edge of the smoothing window achieved the same value as the outer average, was determined. The position of the centre of the smoothing window was then used to calculate the sectional width. This method defined the position where the immuno-reaction intensity began to decline in the outer muscle. The distance between this point and the endometrial-myometrial junction was defined as the sectional thickness of the inner myometrium.

Averages were calculated for the myometrial distribution of the β2 laminin chain and collagen IV. All smoothed data sets for the β2 laminin chain (n=13) and collagen IV (n=12) were aligned separately using the position of the endometrial/myometrial boundary and truncated at a length equal to that of the shortest specimen (12.02mm for the β2 laminin chain and 11.51mm for collagen IV). A combined average was calculated for all the tissue sections throughout the muscle.

The sectional thickness was calculated from the average data set for the β2 laminin chain using a similar method as that described above. The region of outer myometrium selected was approximately 3.5mm in length and an average value density value was calculated for the outer part of the muscle.

The ratio of the β2 laminin chain to collagen IV was also calculated (Excel). Linear and quadratic fits were applied to the ratio of the β2 laminin chain to collagen IV (Excel). The sectional thickness was defined, using the method described above and when the quadratic function reached the maximum.

2.5 RNA Isolation

Total RNA was extracted from four hysterectomy specimens. Immediately after the surgery, the uterus was taken to Pathology, where a full thickness endometrium and myometrium mid corpus slice (~1cm thick) was cut off, by the receiving pathologist, and transferred to the lab in an RNA stabilising solution (RNAlater Ambion, Cat.#7021). The endometrium was removed, under sterile conditions, and discarded. The remaining myometrium was weight and placed into five times the volume of RNAlater solution, stored at 4°C and processed within a month from the date of collection.

Total RNA was isolated from each sample using the Trizol (Life Technologies, Cat.No. 15596) according to the manufacturer method. The tissue was chopped into smaller pieces and homogenised in 1ml of Trizol (per 50-100mg of tissue) using a homogenizer for 50sec. The homogeniser head was cleaned with double-distilled water (DDW) and 70% alcohol before and after the processing of individual samples.

The homogenised sample was aliquoted in 1ml amounts (5-12 tubes), incubated for 5min at 15-30°C. 0.2ml of chloroform (per 1ml of Trizol) was then added to each tube. The tubes were shaken vigorously by hand for 15sec, incubated at 15-3°C for 2-3 min and centrifuged (13,000 rpm) for 15min at 2-8°C. Following centrifugation the mixture was separated into a lower red, phenol-chloroform phase, an interphase and a colourless upper aqueous phase. The aqueous phase was carefully transferred to new tubes using a fine plastic pipette and then 0.5ml of isopropyl alcohol (per 1ml of Trizol used in the initial homogenisation) was added. Samples were incubated for 10min at 15-30°C and centrifuged (13,000 rpm) for 10min at 2-8°C. The supernatant was removed and each RNA pellet was washed once with 1ml of 70% ethanol (per 1ml of Trizol used in the initial homogenisation). Each sample was mixed by vortexing so that the pellet could be seen floating in the solution. At this point all samples were stored at -70°C. After thawing the samples were centrifuged (10,000 rpm) for 5min at 2-8°C, the pellets were

allowed to dry for approximately 20 min. The RNA was dissolved in DEPC treated DDW. The amount of DEPC DDW used depended on the size of the pellet, but no less than 15µl was used. All samples were vortexed, centrifuged and incubated for 5min at 65°C (Techne Dri-Block DB 1M, Genetic Research Instrumentation, Essex, Enlgand). The last three steps were repeated one more time. All aliquots (5-12 tubes) were combined into one tube and kept on ice.

2.5.1 Quantification of RNA

10µl of the RNA sample was added to 990µl of double distilled water in a microcentrifuge tube. This solution was vortexed and transferred into a silica cuvette using a disposable plastic pipette. The absorbance of the solution at 260nm and 280nm was measured using a spectrophotometer. The absorbance of the solution at 260nm and 280nm is directly proportional to the concentration of RNA present in the sample. The ratio of absorbance values obtained is an index of the purity of the RNA sample. A ratio of 2.0 represents a pure RNA sample with very little contamination. The amount of RNA present in 1ml of a sample was calculated by multiplying the absorbance at 260nm by 40, since an optical density of 1 represents 40mg of RNA. The total amount of RNA present was calculated by multiplying the above value by the dilution factor.

2.5.2 Electrophorised examination for RNA samples

The RNA gel was prepared by dissolving 1.2g of agarose in a solution containing 73ml of DDW and 10ml of 10x MOPS. The solution was microwaved at P70 for 2.5min, gently swirling every 20sec. Seventeen millilitres of formaldehyde were added to the above solution and then it was left to cool down for approximately 20min. The above solution was poured into a sealed gel plate containing a plastic comb, 60ml of and the gel was left to set for 30min. The gel was placed in a G-100 gel tank, and filled up with 1xMOPS solution. 10µl of loading buffer was added to the RNA samples, and the tubes were vortexed and incubated at 65°C for 10min before the RNA samples were loaded onto the gel wells. The samples (5µl) were electrophorised at 60V for 2-2.5h. The presence 18S and 28S bands were examined using a transilluminator (TC-312A, purchased from Spectroline, U.K.) A photograph of each gel was taken, using a direct screen instant camera (DS 34, purchased from Polariod, U.K.) with a 0.7x Hood (DS H-7, Polariod, U.K.). All samples were aliquoted in 10µl aliquots and stored at -70 °C.

2.5.3 Reverse transcriptase-polymerase chain reaction analysis of anti-beta 2 (C4) and gamma 1 (D18) laminin chains

Anti-beta 2 (C4) and gamma 1 (D18) laminin chain mRNA expression was examined by reverse transcriptase-polymerase reaction (RT-PCR) using a one step reaction (Qiagen OneStep RT-PCR

kit, Cat. No. 210212). Total RNA was extracted (see **RNA Isolation**) from human myometrial tissue.

RT-PCR was performed in a reaction volume of 50µl (***Table.2***). A volume 10% greater than the required, for the total number of reactions, was prepared according to ***Table.2***. A negative control, lacking the template RNA, was also included in every experiment. The Master mix was vortexed and the appropriate volumes were dispensed into PCR tubes. The template RNA was then added to the individual PCR tubes, vortexed and overlaid with one drop of mineral oil. While the PCR tubes were still on ice, the RT-PCR program was initiated but the PCR tubes were not placed into the thermal cycler until it had reached a temperature of 50°C.

For amplification of the anti-beta 2 laminin chain, the sense primer 5[prime] GCTCGGCAGTTGGATGCTCTC 3[prime] and the antisense 3[prime] GCCCGCTCATTTTCCTCATAG were used. For amplification of the gamma 1 laminin chain, the sense 5[prime] CAAAGCCAAAGATGAAATGAA 3[prime] and the antisense 3[prime] AGAGGAGTGGGGGTCTGAAAA 5[prime] were used. All oligonucleotides were synthesised by Operon Technologies, Inc. The sequence of both sense and antisense primers were kindly provided by John Aplin (St.Mary's Hospital, Manchester). The amplification conditions are summarised in ***Table.3***.

After amplification, the PCR products were electrophorised on a 1% agarose gel for 1.5h at 80V. For the preparation of the gel 1g of agarose (BRL, 5405510UB) was dissolved in 100ml of 1xTBE. The solution was microwaved at P70 for 2.5 min, gently swirling every 25 sec. 1µl of ethidium bromide (Sigma, E1510) was added to the solution which was left to cool for approximately 20min before it was poured into the gel tray and left to set for about 30 min. The gel was placed into G-100 tank and filled with 1xTBE.

Table.2 Reaction components for one-step RT-PCR

Component	Volume/reaction
Master Mix	
RNase-free water	Variable
5x OneStep RT-PCR Buffer *	10.0µl (C4) & 6.0µl (D18)
dNTP Mix	2.0µl
Primer A (sense primer)	1µl
Primer B (antisense primer)	1µl
OneStep RT-PCR Enzyme Mix	2.0µl
Template RNA	
Template RNA	Variable†
Total Volume	50.0

**Contains 12.5 mM $MgCl_2$. The final concentration in the Master mix is 2.5 mM $MgCl_2$. For the anti-beta 2 oligonucleotide 2.5 mM $MgCl_2$ were required but 1.5 mM $MgCl_2$ for the gamma1 oligonucleotide.*

† A final concentration of 2µg was used per reaction.

Table.3 Thermal cycler conditions

Step		Temperature
Reverse transcription	30min	50°C
Number of cycles	1	
Initial PCR activation step	15min	95°C
Number of cycles	1	
Denaturation	1min	94°C
Annealing	1min	57°C (C4) – 51°C (D18)
Extension	1min	72°C
Number of cycles	30	
Final extension	10min	72°C

Chapter.3 Results

3.1 α2, β1, β2, γ1 laminin chains and collagen IV expression in the human uterus

Frozen sections from thirty-two normal specimens (4 menstrual, 15 proliferative, 11 secretory, 1 inactive, 1 postmenopausal) and 12 exposed to exogenous progestagen (Mirena®) for a period of 10 weeks to 9 months, were stained with antibodies directed to the α2, β1, β2, γ1 laminin chains and collagen type IV. The original tissue bank consisted of 70 specimens but due to a freezer failure almost half of the tissue bank was lost, together with cut frozen sections.

3.1.1 *α2, β1, β2, γ1 laminin chains and collagen IV expression in the myometrium and endometrium of normal uteri*

Low magnification scans of sections where the β2 laminin chain (***Plate.1A***) had been immunolocalised revealed myometrial layering. This was in contrast to the more uniform myometrial distribution of the γ1 laminin chain (***Plate.1B***) and collagen IV (***Plate.1C***).

Microscopic images allowed higher resolution examination of the α2, β1, β2, γ1 laminin chains and collagen IV distribution. In the myometrium collagen IV was widely distributed throughout the smooth muscle (***Plate.2A***) and was also present in the vascular smooth muscle and stroma surrounding the blood vessels of both the inner and outer myometrium (***Plate.2A,B***). Collagen IV was immunolocalised in the glandular BM and blood vessels of the endometrium (***Plate.2C,D***). It was also present in the endometrial stroma of the superficial (***Plate.2C***) and basal part (***Plate.2D***) of the endometrium.

The γ1 laminin chain was immunolocalised in the smooth muscle and vascular smooth muscle of the inner myometrium (***Plate.3A***). In the outer myometrium the γ1 laminin chain was present in the smooth muscle and vascular smooth muscle but was absent from the stroma surrounding the blood vessels (***Plate.3B***) in contrast to collagen IV (***Plate.2B***). In the endometrium the γ1 laminin chain was present in the glandular BM, capillaries and arterioles (***Plate3C,D***) but was absent from the endometrial stroma of both the superficial (***Plate.3C***) and basal part of the endometrium (***Plate.3D***).

In the inner myometrium the β2 laminin chain was present in the smooth muscle and vascular smooth muscle (***Plate.4A***). In the outer myometrium the β2 laminin chain was immunolocalised in the smooth muscle and vascular smooth muscle (***Plate.4B***) but was absent from the stroma surrounding the blood vessels (***Plate.4B***). There is an obvious increase in intensity of staining between the smooth muscle of the inner (***Plate.4A***) and outer myometrium (***Plate.4B***). This

difference illustrates the gradient of the β2 laminin chain expression within the human myometrium and can be clearly seen in a low magnification scanned image (***Plate.1A***).

In the endometrium the β2 laminin chain was restricted in the basal portion of the glandular BM of the superficial endometrium (***Plate.4C***). The β2 laminin chain was also present in the spiral arterioles, variably present in the capillaries of the endometrium but absent from the stroma of both the superficial and basal part of the endometrium (***Plate.4C,D***).

Plate.1: Laminin β2, γ1 chains and collagen IV distribution in uterine sections

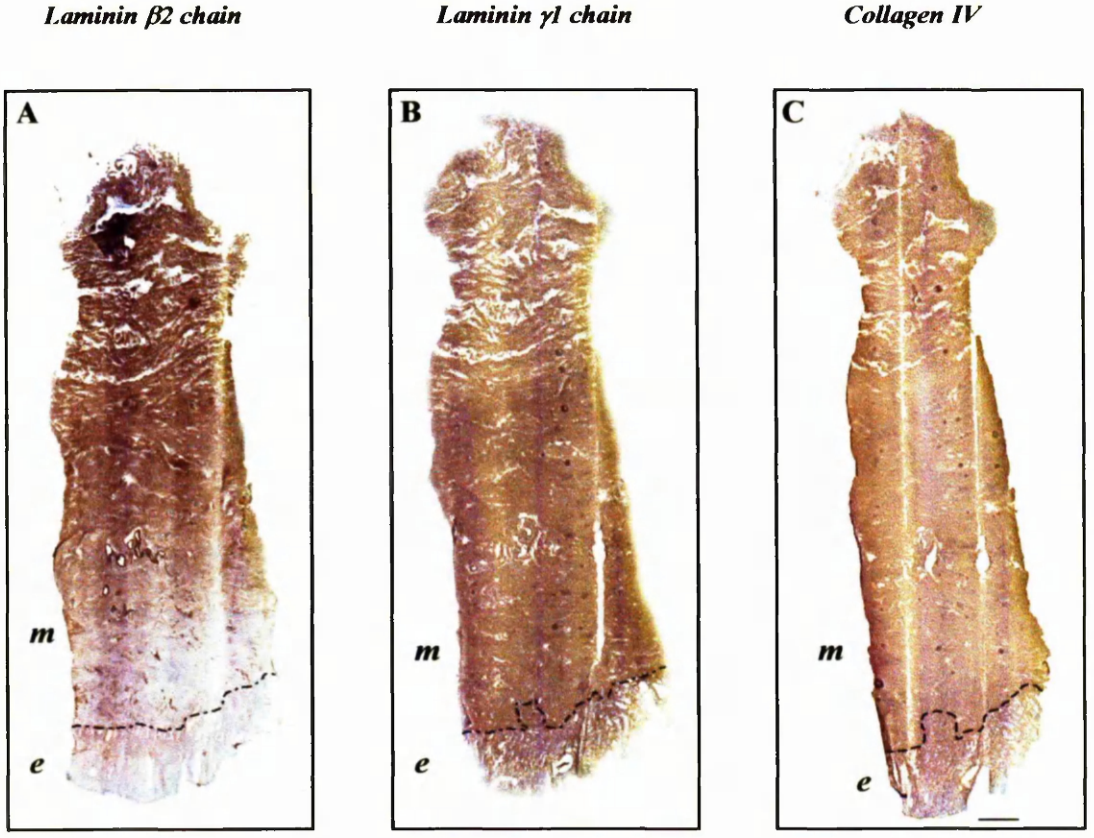

Plate.1: Low magnification scanned images of endometrium and myometrium from cryosections. (**A-C**) Secretory phase specimens where laminin β2 (**A**), γ1 chains (**B**) and collagen IV (**C**) have been localised. The blue colour is Haematoxylin staining of the nuclei. The dotted line marks the boundary between endometrium (*e*) and myometrium (*m*). In (**B**) and (**C**) part of the endometrium is seen to invade the subendometrial myometrium. There is a gradient in the myometrial smooth muscle expression of the β2 laminin chain (**A**) in contrast to the more expression of the γ1 laminin chain (**B**) and collagen IV (**C**). Within the inner myometrium, blood vessels are stained with the β2 laminin chain. Scale bar = 5mm.

Plate.2: Collagen type IV distribution in the human myometrium and endometrium

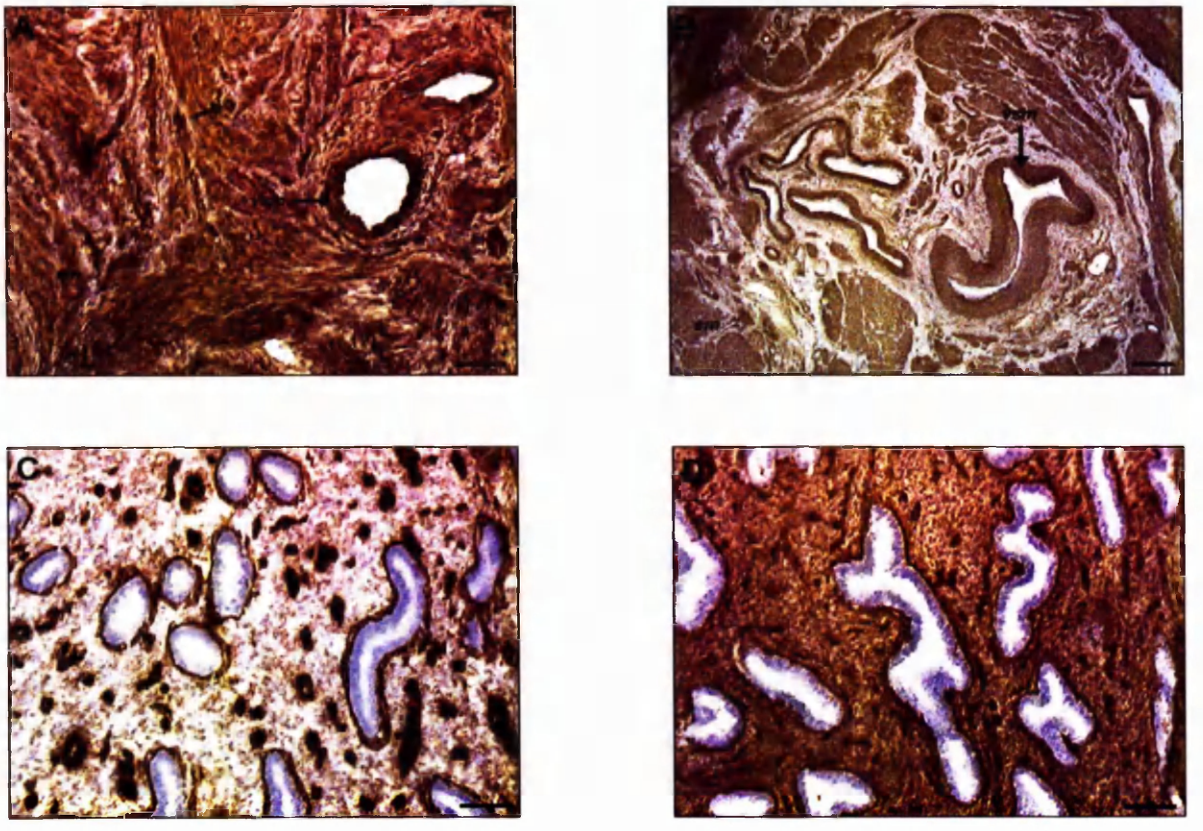

Plate.2*:** Collagen IV in a ubiquitous component of the basement membrane and. It was therefore expected to be uniformly distributed throughout the myometrium and endometrium and so acted as an internal control. (**A**) In this proliferative phase specimen, collagen IV is expressed within the smooth muscle (sm***) of the inner myometrium, capillaries (*c*), vascular smooth muscle (***vsm***) and the peri-vascular stroma. (**B**) Collagen IV is present in the smooth muscle (***sm***) and vascular smooth muscle (***vsm***) of the outer myometrium in this proliferative phase specimen. It is also present in the smaller arteries as well as in the stroma surrounding the blood vessels. (**C**) In the endometrium of this proliferative phase specimen, collagen IV is present in the glandular basement membrane and in the capillaries. Collagen IV is also present in the endometrial stroma in a punctuate pattern. (**D**) Collagen IV is present in the glandular basement membrane and in the capillaries of this proliferative phase specimen. Due to the higher cellular density of the basal stroma, collagen IV is more widely distributed (**C**). Scale bar (**A,C,D**) = 100μm, (**B**) = 200μm.

Plate.3: γ1 laminin chain distribution in the human myometrium and endometrium

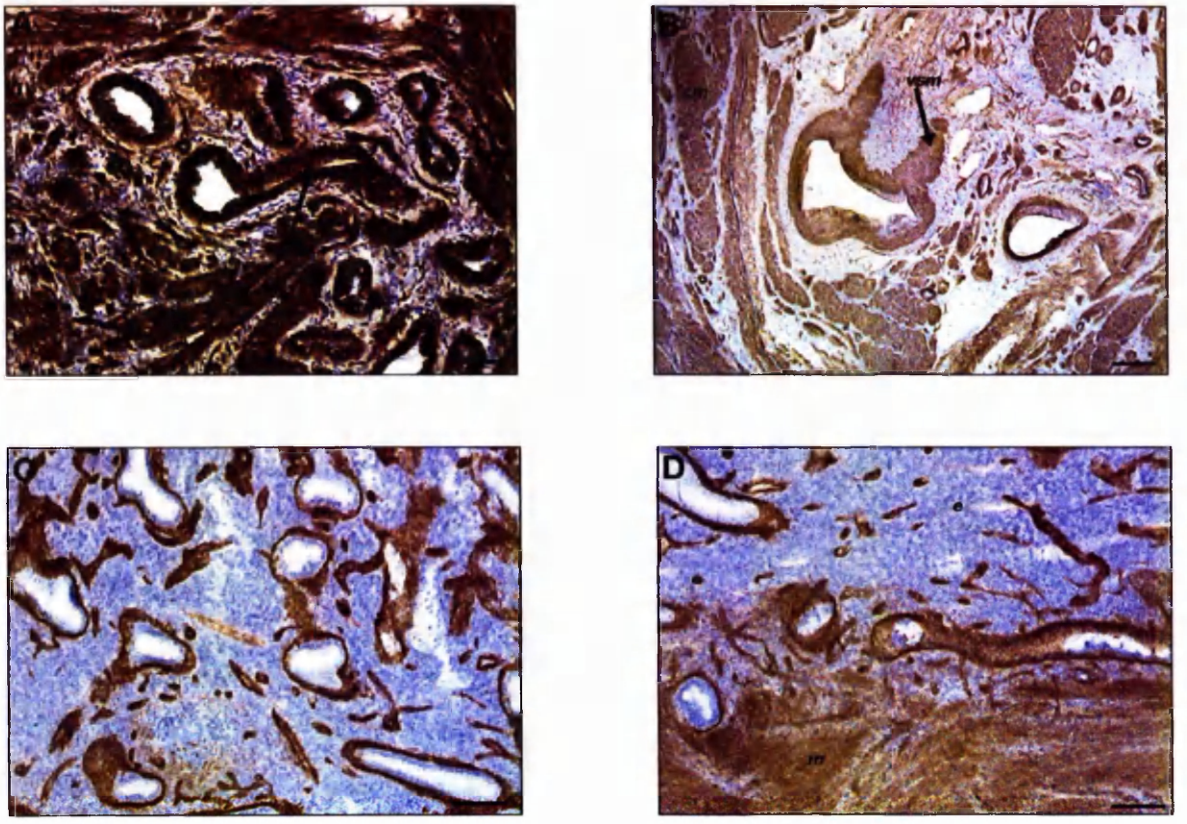

Plate.3*:** The γ1 laminin chain is present in most of the laminin types. It was therefore expected to be found in all the components of the myometrium and endometrium, where BM were present and hence acted as an internal comtrol. (**A**) The γ1 laminin chain is present in the smooth muscle (sm***) and the vascular smooth muscle (***vsm***) of the inner myometrium but is absent from the stroma surrounding the blood vessels, in this proliferative phase specimen. (**B**) In the outer myometrium the γ1 laminin chain is present in the smooth muscle (***sm***), vascular smooth muscle (***vsm***) but is absent from the peri-vascular stroma in this weakly proliferative phase specimen. (**C**) In the basal endometrium of this menstrual phase specimen, the γ1 laminin chain is present in the glandular basement membrane and the blood vessels but is absent from the endometrial stroma. (**D**) Part of the endometrium (***e***) and subendometrial myometrium (***m***) from the same specimen as (**C**) are visible. The γ1 laminin chain is present in the glandular basement membrane and capillaries but is absent from the endometrial stroma. The smooth muscle of the myometrium (***m***) is shown to express the γ1 laminin chain. Scale bar (**A,C,D**) = 100μm, (**B**) = 200μm.

Plate.4: β2 laminin chain distribution in the human myometrium and endometrium

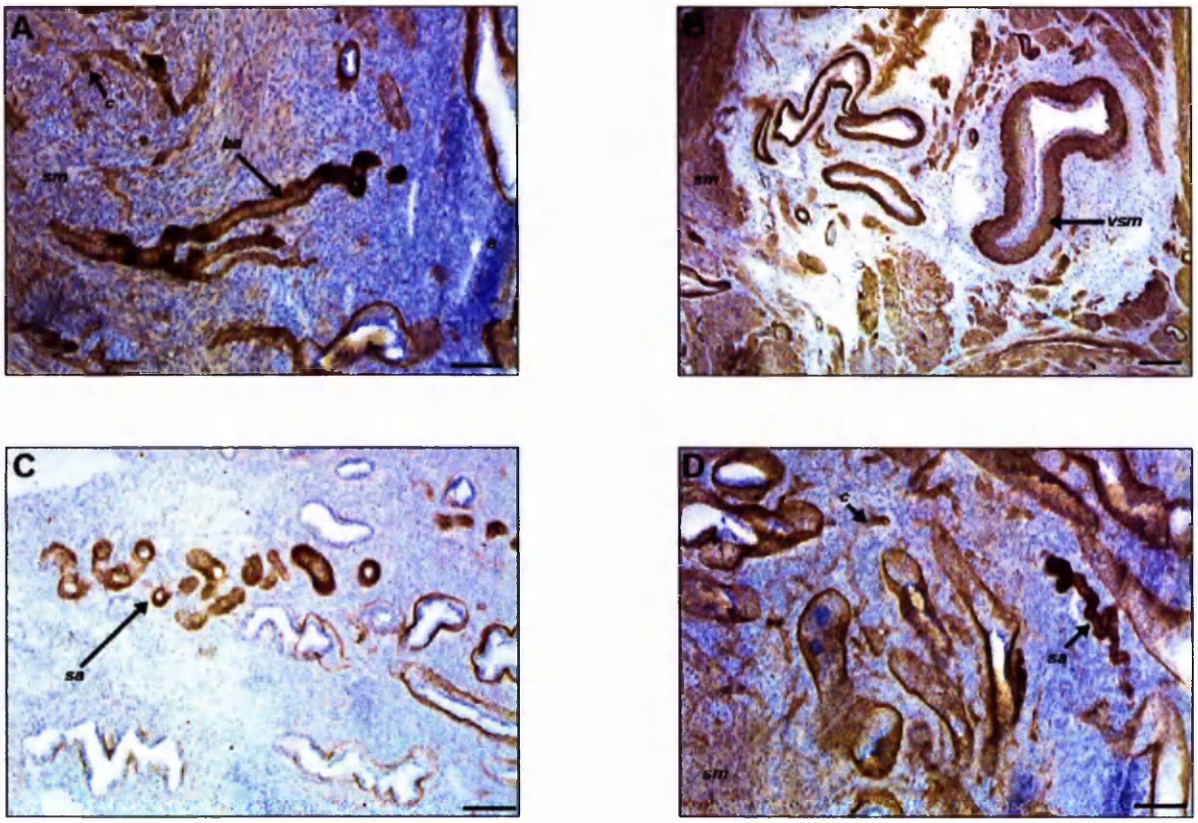

Plate.4*:** Layering in the myometrial distribution of the β2 laminin chain is observed by direct microscopic observation of tissue sections. **(A)** In the inner myometrium of this menstrual phase specimen, the β2 laminin chain is present in the vascular smooth muscle as seen in this branching arteriole (ba***) and only weakly expressed in the smooth muscle (***sm***). The β2 laminin chain is also present in the capillaries (***c***). Part of the basal portion of the adjacent endometrium (***e***) is present. **(B)** In the outer myometrium of the same specimen as **(A)**, the β2 laminin chain is expressed in the smooth muscle (***sm***). The β2 laminin chain is also present in the vascular smooth muscle (***vsm***) but absent from the peri-vascular stroma. Note the difference in the intensity of staining between the smooth muscle of the outer and inner myometrium. This illustrates the myometrial layering of the β2 laminin chain which is shown in ***Plate.1A***. **(C)** In the endometrium the β2 laminin chain is present in the vascular smooth muscle as seen in the spiral arteriole (***sa***) but is absent from the endometrial stroma in this secretory phase specimen. The β2 laminin chain expression is restricted to the basal portion of the glandular basement membrane. **(D)** In the basal endometrium of this weakly proliferative phase specimen, the β2 laminin chain is present in the glandular basement membrane, the vascular smooth muscle as seen in the spiral arteriole (***sa***). The β2 laminin chain is absent from the endometrial stroma but present in the smooth muscle (***sm***) of in the inner myometrium. Scale bar **(A,C,D)** = 100μm, **(B)** = 200μm.

The β1 laminin chain was present in the smooth muscle of the inner myometrium (***Plate.5A***) as well as in the endothelium of the blood vessels (***Plate.5A***). In the outer myometrium the β1 laminin chain was expressed in the smooth muscle but absent from the stroma surrounding the blood vessels (***Plate.5B***). The β1 laminin chain was also present in the endothelium of blood vessels in the outer myometrium (***Plate.5B***) but absent from the vascular smooth muscle (***Plate.5B***).

In the endometrium, the β1 laminin chain was immunolocalised in the glandular BM and endometrial stroma (***Plate.5C,D***). The β1 laminin chain was also present in the capillaries and particularly obvious in the vascular smooth muscle of the arteries (***Plate.5C,D***). The myometrial distribution of the β1 laminin chain is heterogeneous (***Plate.5C,D***).

In the inner myometrium, the α2 laminin chain was present in the smooth muscle but absent from the stroma surrounding the blood vessels and the vascular smooth muscle (***Plate.6A***). In the outer myometrium the α2 laminin chain was present in the smooth muscle but absent from the vascular smooth muscle (***Plate.6B***). The α2 laminin chain was also absent from the vascular endothelium and per-arteriolar stroma (***Plate.6B***).

In the endometrium, the expression of the α2 laminin chain was restricted in the basal portion of the glandular BM (***Plate.6C***). There was no stromal expression of the α2 laminin chain stroma in either the superficial (***Plate.6C***) or basal (***Plate.6D***) part of the endometrium.

Due to the absence of the α2 and β1 laminin chain from the vascular smooth muscle and peri-vascular stroma, structures presumed to be of neural origin appeared to express the α2 and β1 laminin chain antigen (***Plate.7A,B***). Immunolocalization carried out in 13 frozen sections (2 menstrual, 9 proliferative, 2 secretory) with the 68kD neurofilament protein, confirmed that these structures where indeed either nerve fibres or nerve bundles. Nerve bundles were observed in the myometrial smooth muscle (***Plate.7C***) as well as thin fibres innervating the large blood vessels of the outer myometrium (***Plate.7D***).

The distribution of the α2, β1, β2, γ1 laminin chains and collagen IV remained the same within the endometrial stroma and glandular BM during the course of the normal menstrual cycle (not shown). However, a denser distribution of ECM was observed around the endometrial blood vessels of the secretory phase sections (***Plate.8 A-C***)

The above findings are summarised in tabular form (***Table.4***). These results illustrate a clear pattern of tissue specificity of laminin chain expression. No staining was observed in the negative controls (not shown).

Plate.5: β1 laminin chain distribution in the human myometrium and endometrium

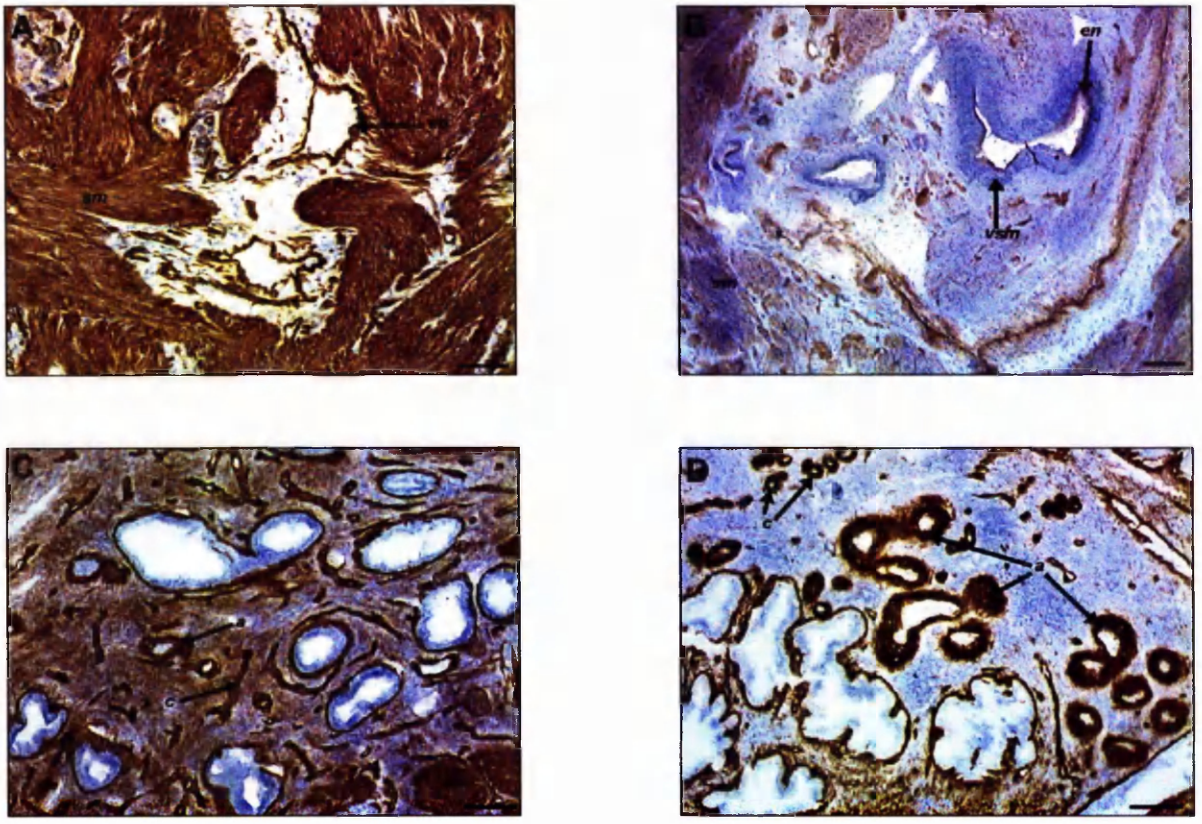

Plate.5*: (A)** In the inner myometrium of this secretory phase specimen the β1laminin chain is present within the smooth muscle (sm***) and endothelium (***en***) of the blood vessels. **(B)** The β1 laminin chain is expressed in the smooth muscle (***sm***) of the outer myometrium and endothelium (***en***) of the blood vessels but absent from the vascular smooth muscle (***vsm***) of this proliferative specimen. **(C)** In the basal endometrium of this secretory phase specimen, the β1 laminin chain is present in the glandular basement membrane, capillaries (*c*) and arterioles (*a*). The β1 laminin chain is also present in the endometrial stroma. **(D)** In the superficial endometrium of the same specimen, the β1 laminin chain is present in the glandular basement membrane, vascular smooth muscle of the arterioles (*a*) and in the endometrial stroma. The stromal distribution of the β1 laminin chain is heterogeneous. The β1 laminin chain expression is widespread within the basal portion of the endometrium (lower bottom corner); punctate in certain areas (upper right corner) and less widely distributed in others. Scale bars **(A,C,D)** = 100μm, **(B)** = 200μm.

Plate.6: α2 laminin chain distribution in the human myometrium and endometrium

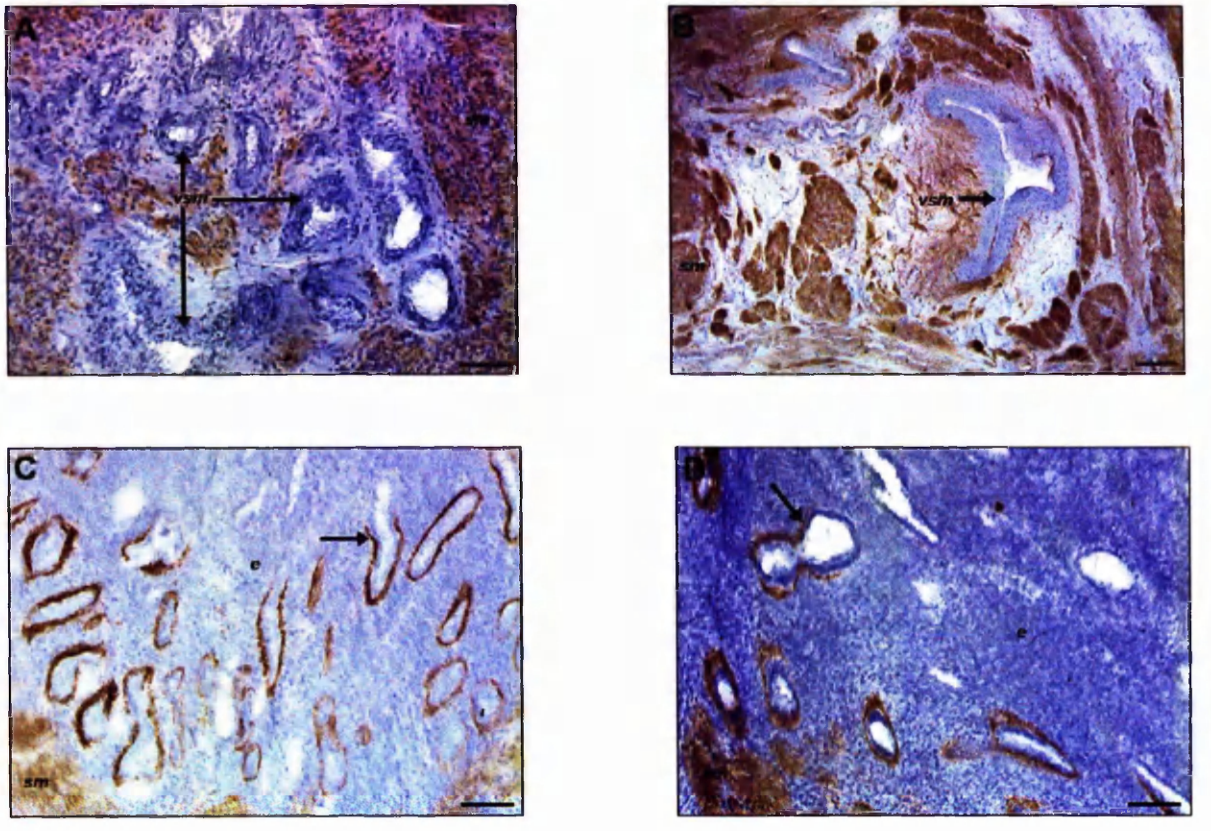

Plate.6*: (A)** In the inner myometrium of this secretory phase specimen, the α2 laminin chain is present in the smooth muscle (sm***) but is absent from the vascular smooth muscle (***vsm***) and the stroma surrounding the blood vessels. **(B)** The α2 laminin chain is expressed in the smooth muscle (***sm***) but is absent from the vascular smooth muscle (***vsm***) of the outer myometrium in this proliferative specimen. **(C)** In the endometrium of this menstrual phase specimen the α2 laminin chain is restricted to the basal portion of the glandular basement membrane but absent from the endometrial stroma. The point of transition is particularly obvious in one glandular cross-section (arrow). The α2 laminin chain was not present in the endometrial blood vessels. Part of the smooth muscle (***sm***) from the subendometrial myometrium is seen to express the α2 laminin chain. **(D)** The α2 laminin chain is present in the basal portion of the glandular basement membrane but absent from the endometrial stroma in this menstrual phase specimen. The point of transition is particularly obvious in one glandular cross-section (arrow). The α2 laminin chain is also expressed in the smooth muscle (***sm***) of the subendometrial myometrium. Scale bars (**A,C,D**) = 100μm, (**B**) = 200μm.

Plate. 7: Distribution of neurofilaments in uterine sections

α2 laminin chain

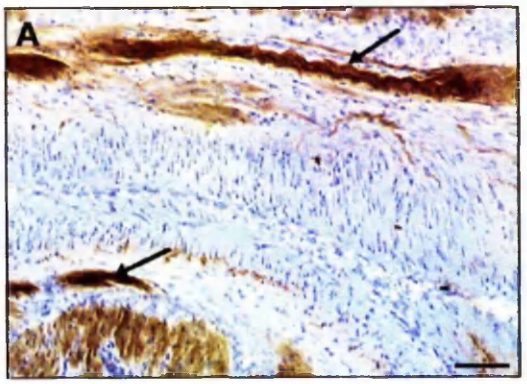

α2 laminin chain

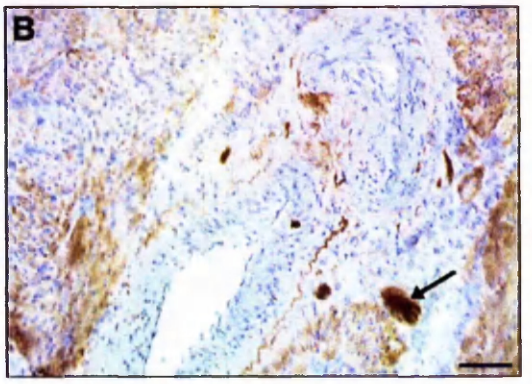

Neurofilament 68kD

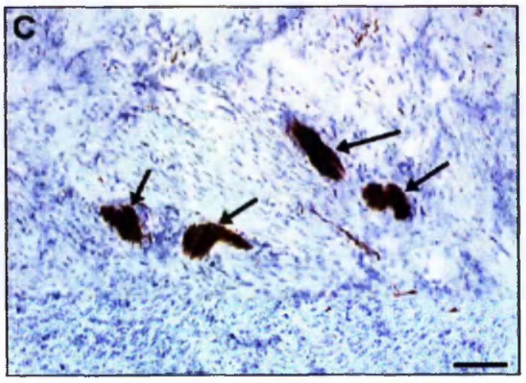

Neurofilament 68kD

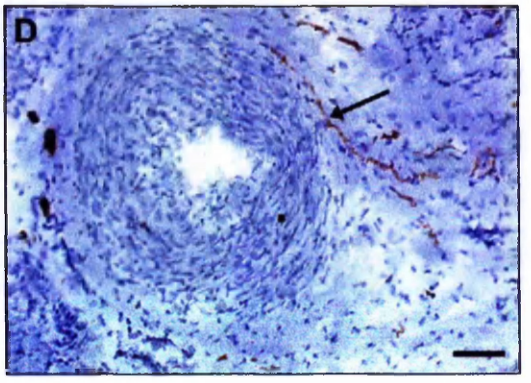

***Plate. 7*: (A,B)** In highly magnified images, structures (arrows) resembling nerve fibres were observed. These structures were particularly obvious with the α2 laminin antibody. **(C,D)** The identity of these structures was confirmed by neurofilament immunolocalisation (arrows). Scale bar = 100μm.

Plate.8: Extracellular matrix deposition around the blood vessels in secretory sections

β1 laminin chain

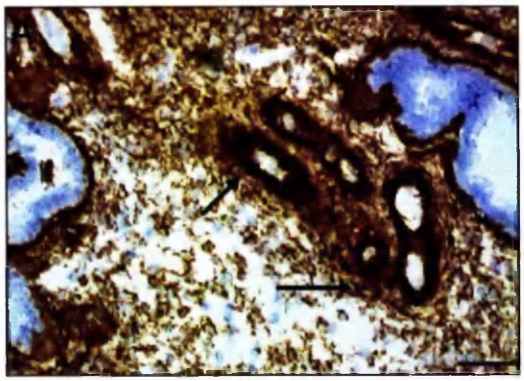

γ1 laminin chain

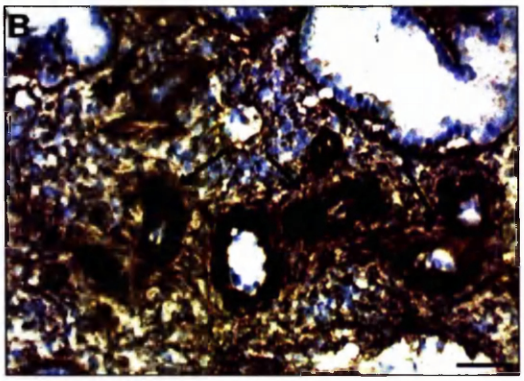

β1 laminin chain

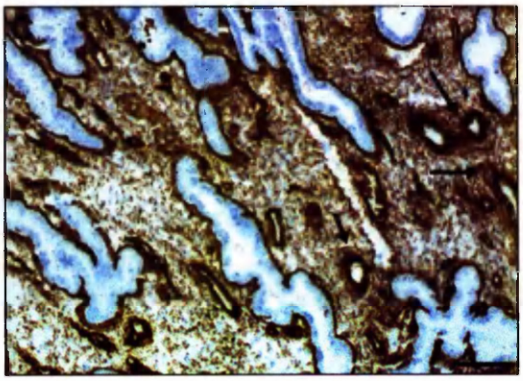

***Plate.8*: (A-C)** Extracellular matrix deposition was observed around the blood vessels (arrows) of the superficial endometrium in secretory sections. This was not observed in specimen from the menstrual and proliferative phases of the normal menstrual cycle. Scale bar = 100μm.

Table.4 Distribution of the α2, β1, β2, γ1 laminin chains and collagen IV in uterine sections

	Laminin α2	Laminin β1	Laminin β2	Laminin γ1	Collagen IV
Endometrium					
Glandular epithelium	*Only in the basal portion*	*Present*	*Only in the basal portion*	*Present*	*Present*
Stroma functionalis	*Absent*	*Heterogeneous distribution*	*Absent*	*Absent*	*Heterogeneous distribution*
Stroma basalis	*Absent*	*Present*	*Absent*	*Absent*	*Present*
Vascular S.M	*Absent*	*Absent*	*Present*	*Present*	*Present*
Endothelium	*Absent*	*Present*	*Variable*	*Present*	*Present*
Myometrium					
Smooth muscle	*Present*	*Present*	*Present (gradient)*	*Present*	*Present*
Vascular S.M	*Absent*	*Absent*	*Present*	*Present*	*Present*
Endothelium	*Absent*	*Present*	*Present*	*Present*	*Present*
Stroma peri-arteriolar	*Absent*	*Absent*	*Absent*	*Present*	*Present*
Nerve fibres	*Present*	*Present*	*	*	*

Key: S.M = smooth muscle
* = due to the abundance of these chains in the smooth muscle, it was difficult to visualise nerve fibres

3.1.2 *α2, β1, β2, γ1 laminin chains and collagen IV expression in the myometrium and endometrium of uteri after exposure to intrauterine levonorgestrel (Mirena®)*

Following treatment with intrauterine levonorgestrel (Mirena®), the myometrial gradient of the β2 laminin chain already described (***Plate.1A***) appeared to remain (***Plate.9.A***), whilst the γ1 laminin chain (***Plate.9B***) and collagen IV (***Plate.9C***) showed a more uniform distribution throughout the smooth muscle of the myometrium.

The α2 laminin chain was present in the smooth muscle of the inner myometrium, but was absent from the vascular smooth muscle (***Plate.10A***). The β1 laminin chain was immunolocalised in the smooth muscle of the inner myometrium but was absent from the vascular smooth muscle (***Plate.10B***). In the inner myometrium the β2 laminin chain was expressed in the vascular smooth muscle and weakly expressed in the smooth muscle and (***Plate.10C***). The γ1 laminin chain (***Plate.10D***) and collagen IV (***Plate.10E***) were present in the smooth muscle and vascular smooth muscle of the inner myometrium.

In the outer myometrium the α2 laminin chain was present in the smooth muscle but was absent from the vascular smooth muscle (***Plate.11A***). The β1 laminin chain was present in the smooth muscle, vascular endothelium but was absent from the vascular smooth muscle (***Plate.11B***). In the outer myometrium the β2 laminin chain was present in the smooth muscle and vascular smooth muscle but was absent from the per-arteriolar stroma (***Plate.11C***). The β2 laminin chain staining in the smooth muscle of the outer myometrium (***Plate.11C***) was more intense than that seen in the smooth muscle of the inner myometrium (***Plate.10C***), illustrating the gradient observed in the low magnification scan (***Plate.9A***). The γ1 laminin chain (***Plate.11D***) and collagen IV (***Plate.11E***) were immunolocalised in the smooth muscle and vascular smooth muscle of the outer myometrium. Collagen IV distribution was similar to the γ1 laminin chain, however collagen IV was present in the stroma surrounding the blood vessels (***Plate.11E***), as seen in untreated patients (***Plate.2A,B***).

In the endometrium of one specimen obtained after exposure to intrauterine levonorgestrel (Mirena®), the β1 laminin chain was present in the highly decidualised areas but was less widely distributed within the basal endometrial stroma (***Plate.12A***). The β1 laminin chain was also present in the glandular BM and in the wall of the arteries and capillaries of the basal part of the endometrium (***Plate.12A***). The γ1 laminin chain was immunolocalised in the areas of decidualised tissue, in the wall of the endometrial vessels and in the glandular BM (***Plate.12B***). However, it was absent from the stroma of the basal part of the endometrium (***Plate.12B***). Collagen IV was present in highly decidualised areas as well as in the stroma of the basal part of

the endometrium (***Plate.12C***). It was also expressed in the BM of the glands and in the wall of arteries and capillaries (***Plate.12C***). More extensive peri-cellular staining was observed with the β1 and γ1 laminin chains.

Staining was absent from the negative controls (not shown).

Plate.9: Distribution of β2 and γ1 laminin chains and collagen IV in uterine sections after exposure to exogenous levonorgestrel

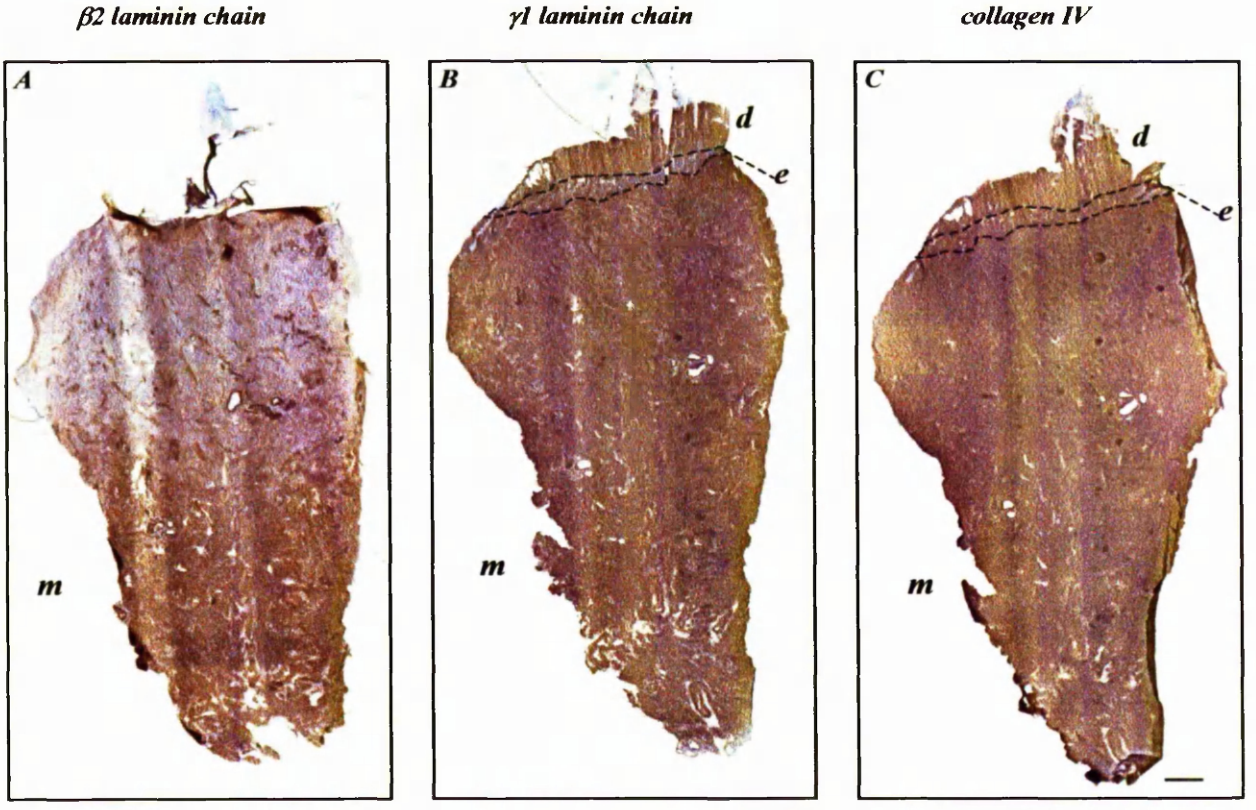

Plate.9*:** Low magnification scanned images of cryosections consisting of endometrium and myometrium. Sections from the same specimen after exposure of 9 months to exogenous levonorgestrel (LNG) where the β2 laminin chain (**A**), γ1 laminin chain (**B**) and collagen IV (**C**) have been immunolocalised. The blue colour is Haematoxylin staining of the nuclei. There is a gradient in the myometrial (m***) distribution of the β2 laminin chain (**A**) in contrast to the more uniform myometrial (***m***) distribution of the γ1 laminin chain (**B**) and collagen IV (C). The area enclosed by the dashed line represents the basal portion of the endometrium (***e***). No endometrium is present in the first section (**A**). Within the more decidualised areas (***d***) the γ1 laminin chain (**B**) and collagen IV (**C**) are very widely distributed. Scale bar = 5mm.

Plate.10: Distribution of the α2, β1, β2 and γ1 laminin chains and collagen IV in the inner myometrium of sections from specimens exposed to intrauterine levonorgestrel between 10 to 36 weeks

α2 laminin chain

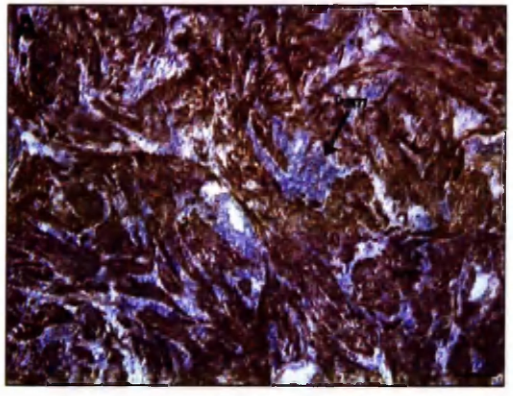

β1 laminin chain

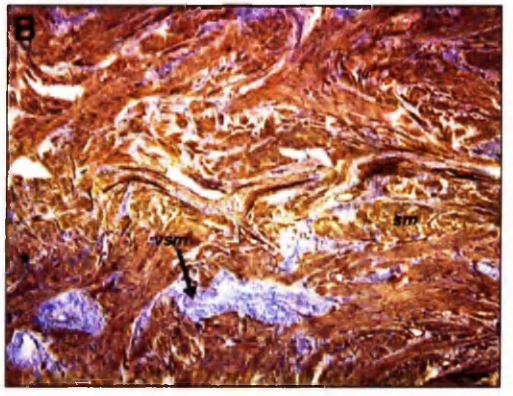

β2 laminin chain

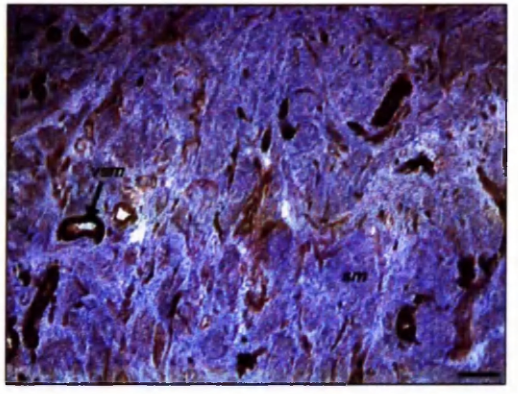

γ1 laminin chain

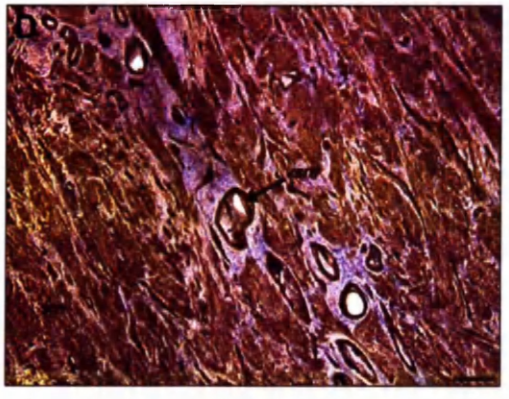

Collagen IV

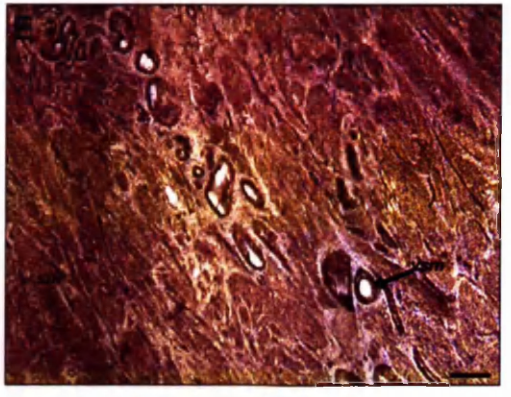

Plate.11: Distribution of the α2, β1, β2 and γ1 laminin chains and collagen IV in the outer myometrium of sections from specimens exposed to intrauterine levonorgestrel between 10 to 36 weeks

α2 laminin chain

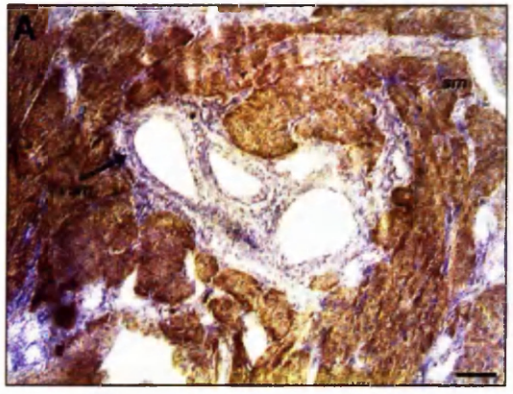

β1 laminin chain

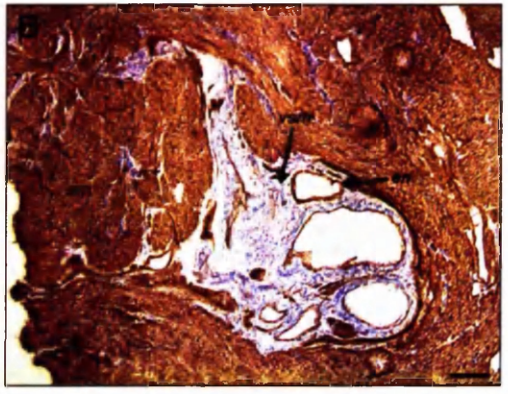

β2 laminin chain

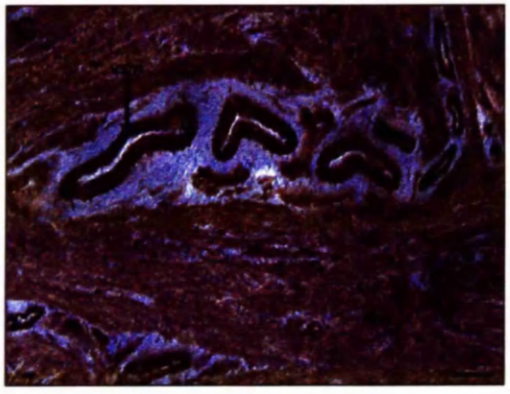

γ1 laminin chain

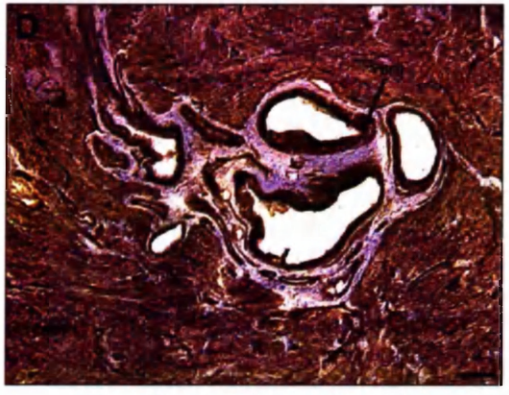

collagen IV

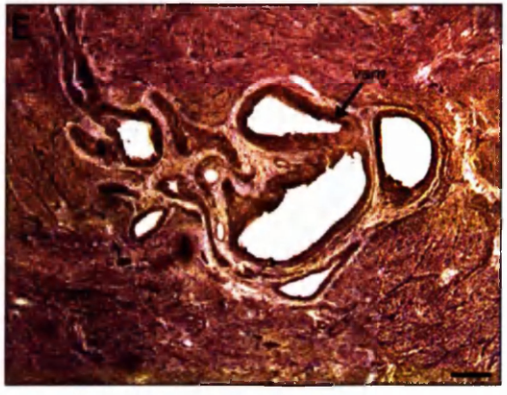

Plate.10*:** Following exposure to exogenous levonorgestrel (Mirena®) the distribution of the α2, β1, β2, γ1 laminin chains and collagen IV in the inner myometrium remained the same as that observed in untreated patients. **(A)** In the inner myometrium the α2 laminin chain is present in the smooth muscle (sm***) but absent from the vascular smooth muscle (***vsm***), after exposure for 10 weeks. **(B)** After exposure to 36 weeks the β1 laminin chain is present in the smooth muscle (***sm***) but absent from the but absent from the vascular smooth muscle (***vsm***) of the inner myometrium. **(C)** In the inner myometrium the β2 laminin chain is present in the vascular smooth muscle (***vsm***) but is weakly expressed in the smooth muscle (***sm***), after exposure for 10 weeks. **(D)** After exposure for 36 weeks, the γ1 laminin chain is present in the smooth muscle (***sm***), vascular smooth muscle (***vsm***) of the inner myometrium but absent from the peri-arteriolar stroma. **(E)** Collagen IV is present in the smooth muscle (***sm***), vascular smooth muscle (***vsm***) and stroma surrounding the blood vessels, after exposure for 9 months. Scale bars = 200μm.

Plate.11*:** There was no difference before or after treatment with the LNG-IUS in the distribution of the α2, β1, β2 and γ1 laminin chains and collagen IV in the outer myometrium. **(A)** In the outer myometrium the α2 laminin chain is present in the smooth muscle (sm***) but absent from the vascular smooth muscle (***vsm***), following 36 weeks of exposure. **(B)** In the outer myometrium the β1 laminin chain is present in the smooth muscle (***sm***), endothelium of the blood vessels (***en***) but absent from the vascular smooth muscle (***vsm***) of the outer myometirum, after 10 weeks of exposure. **(C)** The β2 laminin chain is present in the smooth muscle (***sm***) and vascular smooth muscle (***vsm***) of the outer myometrium but absent from the stroma surrounding the blood vessels, after 36 weeks of exposure. **(D)** In the outer myometrium the γ1 laminin chain is present in the smooth muscle (***sm***) and vascular smooth muscle (***vsm***) but absent from the peri-arteriolar stroma, after 10 weeks of exposure. **(E)** Collagen IV is present in the smooth muscle (***sm***) and vascular smooth muscle (***vsm)*** of the outer myometrium. It is also present in the stroma surrounding the blood vessels, of the same specimen as **(D)**. Scale bars = 200μm.

Plate.12: Distribution of the β1 and β2 laminin chains and collagen IV in endometrial sections from specimen exposed to intrauterine levonorgestrel for a period of 9 months

β1 laminin chain *γ1 laminin chain* *Collagen IV*

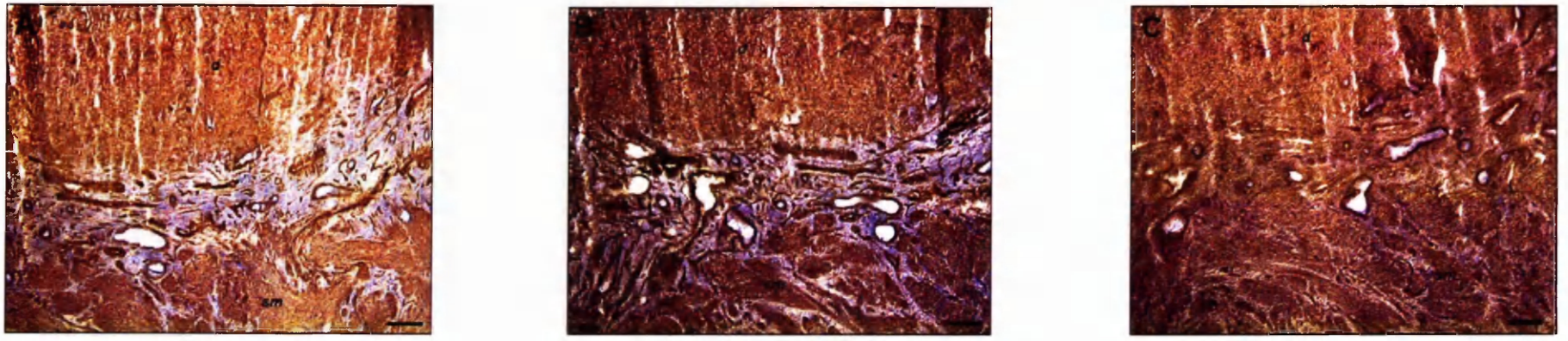

Plate.12: No differences were observed in the distribution of the β1 and γ1 laminin chains and collagen IV in the endometrium of a specimen exposed to exogenous levonorgestrel. (**A-C**) In the more superficially decidualised areas (***d***) of three consecutive sections the β1, γ1 laminin chains and collagen IV are widely distributed, after 9 months of exposure. (**A**) The β1 laminin chain is present in the glandular basement membrane and vascular smooth muscle but is less widely distributed in the non-decidualised basal portion of the endometrial stroma, after 9 months of exposure. The β1 laminin chain is also present in the smooth muscle (***sm***) of the subendometrial myometrium. (**B**) The γ1 laminin chain is present in the glandular basement membrane and vascular smooth muscle but absent from the endometrial stroma. The γ1 laminin is also present in the smooth muscle (***sm***) of the subendometrial myometrium. (C) Collagen IV is expressed in the glandular basement membrane, vascular smooth muscle and endometrial stroma as well as in the smooth muscle (***sm***) of the subendometrial myometrium. Scale bars = 200μm.

3.1.3 *Quantitative analysis of the β2 laminin chain and collagen IV distribution in the myometrium*

Qualitative analysis of the human myometrium revealed layering only in the distribution of the β2 laminin chain. The remaining α2, β1, γ1 laminin chains and collagen IV showed a uniform distribution throughout the smooth muscle of the myometrium. A quantitative examination was undertaken to support the qualitative observations. Line profiles for the intensity of the β2 laminin chain and collagen IV where obtained from twelve higher quality full (1 menstrual, 2 secretory, 1 Mirena®) (***Plate.13A-D***) and partial (1 menstrual, 3 proliferative, 1 secretory, 3 Mirena®) (***Plate.14A-D***) myometrial thickness specimens, where the β2 laminin chain and collagen IV had been immunolocalised without Haematoxylin counterstaining.

All plots (***Plate.13A,C;Plate.14A;Appendix.4A,C,E,G,I,K,M,O***) with the exception of one (***Appendix.4L***) showed a steep increase in the myometrial distribution of the β2 laminin chain, from the inner towards the outer myometrium. The average of the inner part of these data sets (***Plate.13A,C;Plate.14.B***) clearly shows an outer plateau and a decrease in the intensity of the β2 laminin chain immuno-reaction towards the inner myometrium. There was no difference in the distribution of the β2 laminin chain either during the course of the menstrual cycle or after exposure to exogenous levonorgestrel (***Appendix.4***). By contrast, the myometrial distribution of collagen IV (***Plate.13B,D;Plate.14C;Appendix.4)*** was relatively invariant. The average of the truncated data sets (***Plate.14D***) was also relatively constant Line profiles for the myometrial distribution of collagen IV obtained, revealed a uniform distribution (***Appendix.4***).

The sectional thickness (inner myometrium) was calculated from both the individual and average data sets (***Plate.15A-F***). The width values range from 14.76-2.09mm and are shown to exhibit both intra and inter-patient variability (***Table.5***). The average sectional thickness of the inner myometrium was approximately 7-8mm, depending on the method of calculation used (***Table.5***).

Plate.13: Quantitative analysis of the β2 laminin chain and collagen IV distribution in two full thickness myometrial cryosections

Example.1 ***Example.2***

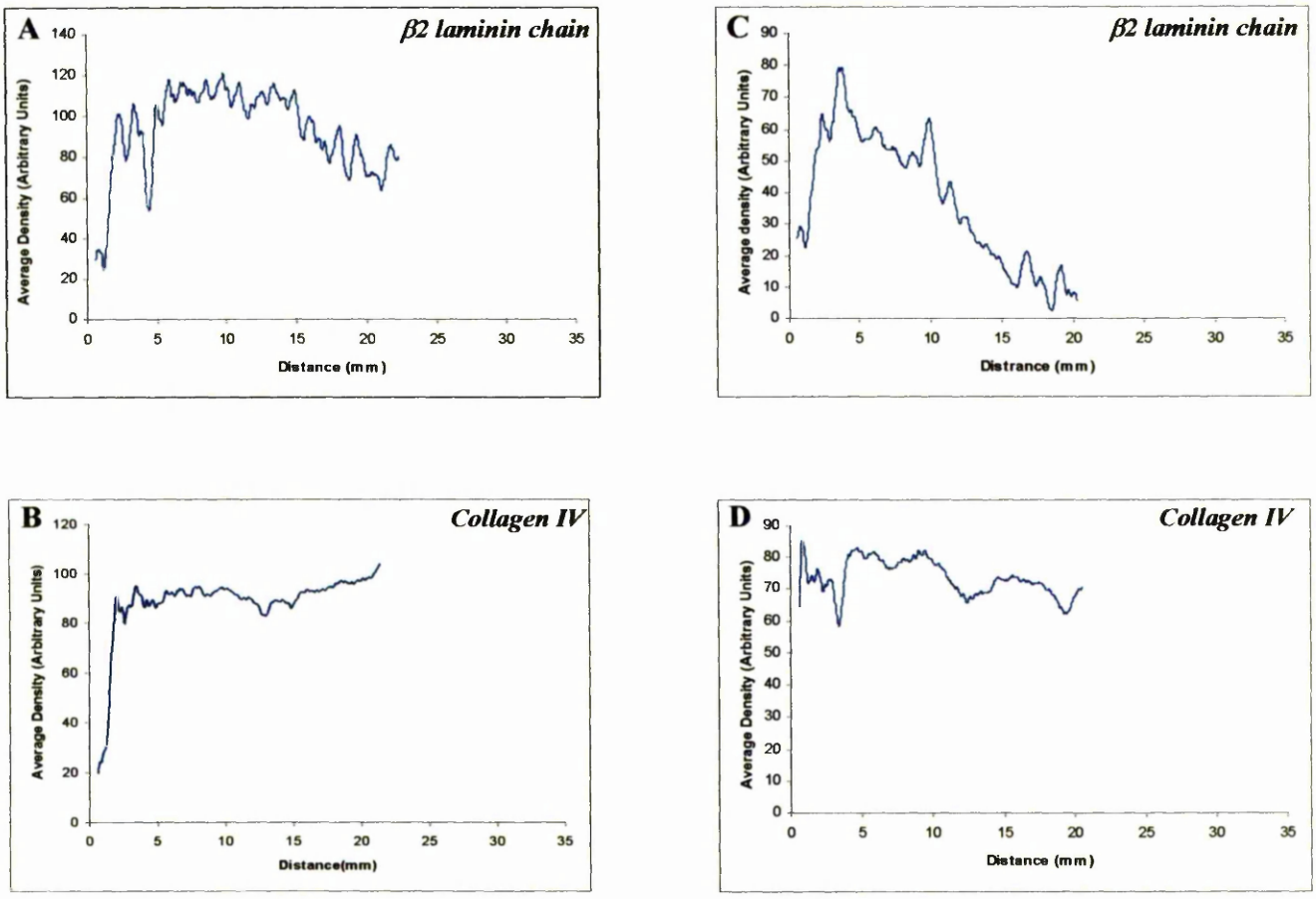

Plate.13: Line profiles for the intensity of β2 laminin chain and collagen IV from low magnification scans of full thickness myometrial sections. Two examples out of the four specimens used are shown. The others had a similar pattern. A gradient is observed in the myometrial distribution of the β2 laminin chain in contrast with the more uniform distribution of the γ1 laminin chain and collagen IV. No endometrial data are shown. (**A**) β2 laminin distribution in a menstrual phase specimen of 22 mm length. (**B**) collagen IV distribution in a consecutive section of 22 mm length. (**C**) β2 laminin distribution after 22 weeks of exposure to intrauterine levonorgestrel in a specimen of 20 mm length. (**D**) collagen IV distribution in a consecutive section of 21 mm length. The X-axis represents distance in mm and the Y-axis measures density in arbitrary units. The peaks are areas of high intensity staining.

Plate.14: Quantitative analysis of the β2 laminin chain and collagen IV myometrial distribution in cryosections

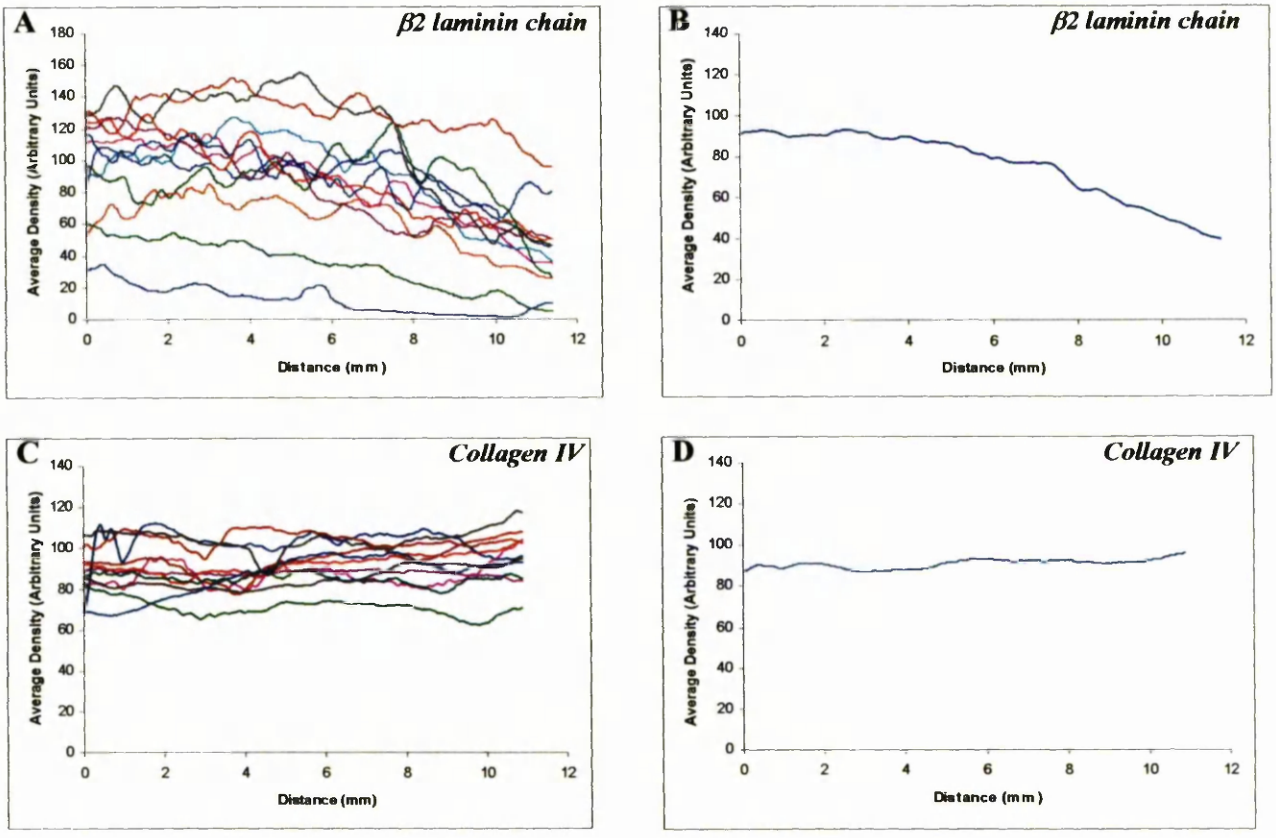

Plate.14: Line profiles for the intensity of the β2 laminin chain and collagen IV from low magnification scans. All data sets were aligned using the position of the endometrium/myometrium boundary and truncated at a length equal to the length of the shortest myometrial specimen (11.40mm for the β2 laminin chain data sets, 10.89mm for the collagen IV data sets), so that the average reflects all specimens. A gradient is observed in the myometrial distribution of the β2 laminin chain in contrast to the more uniform distribution of collagen IV. Endometrial data are shown in ***Appendix.4***. (**A**) β2 laminin chain myometrial distribution in 13 specimens (2 menstrual, 4 proliferative, 3 secretory, 4 exposed to intrauterine levonorgestrel for a period of 8 weeks to 9 months. (**B**) the average data set for the myometrial distribution of the β2 laminin chain from all specimens. (**C**) collagen IV myometrial distribution in 11 specimens (2 menstrual, 4 proliferative, 3 secretory, 2 exposed to intrauterine levonorgestrel for a period of 8 weeks and 9 months respectively. (**D**) the average data set for the myometrial distribution of collagen IV from all 11 specimens. The X-axis represents the distance in mm and the Y-axis measures density in arbitrary units. The coloured line in (**A**) and (**C**) represent the individual patients and bare no relation to the stage of the cycle.

Plate.15 (Plate.14 continued): Sectional thickness measurements in four cryosections with partial myometrial thickness

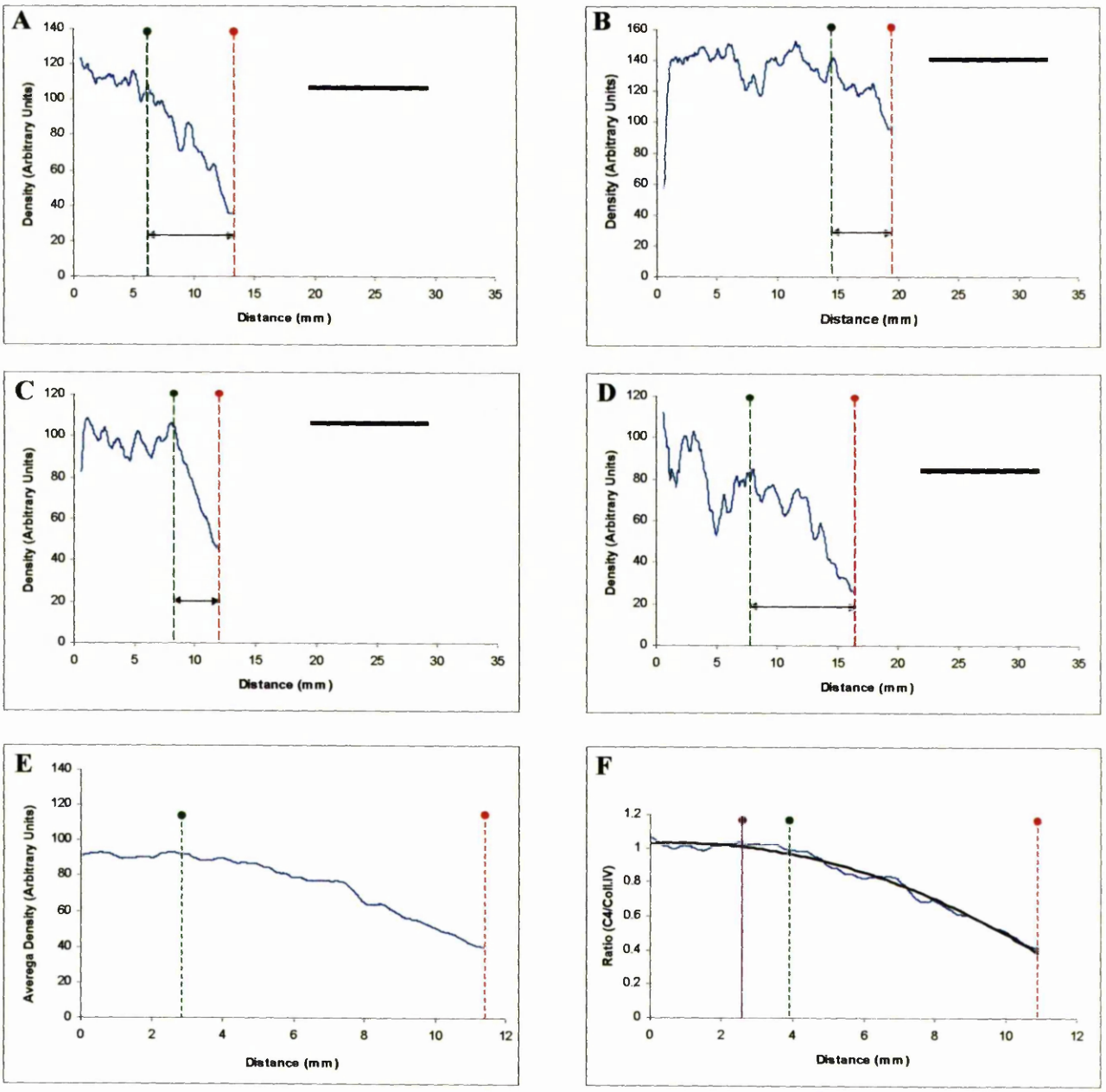

Plate.15*:** Objective methods were used to define the transition point between in the inner and outer myometrium. Data averaging techniques were used to define the point at which the intensity of the immuno-reaction started to decline, within the outer myometrium. For the non-truncated data sets (Plate.15A-D***), a region of the outer myometrium at least 1.25mm from the edge of the sections and approximately 7mm in length, was selected to represent the average density value of the outer myometrium. The average of the 7mm region is marked by the height of the thick horizontal line. However, for the average truncated data sets (***Plate.15E***) a region of approximately 3.5mm was selected. The ratio of the β2 laminin chain to collagen IV was also calculated and both a quadratic (R^2=98.5%) and a linear fit (not shown, R^2=90.3%) were applied. The point at which the continuous smoothed data set achieved the same value as the outer average, counting from the inner towards the outer myometrium, was define as the point at which the immuno-reaction intensity began to decline. (green dashed line). The distance (two sided arrows) between this point and the endometrial-myometrial junction (red dashed line) was defined as the sectional thickness of the inner myometrium. (**A**) a menstrual phase specimen of 13 mm length. (**B**) a proliferative phase specimen of 20 mm length. (**C**) a secretory phase specimen of 19 mm length. (**D**) a specimen of 16 mm length, exposed to intrauterine levonorgestrel for a period of 8 weeks. The purple line represents the maximum of the theoretical quadratic fit. The peaks are areas of high intensity of the β2 laminin chain antibody.

Measurement of layer data from full thickness averages

(**E**) the average data set for the β2 laminin chain myometrial distribution from all 13 specimen. (**F**) the ratio of the β2 laminin chain to collagen IV average myometrial distribution. The purple line represents the maximum of the theoretical quadratic fit. The peaks are areas of higher abundance of β2 laminin.

Table.5 Sectional thickness values of the inner layer in full thickness myometrial specimens

Patient Code	*Sectional thickness (mm)*	*Parity*	*Medication*	*State*
BMM29	*10.51*	*1+5*	*Nil*	*Decidualisation*
BMM33	*5.92*	*3+1*	*Mef.acid*	*Proliferative*
BMM34	*7.35*	*3+1*	*Nil*	*Menstrual*
BMM35	*4.82*	*3+1*	*Nil*	*Secretory*
BMM35(2)	*7.53*	*3+1*	*Nil*	*Secretory*
BMM47	*5.89*	*N/A*	*Nil*	*Inactive*
BMM49	*3.75*	*N/A*	*Nil*	*Proliferative*
BMM52	*2.09*	*1*	*FeS04*	*Proliferative*
BMM55	*8.59*	*2+0*	*Nil*	*Decidualisation*
BMM60	*7.78*	*2+0*	*Nil*	*Secretory*
BMM65	*11.09*	*2+1*	*Asthmatic*	*Decidualisation*
BMM68	*14.76*	*3+1*	*Nil*	*Weakly Prolif.*

Sectional thickness

Calculated from individual data sets

- Median (***Table.5***): 7.440mm
- Q1(quartile): 5.088
- Q3(quartile): 10.03

Calculated from the average data sets

- β2 laminin chain (***Plate.15E***): 8.46mm
- β2 laminin to collagen IV ratio (***Plate.15F***): 6.99mm
- Ratio value of the 99% of the maximum of the quadratic function (***Plate.15F***): 8.82mm

The blue text represents the sectional thickness in specimen after exposure to exogenous progestagen (Mirena®) for a period of 8 weeks to 9 months. BMM29 = 9 months of exposure, BMM55 = 8 weeks of exposure, BMM65 = 22 weeks of exposure, BMM68 = 9 weeks of exposure.

N/A: not available, **Mef.acid**: Mefanamic acid, **Weakly Prolif**: Weakly Proliferative, **n+n**: births+miscarriages.

3.1.4 *Reverse transcriptase-polymerase chain reaction (RT-PCR) for the detection of the β2 and γ1 laminin chain in the human myometrium*

Total RNA was extracted from 4 full thickness hysterectomy specimens. The endometrium was discarded and the remaining myometrium was divided into inner and outer. The integrity of the RNA was confirmed by the presence of intact 18S and 28S (ribosomal RNA) on the agarose gels in all but one of the samples.

The RT-PCR for the γ1 laminin chain gene amplified a major band consisted with the predicted product of 315base pairs (bp) (***Plate.16A,B***). A faint band of approximately 1000bp was observed in the outer, inner and total DNA of the second specimen (***Plate.16A***). The reverse transcribed mRNA free PCR water control was negative (***Plate.16A lane 8***).

For the β2 laminin chain gene the RT-PCR amplified a major band consistent with the predicted product of 305 bp (***Plate.16C,D***). No bands were observed for the fourth specimen total DNA (***Plate.16D, lanes1,2,3***). The reverse transcribed mRNA free PCR water control was negative (***Plate.16C lane 8; D lane 10***). The RT-PCR data show the presence of the γ1 and β2 laminin gene expression chains within the human myometrium, confirming the ICC results.

Plate.16: RT-PRC for γ1 and β2 laminin chains

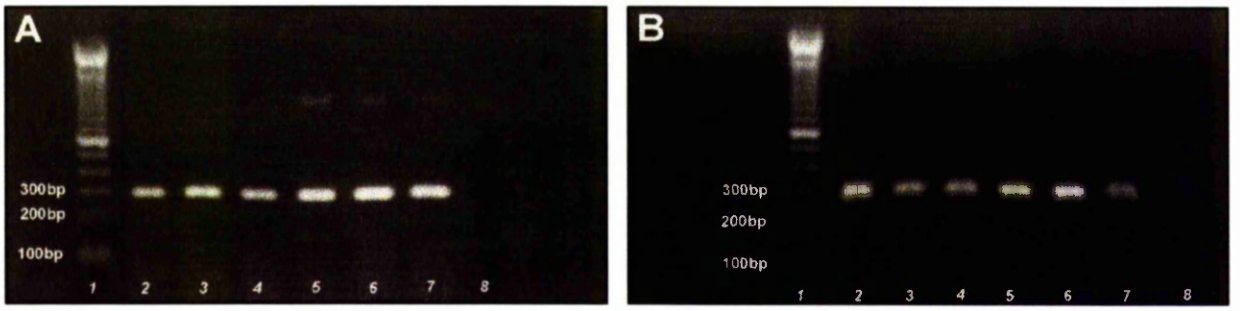

RT-PCR products of the γ1 **(A,B)** gene separated by 1% agarose gel electophoresis. The major product is close to the predicted size of 315bp

(A) Lane 1: DNA ladder
Lane 2: inner myometrium 1st specimen
Lane 3: outer myometrium 1st specimen
Lane 4: total myometrium 1st specimen
Lane 5: inner myometrium 2nd specimen
Lane 6: outer myometrium 2nd specimen
Lane 7: total myometrium 2nd specimen
Lane 8: water negative control

(B) Lane1: DNA ladder
Lane 2: total myometrium 4th specimen
Lane 3: outer myometrium 4th specimen
Lane 4: inner myometrium 4th specimen
Lane 5: total myometrium 3rd specimen
Lane 6: outer myometrium 3rd specimen
Lane 7: inner myometrium 3rd specimen
Lane 8: empty

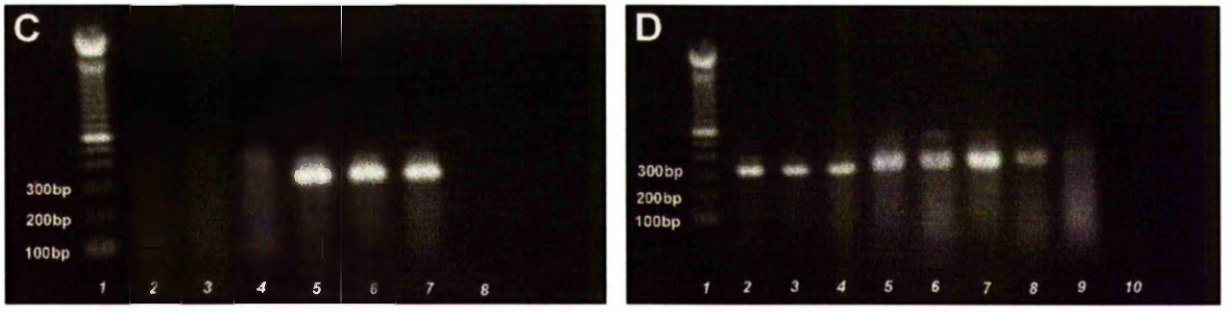

RT-PCR products of the β2 gene **(C,D)** separated by 1% agarose gel electrophoresis. The product is close to the predicted size of 305bp

(C) Lane 1: DNA ladder
Lane 2: inner myometrium 1st specimen
Lane 3: outer myometrium 1st specimen
Lane 4: total myometrium 1st specimen
Lane 5: inner myometrium 2nd specimen
Lane 6: outer myometrium 2nd specimen
Lane 7: total myometrium 2nd specimen
Lane 8: water negative control

(D) Lane 1: DNA ladder
Lane 2: inner myometrium 2nd specimen
Lane 3: outer myometrium 2nd specimen
Lane 4: total myometrium 2nd specimen*
Lane 5: outer myometrium 3rd specimen
Lane 6: total myometrium 3rd specimen
Lane 7: inner myometrium 4th specimen
Lane 8: outer myometrium 4th specimen
Lane 9: total myometrium 4th specimen
Lane 10: water negative control

* No inner myometrial sample was used for the 3rd specimen because no RNA was left.

3.2 Elastin expression in the human uterus

Elastin was immunolocalised in paraffin embedded sections (n=51) from all stages of the menstrual cycle (14 proliferative, 13 secretory, 7 menstrual, 1 inactive, 1 postmenopausal, 15 Mirena®). The duration of exposure to intrauterine levonorgestrel was 1-48 months.

3.2.1 *Elastin expression in the myometrium and endometrium of normal uteri*

Microscopic examination of sections where sufficient myometrial thickness was available for assessment (n=40, 12 proliferative, 10 secretory, 5 menstrual, 13 Mirena®), suggested a decreasing gradient in the distribution of elastin from the outer towards the outer myometrium (***Plate.17A,B,C***). The remaining 11, mainly inner myometrial sections (2 proliferative. 3 secretory, 2 menstrual, 1 inactive, 1 postmenopausal, 2 Mirena®) were only used for endometrial examination. In the smooth muscle of the inner myometrium of all 40 sections, elastin was absent (***Plate.18A***) or of low abundance (***Plate.18B***). The walls and internal elastic laminae of the myometrial arteries were however immunoreactive (***Plate.18A,B***) whereas elastin was absent from the thin walled vessels of the inner myometrium (***Plate.18B***). In the outer myometrium, of all 40 sections, elastin was present in the peri-vascular tissue particularly near the large vessels (***Plate.18C,D,E***). However elastin was absent from the thin walled vessels of the outer myometrium (***Plate.18D***). More peri-vascular and extra-vascular staining was present in the outer myometrium of all cases (***Plate.18E***). Elastin was also located in the smooth muscle of the outer myometrium (***Plate.18F***). Elastin deposition within the smooth muscle of the outer myometrium was neither peri-vascular nor associated with large vessels containing an obviously muscularised wall. No change was observed in the myometrial distribution of elastin during the course of the normal menstrual cycle.

Within the normal human endometrium (n=40) elastin was present in the basal portion of the spiral arterioles (***Plate.19A***) but was absent from the surface epithelium, glandular BM and stroma (***Plate.19B***). Elastin was also absent from thin walled vessels close to the surface epithelium (***Plate.19B***) and from spaces in the basalis assumed to be blood vessels (***Plate.19C***). Despite the absence of elastin in the stroma, 78% (95/122) of cross-sections of lymphoid aggregates had traces of elastin (***Plate.19D***). No difference was observed in the endometrial expression of elastin during the course of the normal menstrual cycle.

Consecutive paired sections (n=24, 2 proliferative, 2 secretory, 2 menstrual, 6 Mirena®) were stained with elastin (n=12) and with a vascular endothelium marker (CD31, n=12) to identify the nature of the presumed vascular spaces seen close to the surface epithelium and within the basalis. The sections were selected on the basis of good quality full thickness endometrium and myometrium being present.

In the inner myometrium small arterioles and thin walled vessels not expressing elastin (***Plate.20A***) were shown to express CD31 within their endothelium (***Plate.20B***). Elastin was absent from the microvessels of the inner myometrium (***Plate.20C***). However similar microvessels were shown to express CD31 in their endothelium (***Plate.20D***). Because of an abundance of elastin staining within the smooth muscle of the outer myometrium, it was difficult to define the wall of the vein and accurately state the presence or absence of elastin (***Plate.20E,G***). However, there seemed to be very little elastin associated with the veins of the outer myometrium (***Plate.20E,G***). The endothelium of the veins or lymphatic vessels present in the outer myometrium was shown to express CD31 (***Plate.20F,H***). Small and large arterioles with little elastin present in their walls (***Plate.20G***) were shown to express CD31 in their endothelium (***Plate.20H***).

Within the endometrium elastin was absent from the thin walled vessels and arterioles close to the surface epithelium (***Plate.21A***), whilst CD31 was expressed within their endothelium (***Plate.21B***). The spaces in the basalis assumed to be blood vessels (***Plate.21C,E***) were shown to express CD31 in their endothelium (***Plate.21D,F***). Elastin was also present in the walls of the basal portions of the spiral arterioles (***Plate.21G***) the endothelium of which was shown to express CD31(***Plate.21H***).

No staining was observed in the negative controls (not shown).

Plate.17: Distribution of elastin in uterine sections

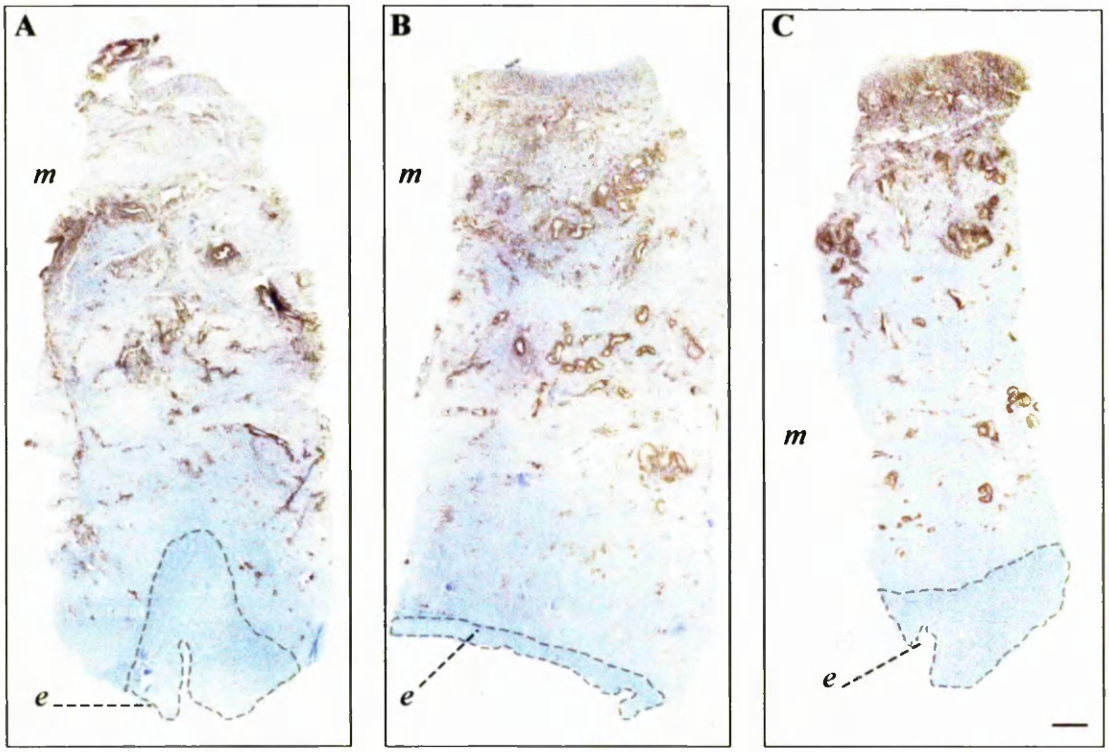

Plate.17: Low magnification scanned images of full thickness endometrial and myometrial paraffin embedded sections. (***A***) secretory (**B**) menstrual (**C**) secretory phase specimens in which elastin has been immunolocalised. The blue colour is haematoxylin staining of the nuclei. The area enclosed with the dotted line represents the endometrium (***e***). There is a gradient in the distribution of elastin within the myometrium (***m***) in each section (**A,B,C**) as determined by inspection of the scanned images and direct microscopic examination of the sections. Elastin is present within the basal portion of the endometrial spiral arterioles but is only visible on the scan when examined at a high magnification. Scale bar = 5mm.

Plate.18 : Elastin distribution in the human myometrium

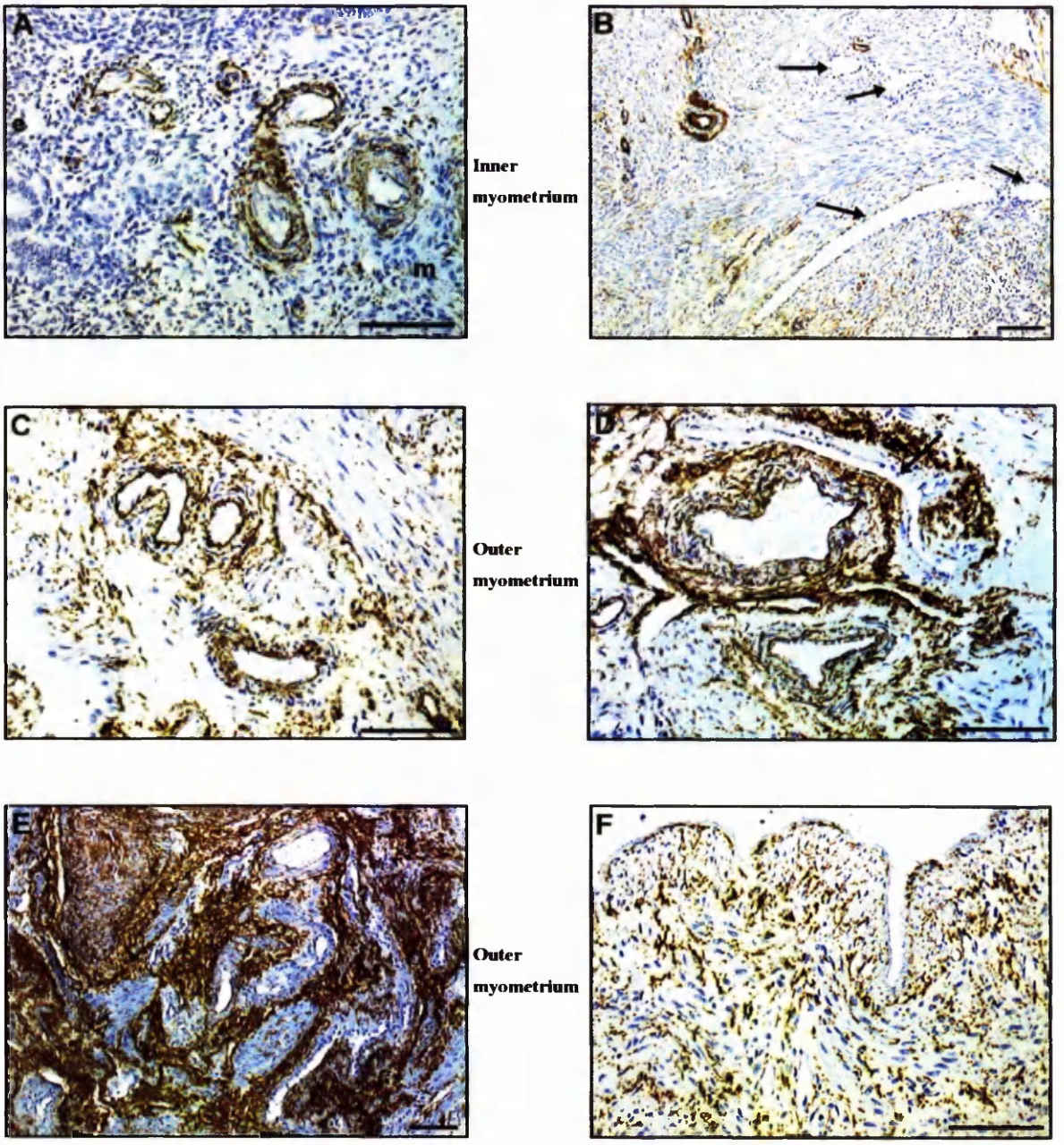

***Plate.18*: (A,B)** Elastin is present within the arteriolar walls but absent or of low abundance in the smooth muscle of the inner myometrium (**m**) close to the endometrium (**e**). (**B**) Elastin is absent from the thin walled vessels in the endometrium (arrows). (**C,D**) Elastin is present in the wall of arteries found in the outer myometrium but absent from the veins (arrows). (**E**) Elastin is widely distributed in areas of the outer myometrium with a high density of large vessel cross-sections. (**F**) Elastin is present in the smooth muscle in areas of the outer myometrium close to the serosa. The reaction product is not associated with blood vessels. This is in contrast to the distribution seen within the smooth muscle of the inner myometrium (**B**). Scale bars =100μm.

Plate.19: Elastin distribution in the human endometrium

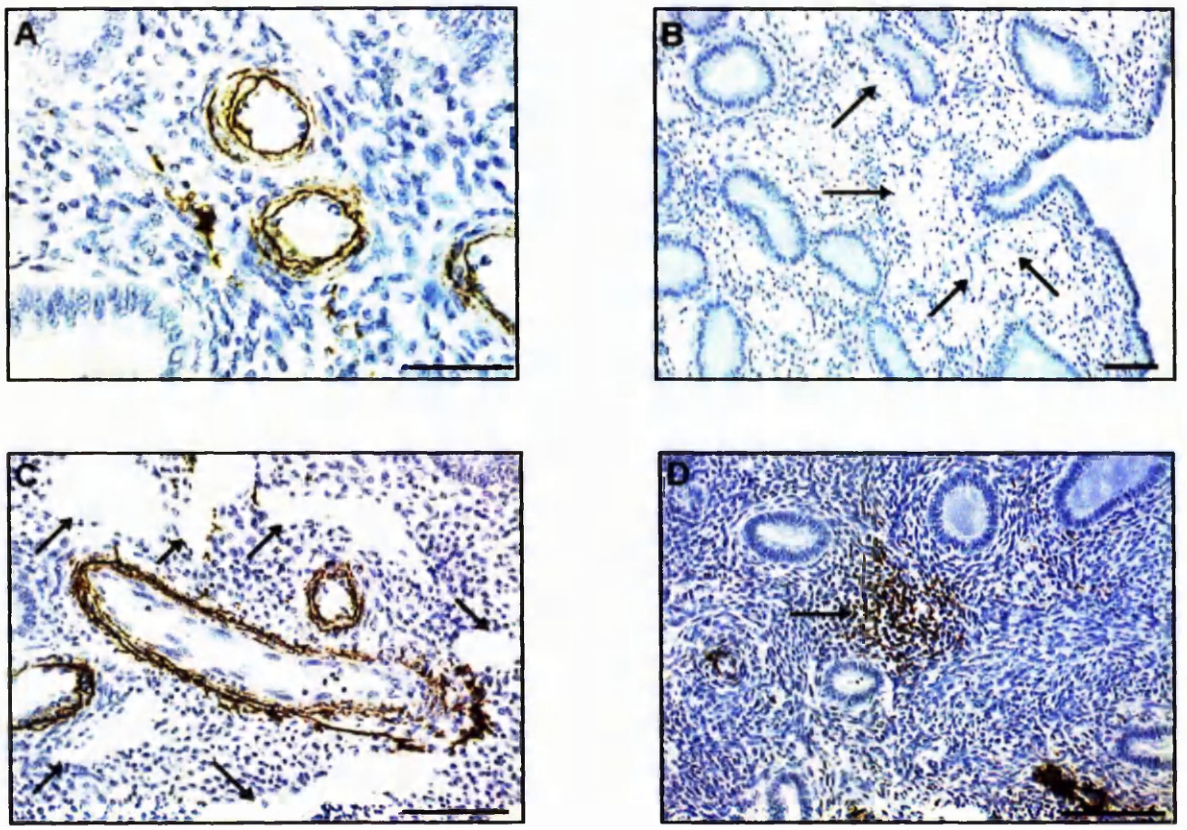

Plate.19*: (A)** Elastic laminae are present in the basal portions of the spiral arterioles, in an early secretory phase specimen. **(B)** Elastin is absent from the blood vessels (arrows) close to the surface epithelium in an early secretory specimen. **(C)** Elastin is expressed in endometrial arterioles but absent from spaces assumed to be veins or lymphatic vessels (arrows) (see ***Plate.21C,E), in an early secretory specimen. **(D)** Traces of elastin were observed in the majority of cross sections of lymphoid aggregates throughout the menstrual cycle. The example shown (arrow) represents a cross-section with the elastin distribution greater than average. Scale bars = 100μm.

Plate.20: Elastin and CD31 expression in blood vessels of the myometrium in consecutive sections

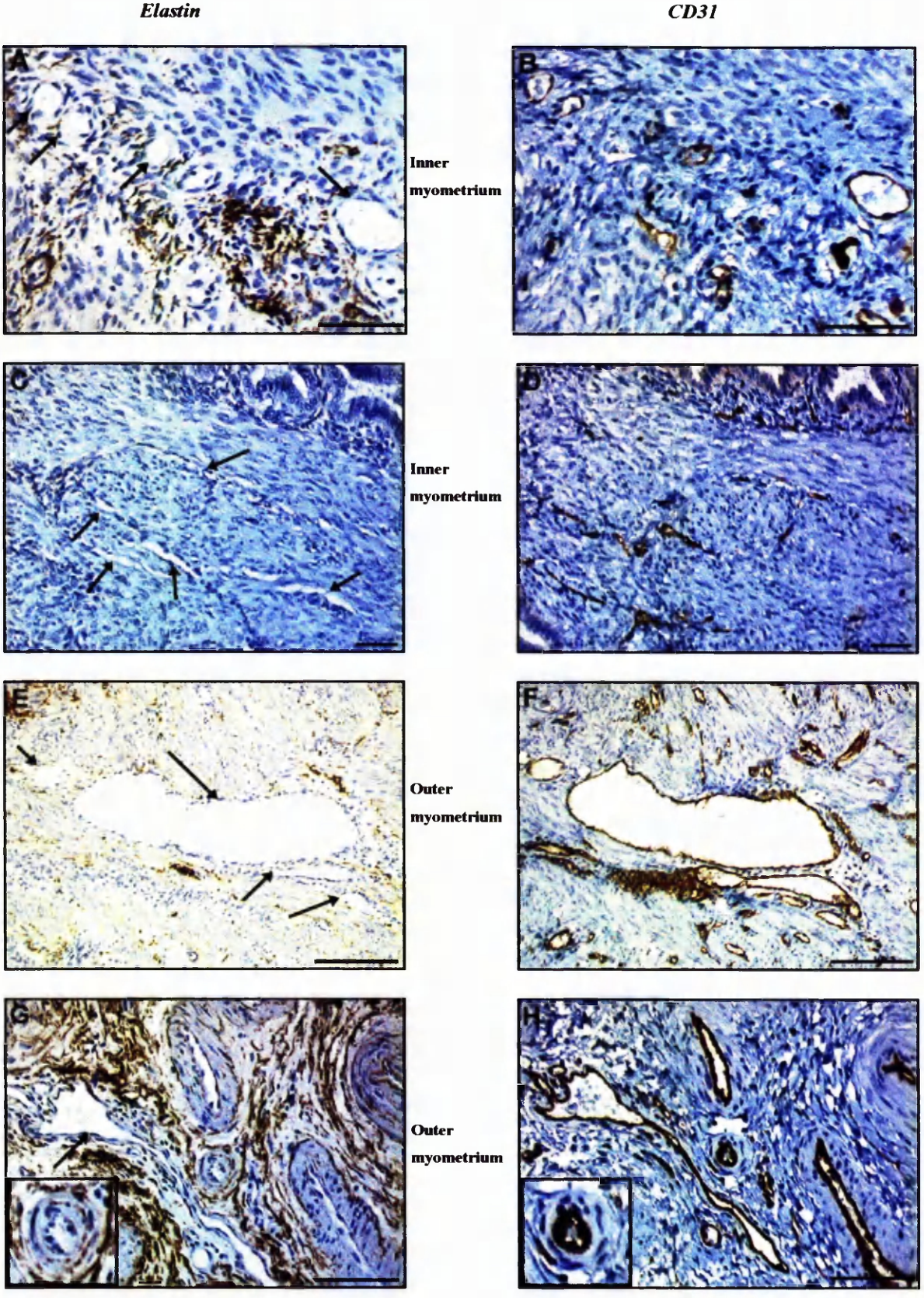

Plate.21: Elastin and CD31 expression in blood vessel of the endometrium in consecutive sections

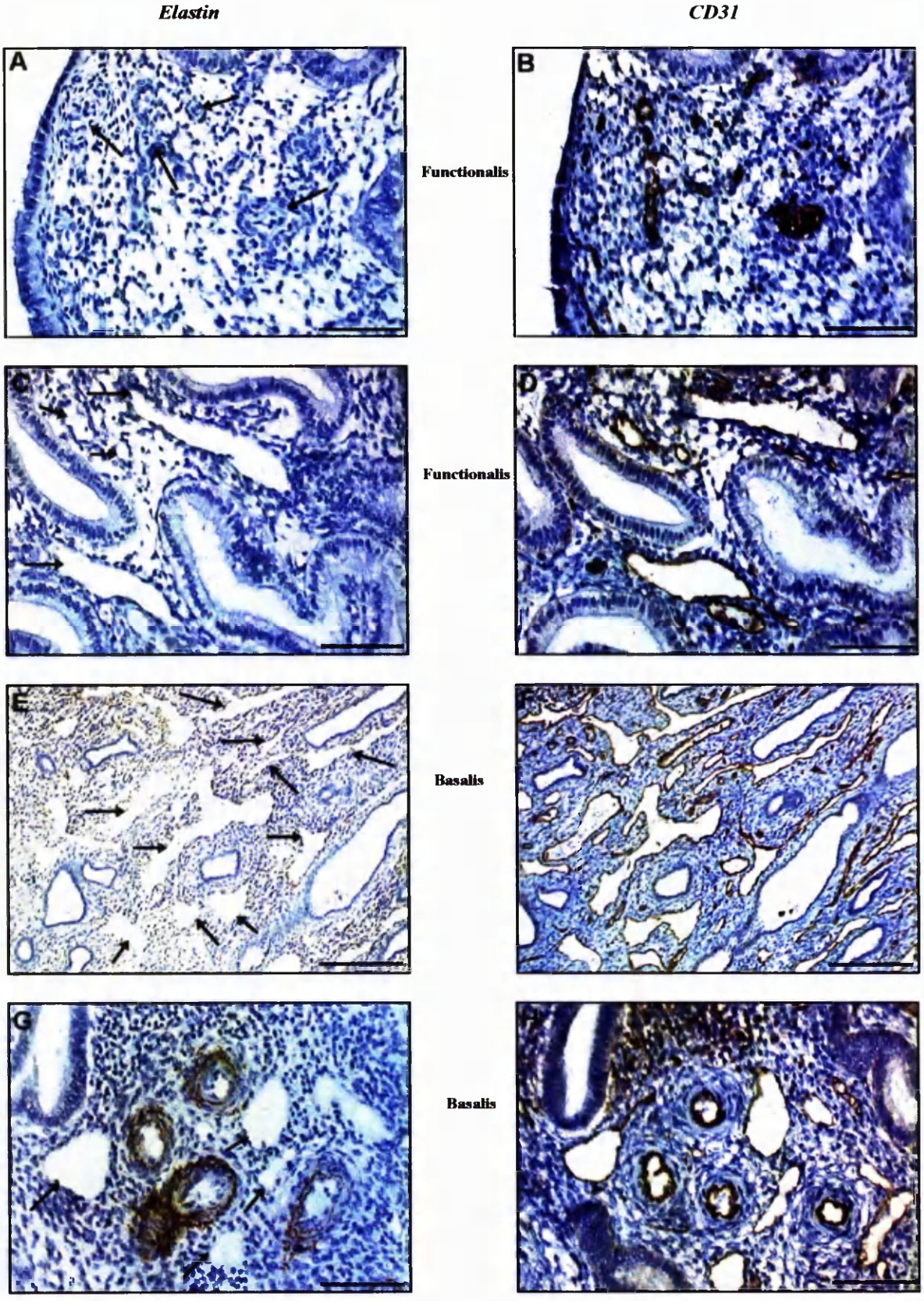

***Plate.20*:** (A) Elastin is weakly distributed within the smooth muscle of the inner myometrium but is absent from the small thin walled vessels (arrow) on the right hand side. Restricted expression of elastin is observed in or near the small arterioles (arrows) of the inner myometrium. **(B)** A consecutive section showing localization of CD31 in the endothelium of the small vessels of the inner myometrium. **(C)** Elastin is absent from vessels (arrows) in the inner myometrium and surrounding smooth muscle. **(D)** The endothelium of similar vessels as those visible in **(C)** is shown to express CD31 in a consecutive section. **(E)** In the outer myometrium elastin is present in the smooth muscle but absent from spaces assumed to be veins (arrows). **(F)** In a consecutive section the spaces seen in **(E)** are lined with CD31 immunopositive endothelium. **(G)** The veins (arrows) of the outer myometrium do not express elastin whereas elastin is present in the internal elastic laminae, walls of the large arterioles and peri-vascular tissue. Restricted expression of elastin is illustrated in the walls of a small arteriole shown in the insert. **(H)** A consecutive section showing CD31 localization in the endothelium of the veins and arteries of the outer myometrium. The insert shows a higher magnification image of the small artery seen in **(H)**. Scale bars = 100μm.

***Plate.21*:** (A) Blood vessels (arrows) close to the surface epithelium do not express elastin. **(B)** In a consecutive section, the endothelial lining of the blood vessels seen in A is shown by CD31 immunolocalization. **(C)** Spaces (arrows) assumed to be veins do not express elastin. **(D)** A consecutive section confirming the vascular nature of the spaces seen in **(C)** by CD31 immunolocalization. **(E)** Elastin is absent from veins in the basal part of the endometrium. **(F)** The endothelium of veins is shown to express CD31. **(G)** Elastin is expressed in the basal portion of the endometrial arterioles seen in this specimen but is absent from veins (arrows). **(H)** A consecutive section showing the endothelium of veins and arterioles by CD31 immunolocalization. Scale bars = 100μm.

3.2.2 *Elastin expression in the myometrium and endometrium of uteri exposed to intrauterine levonorgestrel (Mirena®).*

After exposure to intrauterine levonorgestrel (Mirena®), there was no detectable difference in the myometrial expression of elastin. Within the endometrium (n=13) elastin remained in the basal portion of the spiral arterioles (***Plate.22A***). In one endometrial section although there was elastin present within some spiral arterioles, there were other in which elastin was absent (***Plate.22B***). In 9 out of 12 sections elastin was absent from the stroma of the basalis (***Plate.22A,B***). In the remaining 3 sections elastin was widely distributed within the basal stroma (***Plate.22C***). Elastin was absent from the surface epithelium, glandular BM, thin walled blood vessels and highly decidualised areas (***Plate.22D***). Staining was absent from the negative controls (not shown).

3.2.3 *Orcein staining for elastin detection in the human uterus*

Additional sections (n=26) from all phases of the menstrual cycle (7 proliferative, 6 secretory, 4 menstrual, 1 inactive, 1 postmenopausal) and 7 sections exposed to exogenous progestagen (Mirena®) were stained with orcein. The intensely stained areas within the walls spiral arterioles of the endometrium (***Plate.23A***), and the large and small arteries of the inner and outer myometrium (***Plate.23B,C***) resembled the pattern of elastin immunolocalisation. Nuclei, glandular secretion and red blood cells were also stained (***Plate.23A***) as orcein staining is not selective for the elastic fibre system. Nevertheless orcein stains the elastic components more intensely (***Plate.23D,E,F***). The negative controls (not shown) exhibited no staining

3.2.4 *Quantitative analysis of the distribution of elastin in myometrial sections*

Full thickness sections (n=11), where elastin was immunolocalised without Haematoxylin counterstaining were scanned and then the blue channel was selected converting the color image to a monochrome one. Quantitative examination of the myometrial distribution of elastin in all 11 full thickness sections (1 proliferative, 4 secretory, 2 menstrual, 4 Mirena®) supported the existence of a gradient previously qualitatively observed. However, considerable variability was observed between sections (***Plate.24A-K***). As this analysis was performed on a limited (11/40) set of sections, it was not possible to judge whether the myometrial distribution of elastin was affected by the stage of the menstrual cycle.

A gradient in the myometrial distribution of elastin was observed when the data sets were aligned using the position of the outer myometrium (***Plate.25A***). The outer myometrium is shown to be more elastic than the inner myometrium. However, the analysis was restricted to the outer myometrium. In the second method when the data were normalised by width (***Plate.25B***) a decreasing gradient, from the outer towards the inner myometrium, was observed in the

distribution of elastin. For the second method the analysis was not restricted by the myometrial length and the values from the inner myometrium were included. For both data sets a linear rather than a quadratic fit was statistically justified.

Plate.22: Distribution of elastin in the endometrium of specimens exposed to exogenous levonorgestrel (Mirena®) over a period of 1 month to 3 years

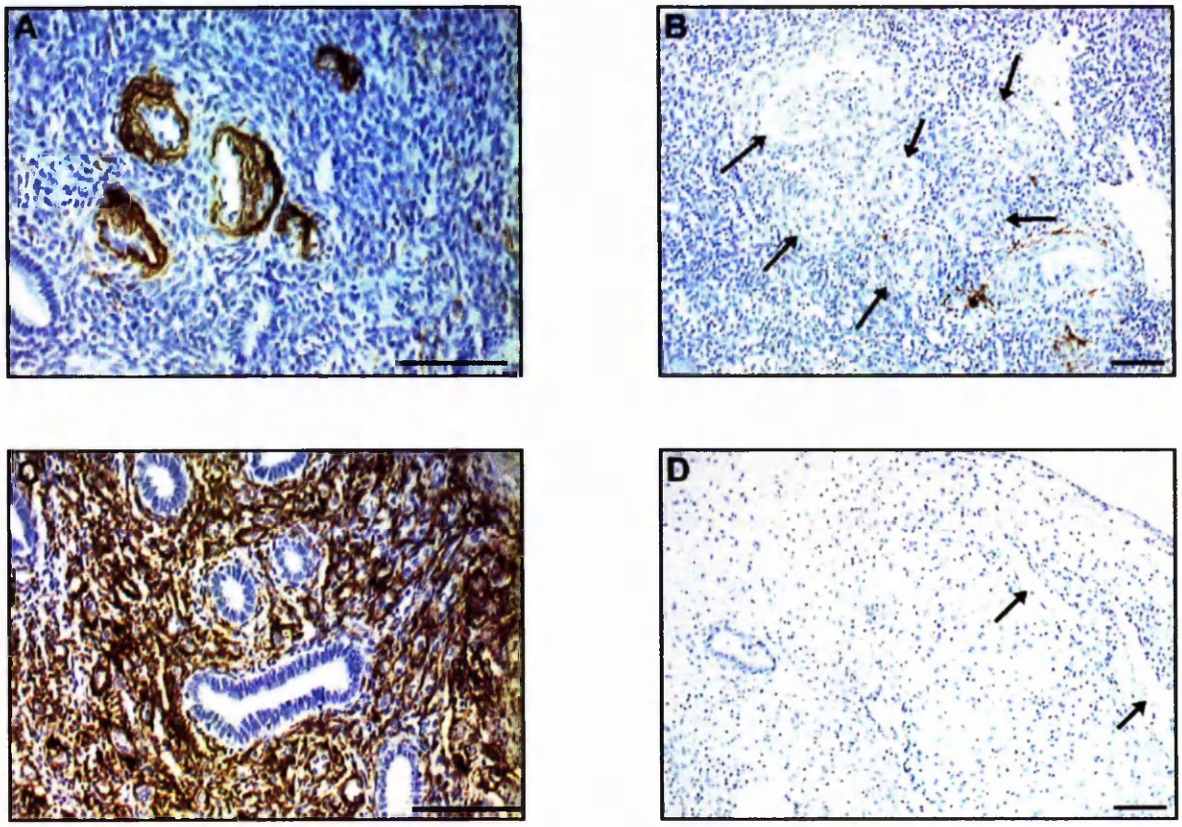

Plate.22*: (A)** Elastin is present in the basal portions of the spiral arterioles but absent from the endometrial stroma after 4 weeks of exposure. **(B)** Elastin is absent from spiral arterioles (arrows) in another region of the same section. This was not observed in tissue obtained from untreated patients (see ***Plate.19). **(C)** Elastin is present in the basal stroma after 10 weeks of exposure. Only 1 out of 2 specimens after this time of exposure displayed this pattern. **(D)** The superficial stroma of this 3-year-treated specimen lacks elastin. The blood vessels (arrows) close to the surface epithelium do not express elastin. Elastin is absent from highly decidualised areas of stroma. Scale bars =100μm.

Plate.23: Orcein staining in uterine paraffin embedded sections

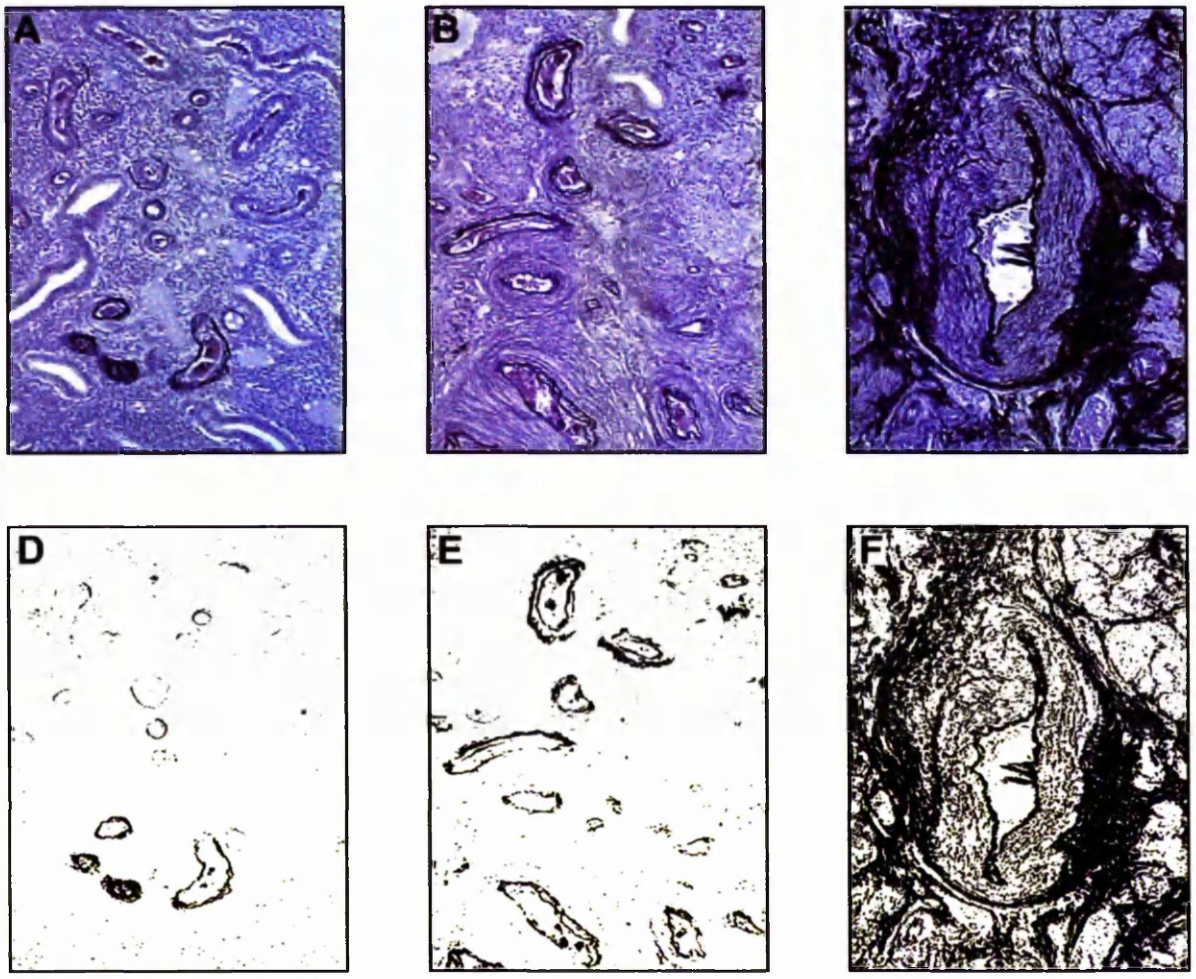

***Plate.23*: (A-C)** Orcein staining of endometrium and myometrium. **(D-F)** Binary images showing corresponding areas of high intensity. **(A)** Orcein stains the endometrial spiral arterioles. **(B)** Arteries in the inner myometrium stained with orcein. **(C)** Intense staining is present in the internal elastic laminae, the vessels walls and the adjoining peri-vascular tissue and smooth muscle of the outer myometrium. Scale bar =100μm.

Plate.24 : Quantitative analysis of elastin distribution in eleven full thickness endometrial and myometrial paraffin embedded sections, for the distribution of elastin within the uterus

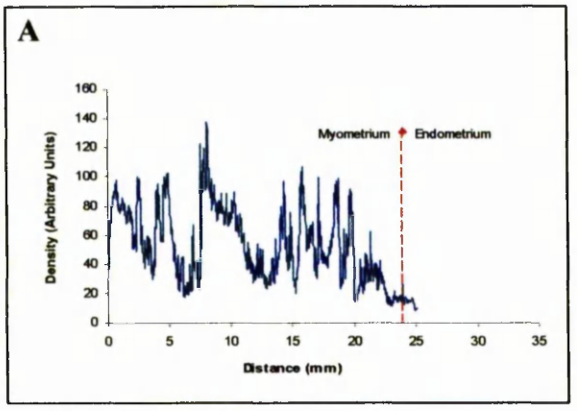

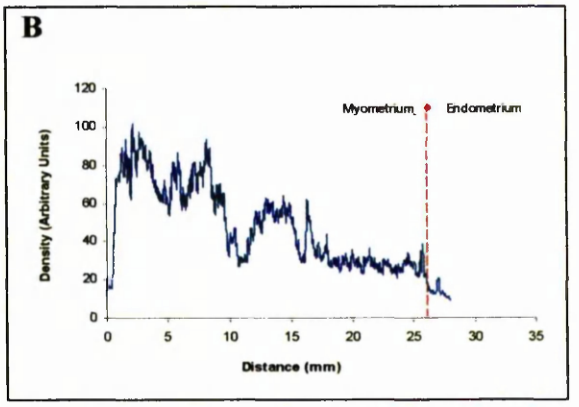

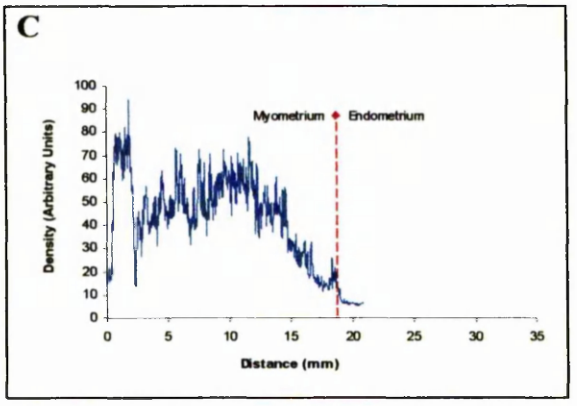

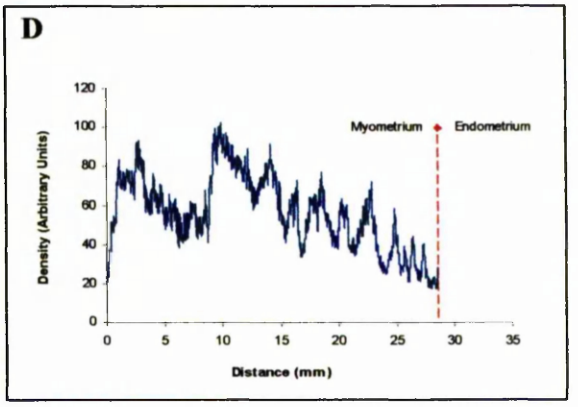

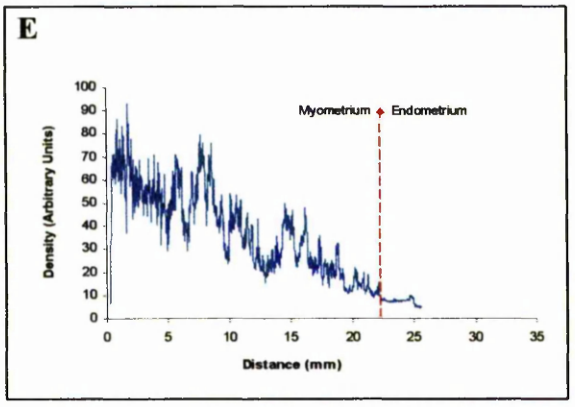

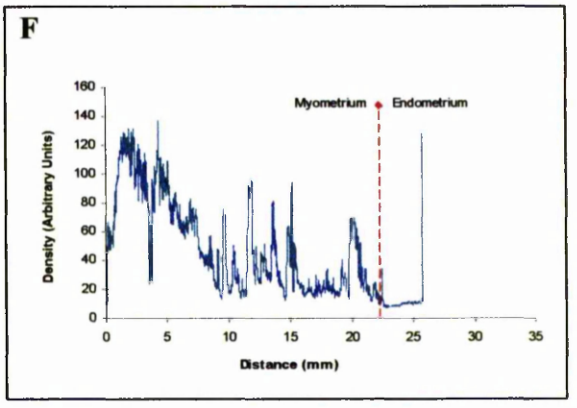

Plate.24 (continued)

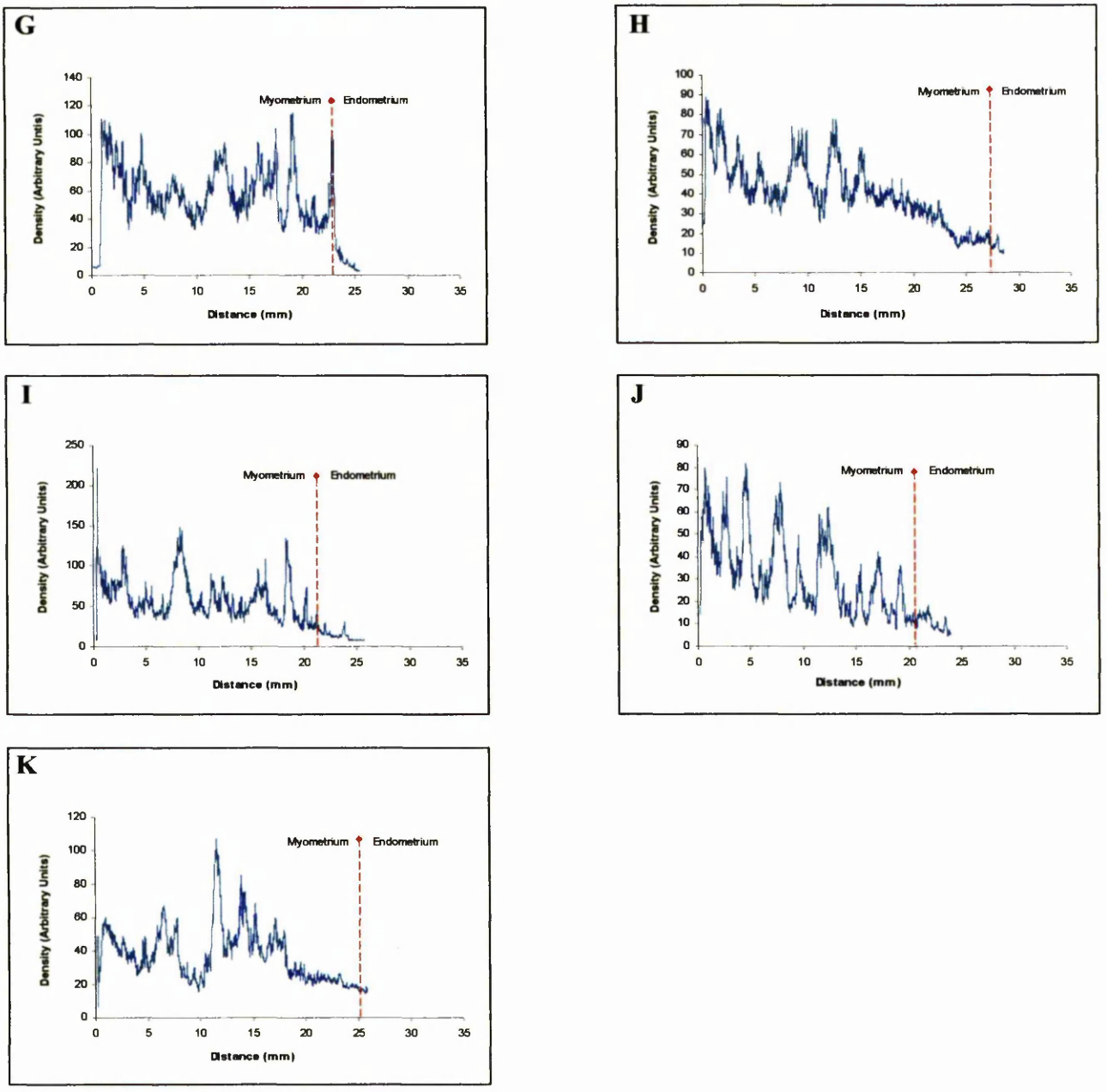

***Plate.24*:** Line profiles for the intensity of elastin staining obtained from 11 low magnification scans of full thickness myometrial and endometrial sections. Elastin distribution in **(A)** a menstrual phase specimen of 25 mm length, **(B)** a menstrual phase specimen of 28 mm length, **(C)** a proliferative phase specimen of 21 mm length, **(D)** an early secretory phase specimen of 28 mm length, **(E)** an early secretory phase specimen of 25 mm length, **(F)** a secretory phase specimen of 25 mm length **(G)** a secretory phase specimen of 25 mm length **(H)** a specimen of 29 mm length after exposure to exogenous levonorgestrel (LNG) for 10 months, **(I)** a specimen of 24 mm length after exposure to exogenous LNG for 10 weeks **(J)** a specimen of 26 mm length after exposure to exogenous LNG for 9 weeks, **(K)** a specimen of 26 mm length after exposure to exogenous LNG for 6 weeks. A decrease in the underlying trend, from the outer towards the inner myometrium, is apparent in most sections. There is nevertheless variability between patients. The X axis represents the distance in mm and the Y axis measures inverted brightness in arbitrary gray level units (0-255). The dashed red line marks the boundary between the endometrium and myometrium. The peaks in the myometrium are areas of intense elastin staining associated with blood vessels and peri-vascular tissue. The peaks in the endometrium represent spiral arterioles stained with elastin.

Plate.25: Average elastin distribution within the human myometrium

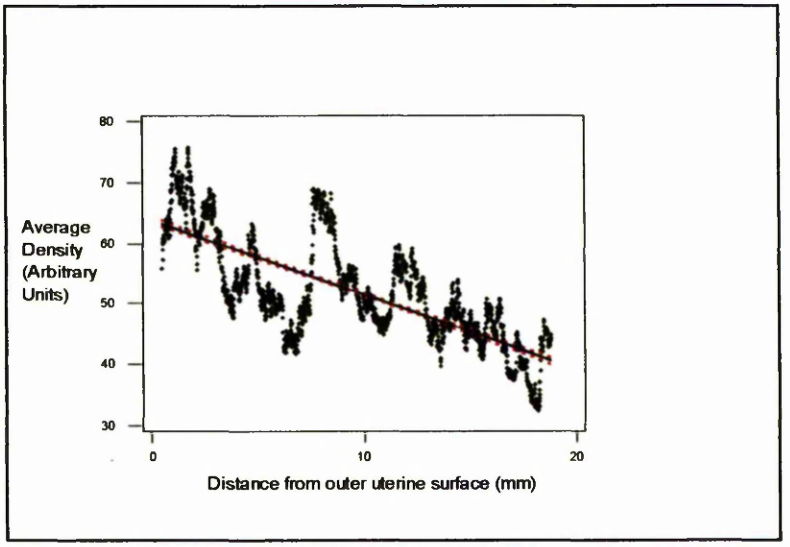

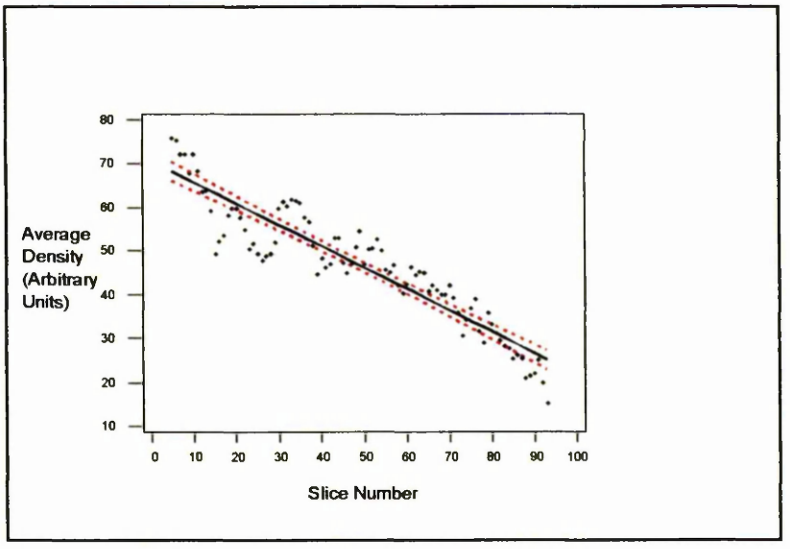

***Plate.25*:** When two methods (**A,B**) were used to average the data from the eleven data set a decrease in the distribution of elastin, from outer towards inner myometrium. (**A**) The data sets were aligned using the position of the outer myometrium and truncated at the length equivalent to the shortest myometrial length (18.8mm). This restricts the analysis to the outer myometrium. Only a linear fit to the data set was statistically justified. The X axis represent distance in mm and the Y axis represents the average density values in arbitrary units. Pearson correlation = -0.740, R^2= 54.7%, P=0.000. The red dotted lines represent the 95% confidence interval. (**B**) A second method was devised in which the complete data set could be used. This permitted the analysis of the inner myometrium and was not restricted by myometrial length. Each specimen was divided into an equal number of slices (n=93). The average for all slices was computed. The data represent the average of approximately 30,000 density values. The X axis represents the slice number and the Y axis represent the average elastin density values in arbitrary units. Pearson correlation = -0.925, R^2= 85.6%, P=0.000. The red dotted lines represent the 95% confidence interval.

Chapter.4 Discussion

4.1 Distribution of the α2, β1, β2, γ1 laminin chains and collagen IV within the human uterus

Low magnification scanned images of frozen sections revealed the presence of a gradient in the myometrial distribution of the β2 laminin chain, whereas the remaining laminin chains (α2, β1, γ1) and collagen IV exhibited a more uniform myometrial distribution. Immunostaining with the β2 laminin chain was weak in the inner myometrium compared to the more intense staining of the outer myometrium.

It was postulated that the observed gradient in the myometrial distribution of the β2 laminin chain provides additional evidence for myometrial layering. So far there are three lines of evidence of myometrial layering MRI, transvaginal ultrasound and histology. Uterine zonal anatomy of women of reproductive age, as visualised on T2-weighted MR images consists of a high-signal-intensity endometrial strip, a subjacent low-signal-intensity junctional zone and a medium-signal-intensity outer myometrium. The low-signal-intensity inner myometrium seen in MRI possibly correlates with the area of the myometrium where weak staining of the β2 laminin chain is observed.

The gradient observed in the myometrial distribution of the β2 laminin chain suggests that the composition of the basement membrane surrounding the myometrial smooth muscle cells varies between inner and outer myometrium. This difference might serve to restrict trophoblast invasion to superficial myometrium overlying the placental bed, or affect the contractile properties of the muscle. This is further discussed below.

McCarthy *et al.* (1989), in an MRI study examining the water content and relaxation properties of the human uterus, also examined the myometrial distribution of laminin and collagen. It was reported that the amount of collagen did differ between the junctional zone and the adjacent myometrium (McCarthy *et al.*, 1989), which is in accordance to the results of this study although it is not stated which type of collagen they were investigating. The same authors also reported that there was no change in the myometrial distribution of laminin. However, once again it was not stated which laminin type was investigated or which chains were used, so no direct comparison could be made with the findings of this study. It is possible that there was no chain specificity of the probes, therefore the authors may have been unable to detect any differences.

Another MRI study, looking for a correlation of MRI and histologic examination of hysterectomy specimens, reported a normal distribution, between the junctional zone and outer myometrium, of collagen IV and laminin (Scoutt *et al.*, 1991). The collagen IV findings are

consistent with the findings of this study. Therefore, a direct comparison between the Scoutt *et al*, (1991) study and this study could not be made on the laminin findings.

In both the studies (McCarthy *et al.,* 1989; Scoutt *et al.*, 1991), no observation about the distribution of collagen and laminin in other cellular compartments, besides the smooth muscle, were not made, possibly because the investigators were only interested in the smooth muscle myometrial distribution of collagen and laminin.

Microscopic images allowed a more detailed examination of the α2, β1, β2, γ1 laminin chains and collagen IV distribution within the human myometrium. Both the γ1 laminin chain and collagen IV were found to be present in smooth muscle, vascular smooth muscle and endothelium. The α2 and β1 laminin chains were present myometrial smooth muscle but absent from the vascular smooth muscle suggesting that there is a phenotypic difference between the VSM and SMC hence a possible functional difference. It is postulated that the mechanical properties of the BM of the VSM maybe different and directly affect the SMC, however at present there is no literature to support this postulation. As well as the postulated phenotypic difference between the VSM and SMC it has been shown that there is tissue specificity of laminin expression.

It has been clear for years that the ECM plays a role in regulating the differentiated phenotype of cells (Watt, 1986). But the mechanisms involved remained largely a mystery until cell-binding on individual ECM glycoproteins and specific ECM receptors were identified (Adams *et al.*, 1993). There are at least three mechanisms by which the ECM can regulate cells behaviour.

One is through the composition of the extracellular matrix. There are several sources of ECM variation one being the diversity in the composition of the ECM in different tissues and at different stages of development arises not only through expression of different matrix molecules but also from the existence of multiple forms of individual molecules (Adams *et al.*, 1993). Different laminin heterotrimers differ in their diversity towards specific cell types (Hunter *et al.*, 1992). Additionally the composition of the ECM is not static, and changing patterns of expression of individual components are observed during development (Leivo & Engvall, 1988; Sanes *et al.*, 1990; Hunter *et al.*, 1992). The existence of these sources of variation makes it clear that, at a given time and place, the ECM has the potential to provide specific environmental information to cells.

The second mechanism by which the ECM can regulate cell behaviour is through synergistic interactions between growth factors and matrix molecules. One type of interaction is the binding of growth factors to the ECM, which affects the local availability and biological activity of growth factors (Adams *et al.*, 1993). The second type of interaction involves regulation of gene

expression and finally ECM molecules can themselves be mitogenic or can influence the responsiveness to growth factors. It is postulated that growth factors and the ECM proteins collaborate in creating distinct cellular environments that regulate proliferation and differentiation (Schofield, 1978).

The third and final mechanism by which the ECM can regulate cell behaviour is through the cell surface receptors that mediate adhesion to ECM components. There are two types of receptors, non-integrin receptors and the integrins (Adams *et al.*, 1993). The ligand specificity of certain integrins appears to be cell-type dependent, for example the α2β1 integrin acts as a collagen receptor in platelets but is a collagen and laminin receptor in endothelial cells (Hynes, 1992). It is possible that there could be a difference in the activation of the receptor thus maintaining or stabilising a different phenotype in muscle cells.

Within the human endometrium, collagen IV and the γ1 laminin chain were found in the glandular BM and endothelium. Collagen IV was also present within the endometrial stromal cells of the both the superficial and basal part. The α2 and β2 laminin chain were present only in the basal portion of the glandular BM and absent from the endometrial stromal cells. The absence of these two laminin chains from the superficial glandular BM, could be a genuine result thus suggesting a possible difference between basement membrane in basal and apical portions of the gland. The reasons for such a change are not defined. Nevertheless, care must be taken when interpreting results from the endometrium of frozen sections because of the relative poor condition. Howerver, these antibodies do not recognise antigens on paraffin embedded sections, ever after antigen retrieval (personal communication A.Young and Dr S.Campbell). The α2 laminin chain was absent from the endometrial blood vessels whereas the expression of the β2 laminin chain was variable. The variability observed in the expression of the β2 laminin chain could be due to the condition of the sections. Once again tissue specificity in laminin expression is exhibited.

The results of this study are in accordance with the preliminary results obtained within the same department (Campbell *et al.*, 1998, abstract). However, I would like to take this opportunity to correct a typing mistake. In the published abstract it was reported that the α2 laminin chain was present throughout the vascular smooth muscle, when it should have read that the β2 laminin chain was present in throughout the vascular smooth muscle.

In secretory sections ECM was deposited around the endometrial blood vessels, compared to the proliferative sections. This ECM deposition was more obvious around blood vessels of the superficial endometrium because of the less dense endometrial stroma. Faber *et al.* (1986), in a immunocytochemical study examining laminin production by human endometrial stromal cells

during the normal menstrual cycle and in pathological condition of the endometrium, reported that laminin immunostaining was observed close to the endometrial small arteries. The same authors also reported that the immunostaining with anti-laminin antibodies failed to identify detectable amounts of laminin associated with the stromal cells, either within the cytoplasm or in the peri-cellular matrix (Faber *et al.*, 1986). Nevertheless, scattered immunoreactive laminin was seen in the cytoplasm of stromal cells, in secretory specimens. However, in this study comparison between in the stromal distribution of the different laminin chains used was not possible due to the poor condition of the endometrial from frozen sections.

Aplin *et al.* (1988) in a immunohistochemical study of human endometrial ECM during the menstrual cycle and first trimester pregnancy, also reported that in secretory specimens laminin immunostaining was seen in the endometrial cells as streaks and spots around the periphery of the cells. The same authors reported that the only immunoreactive endometrial structures with laminin1 ($\alpha1\beta1\gamma1$) and collagen IV, in proliferative specimen, were the blood vessel walls and the glandular BM. The latter statement is in accordance with the results of this study. However, in the Aplin *et al.* (1988) study the antibody used for laminin immunostaining was directed to laminin 1 ($\alpha1\beta1\gamma1$) and not to specific laminin chains. One discrepancy between the Aplin *et al.* (1988) study and this study was the absence of collagen IV in the endometrial stroma. This study has shown that collagen IV was present in the superficial endometrial stroma in a punctate pattern as well as in the basal stroma but in a more compact pattern, due to a higher stromal cell density of the endometrial basal portion.

In a more recent immunocytochemical and ultrastructural study, it was reported that the $\alpha2$ laminin chain and collagen IV were present glandular basement membrane, luminal epithelium, microvascular endothelium and smooth muscle (Kohnen *et al.*, 1998). However, in this study the $\alpha2$ laminin chain was shown to be absent from the vascular smooth muscle and microvascular endothelium, using the same antibody as that used by Kohnen *et al.* (1998) study. Since the same antibody was used and the sections used were of endometrium with attached myometrium. it is difficult to accept the claim that Kohnen and colleagues (1998) made regarding the presence of the $\alpha2$ laminin chain in the vascular smooth muscle and microvascular endothelium, since no evidence is presented in the published paper.

From the results obtained for the distribution of the $\alpha2$, $\beta1$, $\beta2$ and $\gamma1$ laminin chains, potential, hypothetical and infeasible laminin types can be postulated (***Table.6***). The potential laminin types are based on combinations between the different laminin chains present whereas the hypothetical included laminin chains not examined in this study. The infeasible laminin types were based on the documented absence of the specific laminin chains.

Table.6 Possible, hypothetical and infeasible laminin types in different cellular compartments of the myometrium and endometrium.

	Possible laminin types	*Hypothetical laminin chains*	*Infeasible laminin types*
Myometrium			
Inner smooth muscle	Laminin 2 , 4	Laminin 1, 3, 6-11	
Outer smooth muscle	Laminin 2 , 4	Laminin 1, 3, 6-11	
Vascular smooth muscle		Laminin 3, 7, 9, 11	Laminin 2, 4
Endothelium		Laminin 3, 7, 9, 11	Laminin 2, 4
Endometrium			
Glandular BM (Functionalis)		Laminin 3, 7, 9, 11	Laminin 2, 4
Glandular BM (Basalis)	Laminin 2, 4	Laminin 1, 3, 6-11	
Stroma Basalis		Laminin 1, 6, 8, 10	Laminin 2, 3, 4, 7, 9
Stroma functionalis		Laminin 1, 6, 8, 10	Laminin 2, 3, 4, 7, 9
Endothelium		Laminin 1, 3, 6-11	Laminin 2, 4

The cross-hatched box indicate an absence of laminin α2, therefore no laminin trimers.

Key: Laminin 1 - α1β1γ1
Laminin 2 - α2β1γ1
Laminin 3 - α1β2γ1
Laminin 4 - α2β2γ1
Laminin 6 - α3β1γ1
Laminin 7 - α3β2γ1
Laminin 8 - α4β1γ1
Laminin 9 - α4β2γ1
Laminin 10 - α5β1γ1
Laminin 11 - α5β2γ1

4.1.1 *Quantitative analysis of the β2 laminin chain and collagen IV myometrial distribution*

Before discussing the two methods of analysing the distribution of the β2 laminin chain and collagen IV in frozen sections, it should be noted that the analysis was based on the transition between the inner and outer part of the muscle. By contrast, full thickness sections in paraffin embedded sections were used for the analysis of the myometrial distribution of elastin. This difference in specimen thickness was due to technical difficulties encountered in obtaining high quality full thickness myometrial frozen sections.

The difference observed in the intensity of the individual sections might be attributed to the variability in thickness within the sections. Another reason is that it was not possible to carry out the study in distinct phases of collection and ICC, hence ICC was carried out in an on going basis using batches of specimens. A combination of the latter reason and the change in the

secondary antibody and detection system could have resulted in the difference in the intensity of staining.

Nevertheless, a small number of high quality full and partial thickness frozen sections was obtained and the analysis was carried out. In order to quantitatively analyse the gradient observed in the myometrial distribution of the β2 laminin chain, two methods were devised. In the first method, all data sets were aligned using the position of the outer myometrium and truncated at a length equal to the shortest myometrial distance. Although this method restricted the analysis to the outer part of the muscle, a decreasing gradient was observed in the myometrial distribution of the β2 laminin chain, from outer towards inner myometrium. The second method involved aligning all data sets using the position of the endometrial/myometrial boundary and truncating them at a length equal to the shortest myometrial distance. In contrast to the first method, the second method restricted the analysis to the inner myometrium. However, it also allowed observation and examination of the gradient. When the second method was applied to analyse the myometrial distribution of collagen IV, it revealed a more uniform distribution compared to the gradient observed in the β2 laminin chain.

A combined average was calculated for both the β2 laminin chain and collagen IV myometrial distribution, clearly showing the decreasing gradient in the myometrial distribution of the β2 laminin in contrast to the more uniform distribution of collagen IV. The ratio of the β2 laminin to collagen IV was also calculated.

4.1.2 *Sectional thickness of the inner myometrium*

Measurements for the sectional thickness of the inner myometrium were carried out only in sections where the β2 laminin chain and collagen IV were immunolocalised. Sections immunostained with collagen IV were used as controls. In the method devised the sectional thickness was defined as the difference between the point at which the intensity of staining started to decrease from the plateau value and the endometrial/myometrial boundary. However, this method was not dependent on an estimate of the density of the endometrial/myometrial boundary.

In an ideal situation, where high quality frozen sections could be obtained, it might be better to express the sectional thickness as a proportion of the total myometrial thickness. Non-parametric statistical methods could then be used to compare different groups of patients.

The method devised for measuring the sectional thickness of the inner myometrium, was slightly different for the full and partial myometrial thickness sections, the reason for it being the variation in myometrial length (see ***Materials & Methods***). The results obtained from the sectional thickness measurements revealed intra and inter patient variability. Sections obtained

from patients after exposure to intrauterine levonorgestrel were also included in the sectional thickness measurements. Surprisingly the highest values were obtained from these patients, ranging from 8.59-14.76 mm. Two reasons can be given for these high values. One could postulate that the LNG-IUS affects the myometrium as well as the endometrium. A recent study investigating the treatment of grossly enlarged adenomyotic uteri, reported that a marked decrease in uterine size occurred within 12 months of insertion of the LNG-IUS. This result suggests that the LNG-IUS might have an effect on the gross uterine anatomy (Fong & Singh, 1999). The second reason could be that these patients might had a wider inner myometrium before treatment, hence the LNG-IUS might not have a dramatic effect on the thickness of the inner myometrium.

However, the patients exposed to the intrauterine levonorgestrel represented a small number and therefore it can not be treated as a concrete result. In order to investigate if the LNG-IUS has indeed an effect on the myometrial sectional thickness, a larger number of patients should be examined.

The sectional thickness measurements for the rest of the patients ranged between 2.09-7.78mm. Based on the variability of the results a question arises as to what constitutes normal thickness. There is a broad agreement in the literature that the "normal" junctional zone on MR imaging, is regular and measures ≤5mm (Mark *et al.*, 1987) in thickness although there is no consensus on what constitutes and "abnormal" junctional zone. Width between 6 and 12 mm have been reported (Mark *et al.*, 1987). It has also been reported that irregular thickening of the junctional zone is a common finding in women suffering from menstrual dysfunction (deSouza *et al.*, 1995). The latter statement might help to explain numbers above 5 mm obtained, for the sectional thickness, in this study. However, this does not explain sectional thickness values below 5mm, since all the patients included in this study reported a complaint of menorrhagia and dysmenorrhoea.

Nevertheless, caution should be taken when comparing the histological findings of this study and the MRI results of inner myometrial thickness. It is possible that there is no direct biological correspondence between histology and MRI, hence explaining values less than 5mm. However, if there is a direct biological correspondence, these values could be due to the orientation of the section and the way the thickness of the inner myometrium was calculated.

Another factor that affects myometrial zonal anatomy is ovarian steroids. In postmenopausal women and pre-pubertal girls the zonal anatomy is often indistinct with a comparatively low signal intensity from the myometrium (Brosens *et al.*, 1998). Gonadotrophin releasing hormone

analogues were shown to lead to an MR appearance of the uterus similar to that of the postmenopausal women (Demas *et al.*, 1985).

At the day of collection, important patient information was also collected such as the age, LMP, parity, medication and other (not shown). Of the patients from which sectional thickness measurements were obtained, none were reported to have received gonadotrophin releasing hormone analogues and none were post-menopausal. Hence all of the women where sectional thickness measurements were carried out could have been expected to exhibit an MR myometrial layering pattern. However, it should be noted that the reported complain of menorrahgia was not objectively proven.

Further MRI evidence for hormonal responsiveness of the junctional zone is provided by Wiczyk *et al.* (1988). It was demonstrated that the junctional thickness changed throughout the menstrual cycle in conjunction with endometrial thickness changes (Wiczyk *et al.*, 1988). In this study the stage of the cycle was recorded for every patient, however it was not possible to make any conclusions about the effect of cycle stage on the sectional thickness. Firstly because hysterectomy specimens of the type used in this study could only be obtained at a given stage of the menstrual cycle. Secondly no pre-hysterectomy MRI or ultrasound images were taken.

The median for sectional thickness of the inner myometrium was calculated from the individual patients, the average of all patients, the ratio of the β2 laminin chain to collagen IV and from the 99% of the maximum of the quadratic. The advantage of calculating the median from the individual patients was that it gives a better estimate of the biological variability, whereas the average of all patients formulates a picture of the transition, between inner and outer myometrium, that would have been difficult to obtain just by looking at individual data sets. However, calculating the median using the average of all patients could restrict the analysis by not properly defining the true nature of the transition between inner and outer myometrium. Experimental caused variability in the starting and plateau points were used and so the shape of the average transition should not be over-interpreted. The median value obtained from the individual patients (n=7.440mm) and average of all patients (n=8.460mm) were very similar.

The advantage of using the ratio of the β2 laminin chain to collagen IV was that it allowed 24 different data sets to be compressed into one, and so the transition pattern was easier to comprehend. The value for the median obtained (n=6.99mm) using the ratio was closer to the median value calculated from the individual patients than that calculated from the average of all patients. The maximum of the quadratic fit gave an imprecise estimate as it approached its maximum. The 99% of the maximum of the quadratic corresponded more closely to the sectional

thickens estimated by other means. The value obtained in this way (n=8.82mm) was closer to that of the average of all patients.

A quadratic fit was statistically justified for the ratio of the β2 laminin chain to collagen IV. In principal the quadratic function reaches a maximum and then declines, however there were no qualitative experimental evidence of this decline, therefore a better mathematical model of the data might be justified.

4.2 Expression of laminin chain in neurons

The survival and development of neurons are influenced not only by soluble molecules such as neurotransmitters and trophic factors, but also by cells adhesion molecules anchored either on cell membranes or in the extracellular matrix (Nurcombe, 1992).

When motor axons regenerate to denervated muscles after nerve injury, they preferentially re-innervate the original synaptic sites and differentiate there into nerve terminals (Sanes *et al.*, 1990). It was reported that the axons also preferentially form contacts and differentiate at synaptic sites on BL sheaths from which muscle fibres have been removed, implicating components of Bl in the remarkable topographic specificity of re-innervation (Sanes *et al.*, 1978; Glicksman & Sanes, 1983). The laminin α1, β1, γ1 (laminin 1) trimer is adhesive to neurons of many types and is a potent promoter of neurite outgrowth (Sanes, 1989).

Laminin can act synergistically with appropriate target-derived neurotrophic factors to promote neuronal survival during early development both *in vivo* and *in vitro* (Edgar, 1989). It may also play important roles in maintaining the transmitter phenotype of neurons (Acheson *et al.*, 1986). Nevertheless, the intracellular mechanisms responsible for these various activities of laminin remain incompletely understood, although the potency and specificity of laminin effects on neurons point to the existence of a specific transduction mechanism on neural cell surfaces (Nurcombe, 1992).

In this study, nerve-like structures were particularly obvious with the α2 and β1 laminin chains due to the absence of these particular laminin chains from the vascular smooth muscle and peri-vascular stroma. Nerves were visualized, after immunostaining with specific antibodies (NF-68 and NF-200kD) as nerve fibres within the myometrial smooth muscle or innervating large blood vessels localised in the outer part of the myometrium. Nerve bundles were also seen in within the smooth muscle of the myometrium. However, not many nerve fibres and bundles were observed within the sections possibly because of the orientation of the sections.

The rarity of the nerve fibres and bundles preclude the use of the present analytical methods to describe the a variation in the neuronal distribution between inner and outer myometrium.

4.3 Extracellular matrix deposition after exposure to intrauterine levonorgestrel (Mirena®)

The gradient observed in the myometrial distribution of the β2 laminin chain in untreated patients was also observed after exposure to intrauterine levonorgestrel, for a period of 10 weeks to 9 months. The myometrial distribution of β1 and γ1 laminin chains was more uniform and resembled that of the untreated patients. In the individual cellular compartments of both the inner and outer myometrium, the distribution of the α2, β1, β2, γ1 laminin chains was the same as that before exposure to the intrauterine levonorgestrel, suggesting that treatment with the LNG-IUS does not affect the extracellular matrix distribution of the myometrium.

After exposure to intrauterine levonorgestrel, areas of highly decidualised tissue were observed within the superficial part of human endometrium. This is consistent with known effects of the device on the endometrium (Silverberg *et al.*, 1986). In the highly decidualised areas of the superficial endometrium, more extensive peri-cellular staining was observed with the β1 and γ1 laminin chains.

It must be bourn in mind that results for endometrial examination of the extracellular matrix after exposure to the intrauterine levonorgestrel, were reported only from one specimen. As the α2, β1, β2 and γ1 laminin chain antibodies do not react with antigens on wax sections, even after antigen retrieval methods were applied (personal communication A.Young & Dr S.Campbell), analysis was limited by the quality of the frozen sections.

Nevertheless, the results of this study are in accordance to the results of Wewer *et al.*, (1985); Aplin *et al.*, (1988) and Kohnen *et al.*, (1998), who demonstrated that decidualisation of the endometrium of early pregnancy is associated with the new accumulation of peri-cellular BM containing at least type IV collagen and laminin. This cyclical variation suggests that some hormonal influence at or shortly following ovulation may be the stimulus for the laminin synthesis. It was reported that in the non-pregnant endometrium, laminin around the stromal cells cannot be detected in the proliferative phase of the menstrual cycle but this matrix protein begins to accumulate in the cytoplasm and as a peri-cellular layer in stromal cells at the early secretory phase (Loke & King, 1995). However, detailed observation of cyclical variation in laminin expression could not be made in this study.

Additionally, after 1-6 months of exposure to LNG-IUS, extensive peri-cellular laminin and collagen IV were present in some areas of the endometrial stroma in 29 out of 30 biopsies (personal communication, Dr S. Campbell). In other areas, deposition of BM was less extensive. On this basis, an observer with no knowledge of the treatment protocol, was able to deduce the

treatment status of 98% (45/46) of the pipelle biopsies used in a study of the Mirena® effects (personal communication, Dr S. Campbell).

However, the function of the peri-cellular aura of the basement membrane is not clear. It has been speculated that the appearance of the BM material with the onset of the process of decidualisation may have important functional implications for the decidual cells (Wewer *et al.*, 1985). Such functions may include selective permeability of macromolecules and structural support or modulation of other cellular functions essential for the maintenance of pregnancy. The presence of a peri-cellular basement membrane may contribute to the anchorage required by the extra-villous trophoblasts or maternal bone marrow derived cells and to the segregation of decidual cells from other cell populations. The peri-cellular BM may also play a role in the organisation of interstitial matrix (Aplin *et al.*, 1988).

In the basal part of the endometrium, the distribution of the β1, γ1 laminin chains and collagen IV was the same as that observed in the untreated patients. Both laminin chains and collagen IV were found to be present in the glandular basement membranes and vascular smooth muscle but they were less widely distributed in the non-decidualised basal portion of the endometrium, with the exception of collagen IV which was widely distributed. This suggests that possibly the effects of the intrauterine levonorgestrel device might be restricted to the superficial part of the human endometrium.

Collagen IV is a ubiquitous component of basement membranes and the γ1 laminin chain is found in most of the laminin types. As both of theses molecules are components of the BM a question arises as to why collagen IV in widely distributed in the endometrial stroma and peri-vascular myometrial tissue whereas the γ1 laminin chain is spatially more restricted. One possible explanation is that collagen IV might genuinely exist without the production of a defined basement membrane. Another reason could the sensitivity levels of the detection system used in immunocytochemistry. It might be possible that staining could not be detected below a certain threshold value for the γ1 laminin chain. Several parameters during immunocytochemistry, such as the affinity and concentration of the primary antibodies, temperature, the time of antibody and substrate incubation, might produce the difference seen in the γ1 laminin chain and collagen IV distribution within the peri-vascular myometrial tissue.

Even after exposure to the LNG-IUS where there is considerable increase in the distribution of laminin, the γ1 laminin chain was less widely distributed. Therefore it seems reasonable to postulate that this reflects a genuine difference between collagen IV and the γ1 laminin chain expression in the stroma and peri-vascular tissue.

4.4 RT-PCR analysis

The use of RT-PCR in this study confirmed the expression of the LAMB2 and LAMC1 genes in the inner and outer myometrium. However, after 30 cycles the reaction in both the inner and outer myometrium could have reached a plateau, therefore it was not possible to make any quantitative inferences. The size of the products from the gene amplification for both laminin chains was close to the predicted size.

Based on the gradient observed in the myometrial distribution of the β2 laminin chain by ICC, a difference in the amount of RNA present in the inner and outer myometrium was postulated. In order to examine the amount of RNA in the two different myometrial layers, the endometrium had to be separated from the myometrium and the remaining myometrium was divided into inner and outer. In this study the division between inner and outer myometrium was estimated visually. However, visually estimating the transition between inner and outer myometrium is not a reliable method therefore, for future work, the myometrium could be divided into inner and outer, using the ICC on parallel blocks. In other words, once the specimen is collected it could be transversally cut into two specimens, one stored in an RNA stabilising solution and the other used for immunolocalisation of the β2 laminin antibody. After ICC, the specimen intended for RNA isolation could be brought side to side with the sections where the β2 laminin antibody was immunolocalised, and based on the observed gradient the specimen should then be divided into inner and outer myometrium. RT-PCR could then take place and a quantitative RT-PCR could be used to detect differences in the amount of RNA present between the inner and outer myometrium.

4.5 Importance of laminin and collagen IV

Based on the early expression of the α1, β1 laminin chains and the ubiquitous expression of the γ1 laminin chain, it was speculated that mutation causing absence or highly altered structure of these chains would be lethal (Aumailley & Smyth, 1998). This has been confirmed by deletion of functional LAMA or LAMC1 gene in drosophila (Henchcliffe *et al.*, 1993) leading to early embryonic lethality. Similarly, targeted extinction of the ITGBI gene encoding the β1 laminin integrin chain is not compatible with embryonic development and leads to prei-implantation lethality (Stephens *et al.*, 1995). These observations strengthen the absolute prerequisite of functional laminin and laminin-integrin interactions from embryonic development.

In man, laminin and integrin defects cause a subset of skin blistering diseases known as the junctional types of epidermolysis bullosa (Kuster *et al.*, 1997). Laminin and laminin receptor defects are responsible for diseases such as congenital muscular dystrophy (Arahata *et al.*, 1997). Laminins and theirs are presumably involved in other pathologies affecting the basement

membranes, such as diabetes or the invasive growth and metastasis of tumours (Aumailley & Smyth, 1998).

Collagen IV has been involved in a number of human diseases such as the Goodpasture syndrome, which is a lethal form of autoimmune disease, Alport syndrome and diffuse esophageal leiomyomatosis (Hudson *et al.*, 1993). By contrast to the laminin family, collagen IV has been related to a disease affecting the normal function of the uterus. The Ehlers-Danlos syndrome (EDS) is a groups of connective tissue disorders involving defects in collagen synthesis. So far, 10 different types have been described (Brees, 1995). The most lethal of these is type IV EDS with up to 25% maternal mortality (Brees, 1995). Obstetrical complications include premature rupture of membranes, rupture of blood vessels and gravid uterus, tearing of perineum, vagina, urethra and bladder (DePaepe *et al.*, 1989).

Sorokin *et al.* (1994), in a study examining the obstetrics and gynaecologic dysfunction in the EDS, reported that women with EDS were found to have high rates of abortion, preterm delivery, pregnancy-related bleeding and stillbirth. In the same study it was also reported that women with EDS also have high frequency of anovulation, vaginal infections, abnormal cytologic smears and dyspareunia.

All of the above diseases demonstrate the importance of a fully formed basement membrane, either for a normal embryonic development or for later stages in life.

4.6 Elastin expression in the human uterus

4.6.1 *Myometrial gradient of the elastin distribution in the human myometrium*

Quantitative and qualitative analysis carried out in this study revealed a decreasing gradient, from the outer towards the inner myometrium, in the distribution of elastin. Two methods were devised to quantitatively analyse the observed gradient. In the first method the average data sets were aligned using the position of the outer myometrium and truncated at distance equal to the length of the shortest myometrial specimen. However this method restricted the analysis to the outer myometrium. In the second method the data sets were normalised by width and therefore the complete data sets were analysed regardless of myometrium length. The second method of analysis involved dividing the sections into slices and this in itself produced a smoothing effect as it employed a consecutive average. Because the positional data are recorded as slice number, there is an inevitable loss of spatial information.

Both methods demonstrated the presence of a decreasing gradient from the outer towards the inner myometrium and hence verified and supported the qualitative analysis. A linear fit was

statistically justified for the average elastin data in contrast to the non-linear distribution of the β2 laminin chain, where a quadratic fit was statistically justified.

McCarthy and colleagues (1989), undertaking an MRI study of the relaxation properties and water content in the human uteri, reported that the content and nature of elastin did not differ between the junctional zone (inner myometrium) and the adjacent myometrium. There is an apparent discrepancy between the study by McCarthy *et al.* (1989) and the present study. There may be four technical reasons explaining this discrepancy. In the published study it was stated that the uterine sections were taken from the posterior and anterior uterine walls, but it was not specified whether the sections were of full or partial myometrial thickness. The selection of a histochemical stain (elastic-Van Gieson) instead of a monoclonal antibody means that the authors used a less specific detection system with background staining. In addition the use of the elastica kit according to Van Gieson could have made it very difficult to see a gradient in the myometrial distribution of elastin (see ***Materials and Methods***). By contrast orcein staining used in this study produced a clearer distinction between elastic and non-elastic components. McCarthy *et al.* (1989) may have failed to observe a gradient in the myometrial distribution of elastin because their aim was to find a more distinct layering pattern, consistent with MRI. It must be bourn in mind that the myometrial distribution of elastin exhibits a gradient and not layering, as in the case of the β2 laminin chain.

There are three possible components to the observed gradient. The first is a gradient in the distribution of elastin within the smooth muscle. It was demonstrated that in the inner myometrial smooth muscle elastin was absent or of low abundance, whereas in the outer myometrium the average intensity of elastin immunolocalization increased. Additionally, in more superficial parts of the tissue close to the serosal surface, elastin was observed in the smooth muscle of areas remote from arterioles and larger blood vessels. The gradient in the smooth muscle cells of the myometrium suggests a phenotypic difference between the SMC of the inner and outer myometrium (discussed in detail below).

The second component of the gradient is in the peri-vascular tissue. Peri-vascular elastin was predominantly associated with large blood vessels, which are located in the outer and not the inner myometrium. Nevertheless, traces of elastin were observed in the inner myometrium in areas surrounding the largest of the arteries and sometimes close to the thin walled vessels. The difference in the blood size between the inner and outer myometrium may partially explain the variation in peri-vascular elastin (***Diagram.1A,B***).

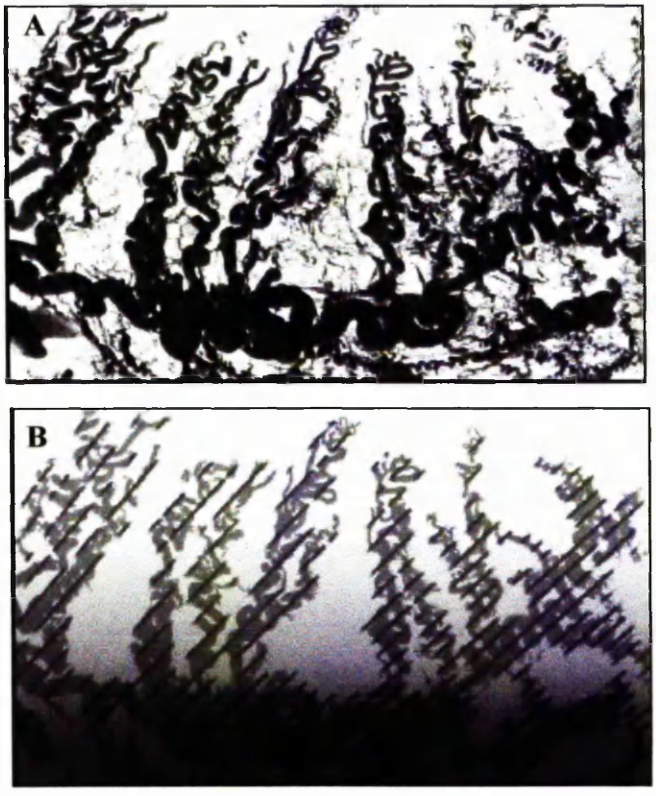

Diagram.1 A conceptual representation of the elastin gradient within the myometrium in relation to the arterial tree. (**A**) The arterial tree as observed in a microradiograph of a transverse uterine slice by Farrer-Brown *et al.* (1970a). (**B**) The three postulated components of the gradient are shown independently. The vascular component is represented by the larger vessels of the arterial tree. The cross-hatching depicts the peri-vascular volume surrounding the coiled vessels. The grey background portrays the gradient of elastin within the myometrial smooth muscle.

(Part (**A**): used with permission from the publishers, Blackwell Scientific
Part (**B**): is reproduced, courtesy of Dr S. Campbell)

The third and final component of the gradient is in the vessel walls *per se*. As the arcuate and radial arteries branch, the cross–section of the individual vessels becomes smaller hence less elastin may be present per cross-sectional unit area of vessel, compared to the highly muscularised larger vessels of the outer myometrium. In other words, there is more elastin in the vascular smooth muscle cells of the large arteries found in the outer myometrium than the thin walled vessels. In addition the images published by Farrer-Brown *et al.* (1970a), suggest that there may be a gradient in the total arteriolar cross-sectional area.

It would not be easily possible to reliably measure the individual components of the gradient using the present methods.

Elastin within the uterus could provide a dynamic function and play a significant role during pregnancy by allowing the uterus to enlarge so that it can accommodate the growing fetus. It has been suggested that elastin may assist in closing the cervix after delivery and thereafter returning it to its non-pregnant configuration (Calder, 1994). This could apply to the whole uterus after parturition. However, the return to the non-gravid size also involves muscular contraction. A combination of passive elastic forces and smooth muscle induced tone, might be necessary to help maintain uterine size and shape, in the gravid and non-gravid state.

The present study suggests that the outer part of the muscle is more elastic compared to the inner part. If the distending force is resolved within the outer part of the muscle it maybe more appropriate for the outer part to be more elastic. This suggestion could be further investigated by devising a method to analyse the elasticity of the uterine muscle.

However, it maybe more appropriate to ask why the inner myometrium is less elastic. Several studies (deVries *et al.*, 1990; Lyons *et al.*, 1991; Chalubinski *et al.*, 1993; Kunz *et al.*, 1996) showed myometrial peristalsis in the human uterus, during the course of the menstrual cycle. These waves emanate from the inner and not the outer myometrium. It appears that the non-peristaltic tissue (outer myometrium) is more elastic than the inner myometrium. The decrease in the amount of elastin present in the inner myometrium may be responsible for a more efficient propagation of the peristaltic waves.

Farrer-Brown *et al.* (1970a,b) in microradiographic studies described the blood supply of the uterus and showed that the anterior and posterior arcuate divisions of the uterine artery and their branches, from which the whole arterial tree is derived, run a markedly tortuous course towards the midline. The branches from the contralateral sides of the uterus then anastomose. These authors postulated that the tortuosity of the myometrial arteries allows expansion of the gravid uterus, which would otherwise be subject to excessive tension. However, it should be noted that the less muscularised venous system does not show similar spiral morphology (Farrer-Brown *et al.*, 1970b). Greater force could be required to distend a muscularised artery than a vein therefore the spiral nature of the arteries may reduce the force required to produce linear elongation of the arcuate artery. Lateral forces acting perpendicularly on the radial arteries may change the pitch of the spiral arteries during pregnancy.

Almost 30 years later, this study has provided the evidence to support the postulation of Farrer-Brown and colleagues (1970a) for it has been demonstrated that the blood vessels of the outer myometrium contain elastin in their walls and does the peri-vascular tissue. Nevertheless, elastin The elastic nature of the blood vessels in combination with the peri-vascular scaffolding of elastin within the arterial walls may not be, by itself, sufficient for very extensive blood vessel stretching. The peri-vascular scaffolding of elastin may be required for the blood vessels to extend during pregnancy.

Gunja-Smith *et al.* (1985), reported that the during pregnancy the elastin content increases fourfold to fivefold and that in the non-gravid uteri the elastin content increased with successive pregnancies. Quantitative analysis of the myometrial distribution of elastin suggested that there is variability within patients. Therefore it was not possible to conclude if successive pregnancies increased the amount of elastin present in the uterus.

The stage of the normal menstrual cycle did not affect the presence of the gradient in the myometrial distribution of elastin. Patients treated with intrauterine levonorgestrel were also included in this study and no differences were observed in the myometrial distribution of elastin when compared to that of the untreated patients. No differences were observed in the myometrial distribution of the different laminin chains and collagen IV myometrial distribution, clearly showing that the intrauterine levonorgestrel system does not affect the gross structure of the myometrium.

Elastin expression in the human endometrium

Within the human endometrium elastin was shown to be restricted in the basal portion of the endometrial arterioles. Elastin was found to be absent from the basal and superficial stroma, the surface epithelium and the muscularised and thin walled blood vessels close to the surface epithelium.

Fleming & Bell, (1997) reported that the human endometrium was free from elastin, while investigating the presence of fibrillin-1, a component of the elastic fibres, in the human endometrium and decidua during the menstrual cycle. Endometrial specimens were collected from regularly cycling women undergoing curettage of hysterectomy. In the published paper the authors do not specify which type of sections (hysterectomy or curettages) they used for the immunolocalization of elastin, which inevitably plays and important role in the interpretation of the results.

If Fleming & Bell (1997) based their description largely on the curettage sections or from hysterectomy specimens with little basal endometrium it is possible that they failed to detect any elastin in the basal part of the endometrium, simply because the part of the tissue is missing. However, if full thickness hysterectomy sections were indeed used, their method for elastin immunolocalization was probably defective. In the published paper the method used for immunolocalization of elastin lacks important details and therefore a direct comparison between their method and the method used in the present study cannot be made.

4.6.2 *Elastin expression in the myometrial and endometrial vascular system*

Elastin was shown to be present in the wall of myometrial arteries. Like most blood vessels, the arterial wall consists of three layers: tunica intima, tunica media and tunica adventitia. In the large arteries, found in the outer part of the muscle, the internal elastic lamina was well marked as a refractile wavy band (***Diagram.2***). The internal elastic lamina is the last layer of the tunica intima. There are different definitions of the composition of the adventitia within standard textbooks In the muscular arteries the tunica adventitia consists of loose connective tissue containing vasa vasorum, nerve fibres, adipose cells, fibroblasts and elastic fibres.

Longitudinally arranged collagen fibres are found in the deeper portion of the adventitia (Zhang, 1999). The tunica adventitia does not have "a clearly defined outer edge", it gradually merges with the loose connective tissue accompanying the vessel (Garven, 1957). However, it proved to be very difficult to distinguish the external elastic lamina because of the elastic fibres found in the arterial wall and peri-vascular area (***Diagram.2***). In the smaller arteries of the outer and inner myometrium elastin was present in the arterial wall but due to the size of the blood vessels it was difficult to distinguish the internal elastic lamina.

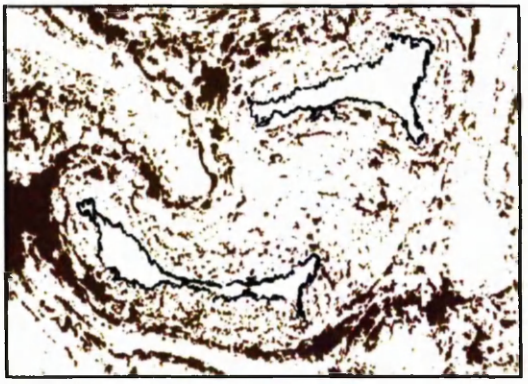

Diagram.2 Diagrammatic representation of the internal elastic lamina (black) of large arteries found in the outer myometrium. The elastin present in the arterial walls and peri-vascular area is also shown (brown).

Despite the presence of elastin in the myometrial arteries and in the basal portion of the endometrial arterioles, spaces assumed to be blood vessels were shown to lack elastin. These assumed vascular spaces were seen in both the endometrium and myometrium. The vascular identity of these spaces was verified using an endothelial marker (CD31). However, a more specific indication of vascular identity was not possible. In other words it was not possible to determine whether these thin walled vessels were veins or lymphatic vessels. One way to distinguish between veins and lymphatic vessels would be the presence or not, respectively, of red blood cells. Nevertheless, a more reliable way to specifically identify the vascular spaces as veins would be to identify endothelial markers, which are spatially restricted within the vascular tree.

4.6.3 ***Elastin in uterine sections after exposure to intrauterine levonorgestrel (Mirena®)***

Within the human endometrium, after exposure to intrauterine levonorgestrel (Mirena®), elastin remained in the basal portion of the endometrial arterioles but was absent from the endometrial stroma in 9 out of 12 sections examined. In the remaining 3 sections elastin was shown to be present in the basal endometrial stroma. Kohnen *et al.* (2000) reported that the stromal cells of the basal endometrium produce α-smooth actin suggesting that endometrial cells have a myofibroblastic phenotype. It may be possible that the presence of the progestagen make these myofibroblasts elastogenic. It seems reasonable to postulate that this is an abnormal feature.

In the human myometrium no differences were observed in the distribution of elastin within the smooth muscle, walls of arteries and in the peri-vascular tissue, when compared to the untreated patients. The vascular abnormalities observed after exposure to the intrauterine levonorgestrel (Campbell *et al.*, 2000 abstract) suggest that the effects of the LNG-IUD may be restricted to the superficial endometrium. However, a recent study examining enlarged adenomyotic uteri, reported a marked decrease in uterine size was observed after 12 months of insertion. Therefore it is possible that the intrauterine levonorgestrel system has an effect on uterine muscle. The myometrial features being examined in this study may not have been sensitive to the effects of the intrauterine levonorgestrel system.

4.6.4 ***Importance of elastin in tissue organisation***

Alterations affecting elastin may either be heritable or acquired and a variety of extrinsic processes may modify elastin during the lifetime of an individual and compromise the funciton of the elastic fibre (Rosenbloom, 1984). However, because of its crucial role in the cardiopulmonary system, the absence of elastin is incompatible with human life. Therefore no diseases in which there is a total absence of elastin have been reported. A literature search carried out for the involvement of elastin in diseases related to the human uterus showed no records so far.

Nevertheless elastin has been reported to play an important role in the pathogenesis of several diseases. Knockout mice lacking elastin died perinatally following obstructive arterial development resulting from sub-endothelial cell proliferation and reorganisation of the smooth muscle. Arterial development in mice lacking elastin was indistinguishable from that of the control mice until 17.5 embryonic day, indicating that elastin is important in the later stages of development. (Dean *et al.*, 1998).

Other diseases in which the involvement of elastin has been implicated include Pseudoxanthoma Elasticum (Altman *et al.*, 1974), Cutis Laxa (Hashimoto & Kanzaki, 1975), and Menses kinky hair syndrome (Menkes *et al.*, 1962), Moyamoya (Yamamoto *et al.*, 1997), supravalvular aortic stenosis (SVAS) (Boeckel *et al.*, 1999) and arteriosclerosis (Yamamoto *et al.*, 1994).

Based on the observed gradient in the uterine myometrial distribution of elastin a literature search for a similar gradient was undertaken in a number of other organs. Although elastic fibre orientation has been described in detail in many tissues such as lung (Starcher *et al.*, 2000) and the bladder (Murakumo *et al.*, 1995) the kind of microscopic description produced in this study does not appear to be available, at least in the research literature.

4.7 Conclusion

The results presented in this thesis suggest that there are important structural differences between the inner and outer myometrial smooth muscle. The anatomy of the human myometrium therefore appears to be more complex than previously reported. In the MRI literature, the muscle of women of reproductive age is said to consist of two distinct layers. As a result of the work carried out in this study, the layering appears to be more subtle and does have an obvious morphological correlate. In addition to layering, within the myometrial smooth muscle, gradients of various kinds may also be present. As a consequence of these findings it is postulated that the outer myometrium is more elastic than the inner and that the variation in BM composition may influence the contractile properties of the muscle.

Although this has been an anatomical study, there is scope for further functional, developmental and molecular genetics studies, to elaborate the basis of human myometrial anatomy.

References

- Abrahamson D.R. Recent studies on the structure and pathology of basement membranes. *Journal of Pathology.* 1986; **149**: 257-278.
- Acheson A.L., et al. Laminin increases levels and activity of tyrosine hydroxylase in calf adrenal medullary cells. *Journal of Cell Biology.* 1986; **102**: 151-159.
- Adams J.C & Watt F.M. Regulation of development and differentiation by the extracellular matrix. *Development.* 1993; **117**: 1183-1198.
- Alberts B., et al. (1994). The extracellular matrix of animals. In *Molecular biology of the cell* (ed. Alberts B., Bray D., Lewis J., Raff M., Roberts K. and Watson J.D.), pp.971-973. Garland Publishing Inc. New York & London.
- Allonen H. The levonorgestrel IUD. In Bardin CW, Mishell DR Jr, eds. *Proceedings from the 4th International Conference on IUDs.* Newton, MA, USA: Butterworth Heinemann, 1994; 284-292.
- Altman L.K., et al. Pseudoxanthoma elasticum: and inderdiagnosed genetically heterogeneous disorder with protean manifestations. *Archives in Internal Medicine.* 1974; **134**: 1048.
- Andersson K., et al. Levonorgestrel-releasing and copper-releasing (Nova T) IUCDs during five years of use: a randomized comparative trial. *Contraception* 1994; **49**: 56-72.
- Andreyko JL., et al. Use of an agonistic analog of GnRH (nafarelin) to treat leiomyomata: assessment by magnetic resonance imaging. *American Journal of Obstetrics and Gynaecology.* 1988; **158**: 903-910.
- Aplin J.D., et al. An immunocytohistochemical study of human endometrial extracellular matrix during the menstrual cycle and first trimester of pregnancy. *Cell and Tissue Research.* 1988; **253**: 231-240.
- Arahata K., et al. Congenital muscular dystrophies. *Current Opinion in Neurology.* 1995; **8**: 385-390.
- Aumailley M., et al. The cellular interactions of laminin fragments. Cell adhesion correlates with two fragment-specific high affinity binding sites. *Journal of Biological Chemistry.* 1987; **262**: 11532-11538.
- Aumailley M., et al. Antibody to integrin α6 subunit specifically inhibits cell-binding to laminin fragment 8. *Experimental Cell Research.* 1990a; **188**: 55-60.

- Aumailley M., et al. Identification of the Arg-Gly-Asp sequence in laminin A chain as a latent cell-binding site being exposed in fragment P1. *FEBS Letters.* 1990b; **262**: 82-86.
- Aumailley M. & Smyth N. Review. The role of laminins in basement membrane function. *Journal of Anatomy.* 1998; **193**: 1-21.
- Autio-Harmainen H., et al. Synthesis of laminin and type IV collagen by trophoblastic cells and fibroblastic stromal cells in the early human placenta. *Laboratory Investigation* 1991; **64(4)**: 483-491.
- Autio-Harmainen H., et al. Simultaneous expression of 70 kilodalton type IV collagenase ans type IV collagen α1(IV) chain genes by cells of early human placenta and gestational endometrium. *Laboratory Investigation.* 1992; **67(2)**: 191-200.
- Azziz R. Adenomyosis: current perspectives. *Obstetric & Gynaecological Clinics of North America.* 1989; **16**: 221-235.
- Barondes S.H., et al. Galectins: a family of animal beta-galactoside-binding lectins. *Cell.* 1994; **76**: 597-598.
- Battaglia C., et al. Basement membrane heparan sulfate proteoglycan binds to laminin by its heparan sulfate chains and to nidogen by sites in the protein core. *European Journal of Biochemistry.* 1992; **208**: 359-366.
- Beck K., et al. Ionic interactions in the coiled-coil domain of laminin determine the specificity of chain assembly. *Journal of Molecular Biology.* 1993; **231**: 311-323.
- Beyer E.C., et al. Antisera directed against connexin 43 peptides react with a 43-kD protein localized to gap junctions in myocardium and other tissues. *Journal of Cell Biology.* 1989; **108**: 595.
- Boeckel T., et al. A new mutation in the elastin gene causing supravascular aortic stenosis. *The American Journal of Cardiology.* 1999; **83(7)**: 1141-1143.
- Bounds W., et al. Clinical experience with a levonorgestrel-releasing intrauterine contraceptive device (LNG-IUCD) as a contraceptive and in the treatment of menorrhagia. *British Journal of Family Planning* 1993; **19**: 193-194.
- Brandenberger R., et al. Native chick laminin-4 containing the β2 chain (s-laminin) promotes motor axon growth. *Journal of Cell Science.* 1991; **135**: 1583-1592.
- Brees C.K. Rupture of the external iliac artery during pregnancy: a case of type IV Ehlers-Danlos syndrome. *Journal of the Kentucky Medical Association.* 1995; **93(12)**: 553-559.

- Brosens J.J., et al. Uterine junctional zone: function and disease. *The Lancet.* 1995; **346(8974)**: 558-560.
- Brosens J.J., et al. Myometrial zonal differentiation and uterine junctional zone hyperplasia in the non-pregnant uterus. *Human Reproduction Update.* 1998; **4(5)**: 496-502.
- Brosens J.J. & Brosens I.A. (1998) Adenomyosis uteri. In In *Clinical disorders of the endometrium and menstrual cycle* (ed. Cameron I.T., Fraser I.S and Smith S.K.), pp.3297-299. Oxford University Press.
- Brown H.K., et al. Uterine junctional zone: correlation between histologic findings and MRI. *Radiology.* 1991; **179**: 409-413.
- Brown J.C., et al. Protein binding and cell adhesion properties of two laminin isoforms (AmB1eB2e.AmB1sB2e) from human placenta. *Journal of Cell Science.* 1994; **107**: 384-391.
- Burgeson R.E., et al. A new nomenclature for laminins. *Matrix Biology.* 1994; **14**: 209-211.
- Calder A.A. (1994). The cervix during pregnancy. In *The uterus* (ed. Chard T. & Grudzinskas C.), pp.295-296. Cambridge University Press.
- Carter W.G., et al. Distinct functions for integrins αaβ1 in focal adhesions and α6β4/bullous pemphigoid antigen in a new stable anchoring contact (SAC) of keratinocytes: relation to hemidesmosomes. *Journal of Cell Biology.* 1990; **111**: 3141-3154.
- Chalubinski K., et al. Vaginosonography for recording of cycle-related myometrial contractions. *Fertility and Sterility.* 1993; **59**: 225-228.
- Campbell S., et al. Laminin β2 distinguishes inner and outer layer of the human myometrium. *Journal of Reproduction and Fertility. Abstract Series.* 1998; **22**: 12.
- Campbell S., et al. Variations in laminin expression in uterine blood vessels and smooth muscle. *Journal of Reproduction and Fertility. Abstract Series.* 2000; **26**: 17.
- Chamley-Campbell J., *et al.* The smooth muscle cell in culture. *Physiological Reviews.* 1979; **59(1)**: 1-61.
- Champliaud M.F., et al. Human amnion contains a novel laminin variant, laminin 7, which like laminin 6, covalently associates with laminin 5 to promote stable epithelial-stromal attachment. *Journal of Cell Biology.* 1996; **132**: 1189-1198.

- Chan F.L., *et al.* The basement membranes of cryofixed or aldehyde-fixed, freeze-substituted tissues are composed of a lamina densa and do not contain a lamina lucida. *Cell Tissue Research.* 1993; **273**: 41-52.
- Chan F.L. & Wong Y.C. Ultrastructural localization of proteoglycans by cationic dyes in the epithelial-stroma interface of the guinea pig lateral prostate. *Prostate.* 1989; **14**: 147-162.
- Chen M., et al. Interactions of the amino-terminal noncollagenous (NC1) domain of type VII collagen with extracellular matrix components. A potential role in epidermal-dermal adherence in human skin. *Journal of Biological Chemistry.* 1997; **272**: 14516-14522.
- Cheng Y.S., et al. Self-assembly of laminin isoforms. *Journal of Biological Chemistry.* 1997; **272**: 31525-31532.
- Church J. Heather., et al. Laminin 2 and 4 are expressed by human decidual cells. *Laboratory Investigations.* 1996; **74(1)**: 21-32.
- Cochat P., et al. *Journal of Pediatrics.* 1988; **113**: 339-343.
- Cooper A.R., et al. Studies on the biosynthesis of laminin by murine parietal endoderm cells. *European Journal of Biochemistry.* 1981; **119**: 189-197.
- Csapo A.I. Smooth muscle as a contractile unit. *Physiology Reviews.* 1962; **5**: 7-33.
- Csapo A.I. (1981) Force of labour. In *Principles and Practice of Obstetrics and Perinatology* (ed. Iffy L. & Kamientzky H.A.), pp.761-799. John Wiley and Sons, NY.
- Daels J., Uterine contractility patterns of the outer and inner zones of the myometrium. *Journal of Obstetrics and Gynaecology.* 1974; **44**: 315-326.
- Daga-Gordini D., et al. Detection of elastin by immunoelectronmiscroscopy. A comparison of different procedures. *Hhistochemsitry.* 1987; **87**: 573-578.
- Dallenbach G. & Hellweg. (1981). The normal histology of the endometrium. In *Histopathology of the Endometrium* (ed), pp.23-83.
- Damiano V., et al. Secretion of elastin in the embryonic chick aorta as visualised by immunoelectron microscopy. *Collagen related Research.* 1984; **4**: 153-164.
- Dean Li, et al. Elastin is an essential determinant of arterial morphogenesis. *Nature.* 1998; **393(6682)**: 276-280.
- DeLuca M., et al. Polarized integrin mediates human keratinocyte adhesion to basal lamina. *Proceedings of the National Academy of Sciences of the USA.* 1990; **87**: 6888-6892.

- Demas B.E., et al. Uterine MR imaging: effects of hormonal stimulation. *Radiology.* 1985; **159**: 123-126.
- De Paepe A. et al. Obstetrical problems in patients with Ehlers-Danlos syndrome type IV; a case report. *European Journal of Obstetrics, Gynaecology & Reproductive Biology.* 1989; **33(2)**: 189-193.
- deSouza N.M. *et al.* The potential value of magnetic resonance imaging in infertility. *Journal of Radiology.* 1995; **50**: 75-79.
- Deutzmann R., et al. Cell adhesion, spreading and neurite stimulation by laminin fragment E8 depends on maintenance of secondary and tertiary structure in its rod and globular domain. *European Journal of Biochemistry.* 1990; **191**: 513-522.
- De Vries K., et al. Contractions of the inner third of the myometrium. *American Journal of Obstetrics and Gynaecology.* 1990; **162**: 679-682.
- Dölz R., et al. Folding of collagen IV. *European Journal of Biochemistry.* 1988; **178**: 357-366.
- Dziadek M. & Timpl R. Expression of nidogen and laminin in basement membranes during mouse embryogenesis and in teratocarcinoma cells. *Developmental Biology.* 1985; **111**: 372-382.
- Eble J.A., et al. The $\alpha 1\beta 1$ integrin recognition site for the basement membrane collagen molecule $[\alpha 1(IV)]_2\alpha 2(IV)$. *EMBO Journal.* 1993; **12**: 4795-4802.
- Edgar D. Neuronal laminin receptors. *Trends in Neuroscience.* 1989; **12**: 248-251.
- Ehrig K., et al. Merosin, a tissue-specific basement membrane protein is a laminin-like protein. *Sciences of the USA.* 1990; **87**: 3264-3268.
- Ekblom P., et al. Laminin isoforms and their receptors in the developing kidney. *American Journal of Kidney Diseases.* 1990; **17**: 603-605.
- Engvall E., et al. Distribution and isolation of four laminin variants: tissue restricted distribution of heterotrimers assembled from five different subunits. *Cell Regulation.* 1990; **1**: 731-740.
- Faber M., et al. Laminin production by human endometrial stromal cells relates to the cyclic and pathologic state of the endometrium. *American Journal of Pathology.* 1986; **124(3)**: 384-391.
- Falk B., et al. Reduction by progesterone of the estrogen-induced increase in transmitter level of the short adrenergic neurons innervating the uterus. *Endocrinology.* 1975; **84**: 958-969.
- Farrer-Brown G., et al. The blood supply of the uterus. I. Arterial vasculature. *Journal of Obstetrics and Gynaecology.* 1970a; **77**: 673-681.

- Farrer-Brown G. & Tarbit M.H. The blood supply of the uterus. II Venous pattern. *Journal of Obstetrics and Gynaecology.* 1970b; **77**: 682-689.
- Fleming S. & Bell. S.C. Localization of fibrillin-1 in human endometrium and decidua during the menstrual cycle and pregnancy. *Human Reproduction.* 1997; **12(9)**: 2051-2056.
- Fong Y.F. & Singh K. Medical treatment of a grossly enlarged adenomyotic uterus with the levonorgestrel-releasing intrauterine system. *Contraception.* 1999; **60(3)**: 173-175.
- Fox J., et al. Recombinant nidogen consists of three globular domains and mediates binding of laminin to collage IV. *EMBO Journal.* 1991; **10**: 3137-3146.
- Gardner R.M. & Stancel G.M. Blockade of epidermal growth factor-induced uterine contractions by indomethacin and nordihydroguaritic acid. *Journal of Pharmacological Experimental Theory.* 1989; **258**: 882-886.
- Garfield R.E., et al. Control of myometrial contractility: role and regulation of gap junctions. *Oxford Reviews in Reproductive Biology.* 1988; **10**: 436.
- Garfield R.E. & Yallampalli C. (1994). Structure and function of uterine muscle. In *The uterus* (ed. Chard T. & Grudzinskas C.), pp.54-84. Cambridge University Press.
- Garven H.S.D. (1957). The circulatory system. In *A student's Histology.* (ed. Garven H.S.D.), pp. 145-224. E. & S. Liningstone Ltd. Edinburgh.
- Glicksman M. & Sanes J.R Development of motor nerve terminals formed in the absence of muscle fibres. *Journal of Neurocytology.* 1983; **12**: 661-671.
- Goldberg M. & Esgaig-Haye F. Is the lamina lusida of the basement membrane a fixation artifact? *European Journal of Cell Biology.* 1986; **42**: 365-368.
- Goodman S.L., et al. Two distinct cell-binding domains in laminin can independently promote nonneural cell adhesion and spreading. *Journal of Cell Biology.* 1987; **105**: 589-598.
- Grosso L. & Mecham R.P. In vitro processing of tropoelastin: Investigation of a possible transport function associated with the carboxy-terminal domain. *Biochemical and Biophysiological Research Communications.* 1988; **151**: 822-826.
- Gunja-Smith Z. & Woessner J.F. Content of the collagen and elastin cross-links pyridinoline and the desmosines in the human uterus in various reproductive states. *American Journal of Obstetrics and Gynaecology.* 1985; **153**: 92-95.

- Hall H., et al. HNK-1 carbohydrate-mediated cell adhesion to laminin-1 is different from heparin-mediated and sulfatide-mediated cell adhesion. *European Journal of Biochemistry.* 1997; **246**: 233-242.
- Hashimoto K. & Kanzaki T. Cutis laxa: ultrastructural and biochemical studies. *Archives of Dermatology.* 1975; **111**: 861.
- Heinricius G. En metod att grafiskt atergiva Kontraktioner hos en icke gravid livmoder. *Finsk Lakaresallsk Handl.* 1889; **31**: 349.
- Henchcliffe C. et al. Genetic analysis of laminin A reveals diverse functions during morphogenesis in Drosophila. *Development.* 1995; **118**: 325-337.
- Hendrickson M.R. & Kemmson R.L. The differential diagnosis of endometrial adenocarcinoma. Some viewpoints concerning a common diagnostic problem. *Pathology.* 1980; **12(1)**: 35-61.
- Henry M.D. & Campbell K.P. Dystroglycan-an extracellular matrix receptor linked to the cytoskeleton. *Current Opinion in Cell Biology.* 1996; **8**: 625-631.
- Hieber A.D., et al. Detection of elastin in the human fetal membranes: Proposed molecular basis of elasticity. *Placenta.* 1997; **18**: 301-312.
- Hinek A., et al. The elastin receptor is a galactoside binding protein. *Science (Washington, D.C.)* 1988; **239**: 1539-1541.
- Hinek A., et al. The 67-kD elastin/laminin-binding protein is related to an enzymatically incative, alternatively spliced form of beta-galactosidase. *The Journal of Clinical Investigation.* 1993; **91(3)**: 1198-1205.
- Hostikka S.L., et al. Identification of a distinct type IV collagen alpha chain with restricted kidney distribution and assignment of its gene to the locus of X chromosome-linked Alport syndrome. *Proceedings of the National Academy of Science USA.* 1990; **87**: 1606-1610.
- Hricak H., et al. Magnetic resonance imaging of the female pelvis initial experience. *American Journal of Obstetrics and Gynaecology.* 1983; **141**: 1119-1128.
- Hudson B., et al. Type IV collagen: Structure, Gene Organization and Role in human diseases. *The Journal of Biological Chemistry.* 1993; **268(35)**: 26033-26036.
- Hunter D.D. *et al.* S-laminin expression in adult and developing retinae: a potential cue for photoreceptor morphogenesis. *Neuron.* 1992; **8**: 399-413.
- Hynes R.O. Integrins: versatility, modulation, and signaling in cell adhesion. *Cell.* 1992; **69**: 11-25.

- Inove S. & Leblond C.P. Three-dimensional network of cords: the main component of basement membranes. *American Journal of Anatomy.* 1988; **181**: 341-358.
- Iwahashi M., et al. Alterations in distribution and composition of the extracellular matrix during decidualization of the human endometrium. *Journal of Reproduction and Fertility.* 1996; **108**: 147-155.
- Janne O. & Ylostalo P. Endometrial oestrogen and progestin receptors in women bearing a progesterone-releasing intrauterine device. *Contraception* 1980; **22**: 19-23.
- Jaques A. & Serafini-Francassini A. Morphogenesis of elastic fibers: An immunoelectronmicroscopy investigation. *Journal of Ultrastructural Research.* 1985; **92**: 201-210.
- Kao C.Y. (1989) Electrophysiological properties of uterine smooth muscle. In *Biology of the Uterus 2nd edition* (ed. Wynn R.M. & Jollie W.P.), pp.403. Plenum Press, New York.
- Karr S.R. & Foster J.A. Primary structure of the signal peptide of tropoelastin b. *Journal of Biological Chemistry.* 1981; **265**: 5946-5949.
- Kohnen G. *et al.* Endothelin receptor expression in human deciduas. *Molecular Human Reproduction.* 1998; **4(2)**: 185-193.
- Kohnen G. *et al.* Spatially regulated differentiation of endometrial vascular smooth muscle cells. *Human Reproduction.* 2000; **15(2)**: 284-292.
- Kramer R.H., et al. Laminin-binding integrin $\alpha 7\beta 1$: functional characterization and expression in normal and malignant melanocytes. *Cell Regulation.* 1991; **2**: 805-817.
- Kreidberg J.A., et al. $\alpha 3\beta 1$ integrin has a crucial role in kidney and lung organogenesis. *Development.* 1996; **122**: 3537-3547.
- Kühn K. Basement Membrane (Type IV) collagen. *Matrix Biology.* 1994; **14**: 439-445.
- Kunz G., et al. The dynamics of rapid sperm transport through the female genital tract: evidence from vaginal sonography of uterine peristalsis and hysterosalpingoscintigraphy. *Human Reproduction.* 1996; **11(3)**: 627-632.
- Kuster J.E., et al. IAP insertion in the murine LamB3 gene results in junctional epidermolysis bullosa. *Mammalian Genome.* 1997; **8**: 673-681.
- Laurie G.W. et al. Fine structure of the glomerular basement membrane and immunolocalization of five basement membrane components to the lamina densa (basal lamina) and its extensions in both glomeruli and tubules of the rat kidney. *American Journal of Anatomy.* 1984; **169**: 463-481.

- Lee J.K.T., et al. The uterus: in vitro MR-anatomic correlation of normal and abnormal specimens. *Radiology.* 1985; **157**: 175-179.
- Leivo I. & Engvall E. Merosin, a protein specific for basement membrane of Schwann cells, striated muscle and trophobalsts, is expressed late in nerve and muscle development. *Proceedings of the National Academy of Science of USA.* 1988; **85**: 1544-1548.
- Leppert P.C. & Shiu Yeh Yu. Three-dimensional structures of uterine elastic fibers: Scanning electron microscopic studies. *Connective Tissue.* 1991; **27**: 15-31.
- Lodge S. & Sproat J.E. Resting membrane potentials of pacemaker and nonpacemaker areas in rat uterus. *Life Science.* 1981; **28**: 2251.
- Loke Y.W. & King A. (1996) In: *Humam Implantation: Cellular Immunology.* (ed. Loke Y.W. & King A). Cambridge University Press.
- Ludwig et al. (1990). Endometrium: tissue remodeling and regeneration. In *Contraception and mechanisms of endometrial bleeding* (ed. D'Arcangues C.D., Fraser I.S., Newton J.R. and Odlind V.), pp.441-446. Cambridge University Press.
- Luukkainen T., et al. Levonorgestrel-releasing intrauterine device. *Annals in Medicine* 1990; **22**: 85-90.
- Lyons A.E., et al. Characterization of subendometrial myometrial contractions throughout the menstrual cycle in normal fertile women. *Fertility and Sterility.* 1991; **55(4)**: 771-774.
- MacKenzie L.W. & Garfield R.E. Hormonal control of gap junctions in the myometrium. *American Journal of Physiology.* 1985; **248**: C296-308.
- Malak M.T. & Stephen C.B. Distribution of fibrillin-containing microfibrils and elastin in human fetal membranes: A novel molecular basis for membrane elasticity. *American Journal of Obstetrics and Gynaecology.* 1994; **171(1)**: 195-205.
- Marinkovich M.P., et al. The dermal-epidermal junction of human skin contains a novel laminin variant. *The Journal of Cell Biology.* 1992; **119(3)**: 695-703.
- Mariyama M., et al. Colocalization of the genes for the α3(IV) and α4(IV) chains of type IV collagen to chromosome 2 bands q35-q37. *Genomics.* 1992; **13**: 809-812.
- Mark A.S. *et al.* Adenomyosis and leiomyoma: differential diagnosis by means of magnetic resonance imaging. *Radiology.* 1987; **163**: 527-529.
- Marshall J.M. Regulation of activity in uterine smooth muscle. *Physiology Reviews.* 1962; **42**: 213.

- Mayer U., et al. A single EGF-like motif of laminin is responsible for high affinity nidogen binding. *FENS Letters.* 1993; **12**: 1879-1885.
- Mayer U., et al. Low nidogen affinity of laminin-5 can be attributed to two serine residues in EGF-like motif γ2III4. *FEBS.* 1995; **365**: 129-132.
- McCarthy S. et al. Female pelvic anatomy: MR assessment of variations during the menstrual cycle with use of oral contraceptive. *Radiology.* 1986; **160**: 119-123.
- McCarthy S., et al. Uterine junctional zone: MR study of water content and relaxation properties. *Radiology.* 1989; **171**: 241-243.
- Mecham R.P. et al. Ligand affinity of 67kD elastin/laminin binding protein is modulated by the protein's lectin domain: visulaisation if elastin/laminin-receptor complexes with gold-tagged ligands. *Journal of Cell Biology.* 1991; **113**: 187-194.
- Mecham R.P. & Davis E.C. Elastic fiber structure and assembly. In *Extracellular matrix assembly and structure* (ed.Yurchenko P.D., Birk D.E. and Mecham R.P.), pp.281-310. Academic Press.
- Menkes J.H et al. A sex linked recessive disorder with retardation of growth, peculiar hair and focal cerebral and cerebellar degeneration. *Pediatrics.* 1962; **29**: 764.
- Minner J.H., et al. The laminin α chains: expression, developmental transitions and chromosomal locations of α1-5, identification of heterotrimeric laminins 8-11 and cloning of a novel α3 isoform. *Journal of Cell Biology.* 1997; **137**: 685-701.
- Mosler K., editor (1968). The dynamic of uterine muscle. Basel-New York: S. Karger-Verlag.
- Murakumo M. et al. Three-dimensional arrangement of collagen and elastin fibers in the human urinary bladder: a scanning electron microscopic study. *Journal of Urology.* 1995; **154(1)**: 251-6.
- Nakamura H. Electron microscopic study of the prenatal development of the thoracic aorta in the rat. *American Journal of Anatomy.* 1988; **181**: 406-418.
- Niessen C.M., et al. Deficiency of the integrin β4 subunit in junctional epidermolysis bullosa with pyloric atresia: consequences for hemidesmosome formation and adhesion properties. *Journal of Cell Science.* 1996; **109**: 1695-1706.
- Nilsson CG., et al. Endometrial morphology of women using a d-norgestrel-releasing intrauterine device. *Fertility and Sterility.* 1978; **21**: 155-164.
- Noes R.W. et al. Dating the endometrial biopsy. *Fertility & Sterility.* 1950; **1(1)**: 3-25.

- Nomizu M., et al. Identification of cell binding sequences in mouse laminin γ1 chain by systematic peptide screening. *Journal of Biological Chemistry.* 1997; **272**: 32198-322205.
- Nurcombe V., et al. The high affinity binding of laminin to cells. Assignation of a major cell-binding site to the long arm of laminin and a latent cell-binding site to its short arms. *European Journal of Biochemistry.* 1989; **180**: 9-14.
- Nurcombe V. Laminin in neural development. *Pharmaceutical Theories.* 1992; **56**: 247-264.
- Odlind V. Long-term experience of a levonorgestrel-releasing intrauterine system. *The European Journal of Contraception and Reproductive Health Care.* 1996; **1**: 319-323.
- Okkels H. & Engle E.T. Studies on the finer structure of the uterine blood vessels of the macacus monkey. *Acta Pathologica Microbiolical Scandinavia.* 1938; **15**: 150-168.
- Ortiz, Maria Elena; Croxatto, Horacio B.; Bardin, C. Wayne. Mechanisms of action of intrauterine devices. *Obstetrical & Gynecological Survey.* 1996; **51(12)Supplement**: 42S-51S.
- Osa T. & Katase T. Physiological comparison of the longitudinal and circular muscles of the pregnant rat uterus. *Japan Journal of Physiology.* 1975; **25**: 153-164.
- Ott U., et al. Protease resistance and conformation of laminin. *European Journal of Biochemistry.* 1982; **123**: 63-72.
- Paulsson M., et al. Structure of the low density heparan sulfate proteoglycan isolated from a mouse tumour basement membrane. *Journal of Molecular Biology.* 1987; **197**: 297-313.
- Paulsson M., et al. Structure of laminin variants. The 300-kDa chains of murine and bovine heart laminin are related to the human placenta merosin heavy chain and replace the α chain in some laminin fragments. *Journal of Biological Chemistry.* 1991; **266**: 17545-17551.
- Piez K.A. (1984) Molecular and aggregate structures of the collagens. In *Extracellular Matrix Biochemistry* (ed. Piez K.A. and Reddi A.H.), pp.1-39.
- Pijenborg R., et al. The pattern of interstitial trophoblastic invasion of the myometrium in early human pregnancy. *Placenta.* 1981; **2**: 303-316.
- Pijenborg R. Trophoblast invasion and placentation in the human: morphological aspects. *Trophoblast Research.* 1990; **4**: 33-47.
- Ramsey M.E. (1967). Vascular anatomy of the uterus. In *Cellular biology of the uterus* (ed.Wynn R.M.), pp.33-39. North Holland, Amsterdam.
- Ramsey M.E. (1994). Anatomy of the human uteus. In *The uterus* (ed. Chard T. & Crudzinskas G.), pp.18-29. Cambridge University Press.

- Raudaskoski T., et al. Transdermal oestrogen with a levonorgestrel-releasing intrauterine device for climacteric complains: Clinical and endometrial responses. *American Journal of Obstetrics & Gynecology.* 1994; **179**: 114-119.
- Reale E. & Luciano L. The laminae rarae of the glomerular basement membrane. Their manifestation depends on the histochemical and histological techniques. In *Hereditary Nephritis* (ed. Sessa A., Meroni M. and Battini G), pp.32-40. Contridutions in Nephrology, vol.80. Karger, Basel.
- Richards P.A. & Tiltman A.J. Anatomical variation of the oestrogen-receptor in normal myometrium. *Virchows Arch., Abt. A. Pathol. Anat.* 1995; **427**: 303-307.
- Rogers P. (1998). The endometrial vascular bed. In *Clinical disorders of the endometrium and menstrual cycle* (ed. Cameron I.T., Fraser I.S and Smith S.K.), pp.31-37. Oxford University Press.
- Rosenbloom J. Elastin: Relation of protein and gene structure to disease. *Laboratory Investigation.* 1984; **51(6)**: 605-623.
- Ross R. & Klebanoff S.J. Fine structural changes in uterine smooth muscle and fibroblasts in response to oestrogen. *Journal of Cell Biology.* 1967; **32**: 155-167.
- Russell P. & Fraser S. (1998). The practical assessment of endometrial morphology and function. In *Clinical disorders of the endometrium and menstrual cycle* (ed. Cameron I.T., Fraser I.S and Smith S.K.), pp.53-59. Oxford University Press.
- Ryan M.C., et al. Cloning of the LamA3 gene encoding the α3 chain of the adhesive ligand epiligrin. Expression in wound repair. *Journal of Biological Chemistry.* 1994; **269**: 22779-22787.
- Saez J.C., et al. Gap junctions: multiplicity of controls in differentiated and undifferentiated cells and possible functional implications. *Advances in second messenger and phosphoprotein research.* 1993; **27**: 163-198.
- Sanes J.R., *et al.* Reinnervation of muscle fibre basal laminin after removal of myofibres. Differentiation of regenerating axons at original synaptic clefts. *Journal of Cell Biology.* 1978; **102**: 420-431.
- Sanes J.R. Extracellular matrix molecules that influence neural development. *Annual Reviews of Neuroscience.* 1989; **12**: 491-497.

- Sanes J.R., et al. Molecular heterogeneity of basal laminae: Isoforms of laminin and collagen IV at the neuromuscular junction and elsewhere. *The Journal of Cell Biology.* 1990; **111**: 1685-1699.
- Sasaki T., et al. Binding of mouse and human fibulin-2 to extracellular matrix ligands. *Journal of Molecular Biology.* 1995; **254**: 892-899.
- Saunders N.A. & Grant M.E. The secretion of tropoelastin by chick embryo artery cells. *Biochemistry Journal.* 1985; **230**: 217-225.
- Scarcelli G., et al. Levonorgestrel-Nova-T and precancerous lesions of the endometrium. *European Journal of Gynaecological Oncology.* 1987; **9**: 284-286.
- Schofield R. The relationship between the spleen-colony forming cell and the haematopoietic stem cell. *Blood Cells.* 1978; **4**: 7-25.
- Schuler F. & Sorokin L.M. Expression of laminin isoforms in mouse myogenic cells in vitro and in vivo. *Journal of Cell Science.* 1995; **108**: 3795-3805.
- Scoutt L.M., et al. Junctional zone of the uterus: Correlation of MR Imaging and histologic examination of hysterectomy specimens. *Radiology.* 1991; **179**: 403-407.
- Seif M.W. et al. A novel approach for monitoring the endometrial cycle and detecting ovulation. *American Journal of Obstetrics & Gynecology.* 1989; **160(2)**: 357-362.
- Seif M.W. et al. Luteal phase defect: the possibility of an immunohistochemical diagnosis. *Fertility & Sterility.* 1989; **51(2)**: 273-279.
- Shearman R.P (1985). Endocrine response in the female genital tract. In: *Clinical Reproductive Endocrinology.* (ed. Shearman R.P.), pp.109-163. Churchill Livingstone, Edinburgh.
- Siebold B., et al. Construction of a model for the aggregation and cross-linking region (7S domain) of type IV collagen based upon an evaluation of the primary structure of the α1 and α2 chains in this region. *European Journal of Biochemistry.* 1987; **168**: 569-575.
- Siebold B., et al. The arrangement of intra- and intermolecular disulfide bonds in the carboxy-terminal, non-collagenous aggregation and cross-linking domain of basement-membrane type IV collagen. *European Journal of Biochemistry.* 1988; **176**: 617-624.
- Silverberg S.G., *et al.* Endometrial morphology during long-term use of levonorgestrel-releasing devices. *International Journal of Gynaecological Pathology.*1986; **5**: 234-241.

- Snijder M.P.M.L., et al. Use of immunocytochemistry of oestrogen receptors and progesterone receptors in the human uterus throughout the menstrual cycle and after the menopause. *Journal of Reproduction and Fertility.* 1992; **94**: 363-371.
- Somlyo A.V. (1980). Ultrastructure of vascular smooth muscle. In *Handbook of Physiology. The Cardiovascular System Vol.2* (ed. Bohr D.F., Somlyo A.P. and Sparks H.V.), pp. 33-71. American Physiology Society, Bethesda, MD.
- Sonnenberg A., et al. Integrin recognition of different cell-binding fragments of laminin (P1, E3, E8) and evidence that α6β1 but not α6β4 functions as a major receptor for fragment E8. *Journal of Cell Biology.* 1990; **110**: 2145-2155.
- Sorokin L., et al. Recognition of the laminin E8 cell-binding site by an integrin possessing the α6 subunit is essential for epithelial polarization in developing kidney tubules. *Journal of Cell Biology.* 1990; **111**: 1265-1273.
- Sorokin L., et al. Monoclonal antibodies against laminin A chain fragment E3 and their effects on binding to cells and proteoglycan and on kidney development. *Experimental Cell Research.* 1992; **201**: 137-144.
- Sorokin L., et al. Expression of the novel 400-kDa laminin chain by mouse and bovine endothelial cells. *European Journal of Biochemistry.* 1994; **223**: 603-610.
- Sorokin L.M., et al. Developmental regulation of the laminin α5 chain suggests a role in epithelial and endothelia cell maturation. *Developmental Biology.* 1997a; **189**: 285-300.
- Starcher BC. Lung elastin and matrix. *Chest.* 2000; **117(5)(Supplement 1)**: 229-34.
- Stephens L.E. et al. Deletion of β1 integrins in mice results in inner cell mass failure and peri-implantation lethality. *Genes & Development.* 1995; **9**: 1883-1895.
- Stjernquist M. & Sjöberg N.O. Neurotrasmitters in the myometrium. In *The uterus* (ed. Chard T. & Grudzinskas C.), pp.193-229. Cambridge University Press.
- Sturridge F. & Guillebaud J. Gynaecological aspects of the levonorgestrel-releasing intrauterine system. *British Journal of Obstetrics & Gynaecology.* 1997; **104(3)**: 285-289.
- Sung U. et al. Cell and heparin binding in the distal long arm of the laminin: identification of active and cryptic sites with recombinant and hybrid glycoprotein. *Journal of Cell Biology.* 1993; **123**: 1255-1268.

- Takada Y., et al. Molecular cloning and expression of the cDNA for α3 subunit of human α3β1 (VLA-3) an integrin receptor for fibronectin, laminin, and collagen. *Journal of Cell Biology.* 1991; **115**: 257-266.
- Terranova D., et al. Role of laminin in attachment of PAM212 (epithelial) cells to basement membrane collagen. *Cell.* 1980; **22**: 719-726.
- Thorbert G. Regional changes in structure and function of adrenergic nerves in guinea pig uterus during pregnancy. *Acta Obstetrica Gynecologica Scandinavica.* 1978; **305(Supplement)**: 1-32.
- Thyberg J., *et al.* Regulation of differentiated properties and proliferation of arterial smooth muscle cells. *Arteriosclerosis.* 1990; **10(6)**: 966-989.
- Timpl R., et al. Laminin-a glycoprotein from basement membranes. *Journal of Biological Chemistry.* 1979; **254**: 9933-9937.
- Timpl R., et al. A network model for the organization of type IV collagen molecules in basement membranes. *European Journal of Biochemistry.* 1981; **120**: 203-211.
- Timpl R., et al. Characterization of protease-resistant fragments of laminin mediating attachment and spreading of rat hepatocytes. *Journal of Biological Chemistry.* 1983; **258**: 8922-8927.
- Timpl R. Structure and biological activity of basement membrane proteins. *European Journal of Biochemistry.* 1989; **180**: 487-502.
- Timpl R. & Brown C. Judith. Supramolecular assembly of basement membranes. *BioEssays.* 1995; **18(2)**: 123-132.
- Turnbull L.W., et al. Magnetic resonance imaging changes in uterine zonal anatomy during a conception cycle. *British Journal of Obstetrics and Gynaecology.* 1995; **102**: 330-331.
- Vanderberg P., et al. Characterization of a type IV collagen major cell binding site with affinity to the α1β1 and the α2β1 integrins. *Journal of Cell Biology.* 1991; **113**: 1475-1483.
- Utani A., et al. Fibulin–2 binds to the short arms of laminin-5 and laminin-1 via conserved amino acid sequences. *Journal of Biological Chemistry.* 1997; **272**: 2814-2820.
- Watt F.M. The extracellular matrix and cell shape. *TIBS.* 1986; **5**: 287-294.
- Wewer U.M., et al. Immunochemical and ultrastructural assessment of the nature of the pericellular basement membrane of human decidual cells. *Laboratory Investigation.* 1985; **53(6)**: 624-632.
- Wiczyk H.P., et al. Comparison of MRI and US in evaluating follicular and endometrial development throughout the normal cycle. *Fertility and Sterility.* 1988; **49**: 969-972.

- Willms A.B., et al. Anatomic changes in the pelvis after uncomplicated vaginal delivery: evaluation with serial MR imaging. *Radiology.* 1995; **195**: 91-94.
- Woessner J.F. Jr. & Brewer T.H. Formation and breakdown of collagen and elastin in the humna uterus during pregnancy and post-partum involution. *Biochemistry Journal.* 1963; **89**: 75.
- Worthington B.S. et al. The low-intensity band on spin-echo images of the uterus: an anatomic and clinicopathologic study. *Radiology.* 1985; **157(P)**: 310.
- Xiao B.L., et al. Pharmacokinetic and pharmacodynamic studies of levonorgestrel-releasing intrauterine device. *Contraception.* 1990; **41**: 353-362.
- Yamamoto Kiyotaka, et al. Role of elastin in the differentiated properties of vascular smooth muscle cells in culture. *Connective Tissue.* 1994; **26**: 245-254.
- Yamamoto M., et al. Increase in elastin gene expression and protein synthesis in arterial smooth muscle cells derived from patients with Moyamoya disease. *Stroke.* 1997; **28(9)**: 1733-1738.
- Yaoita H., et al. Localization of the collagenous component in skin basement membrane. *Journal of Investigation in Dermatology.* 1978; **70**: 191-193.
- Yurchenko P.D. & Schittny J.C. Molecular architecture of basement membranes. *FASEB Journal.* 1990; **4**: 1577-1590.
- Yurchenko P.D. & Cheng Yi-Shan. Self-assembly and calcium-binding sites in laminin. *The Journal of Biological Chemistry.* 1993; **268(23)**: 17286-17299.
- Yurchenko P.D. (1994) Assembly of laminin and type IV collagen into basement membrane networks. In *Extracellular matrix assembly and structure* (ed.Yurchenko P.D., Birk D.E. and Mecham R.P.), pp351-380.
- Zhang Shu-Xin (1999). Circulatory System. In *An Atlas of Histology.* (ed Zhang Shu-Xin), pp.118-127. Springer-Verlag New York, Inc.
- Zhao Gu., et al. A morphometric study on the endometrial activity of women before and after one year with LNG-IUD in situ. *Contraception.* 1995; **52**: 51-56.
- Zhou J., et al. Deletion of the paired α5(IV) and α6(IV) collagen genes in inherited smooth muscle tumours. *Science.* 1993; **261**: 1167-1169.

Appendix.1

ENDOMETRIAL BREAKTHROUGH BLEEDING

Uterine Sampling Protocol

If the pathologist feels the uterus is grossly normal, and that it does not need to be sampled otherwise, please trim the specimen as illustrated below:

- Please cut the uterus transversely and provide the researcher with a slice that is 0.5 - 1 cm thick
- The researcher will divide the slice into pieces for wax embedding and cryo-sectioning
- The researcher will ensure that relevant clinical details are provided on the request form

Mid Corpus Slice

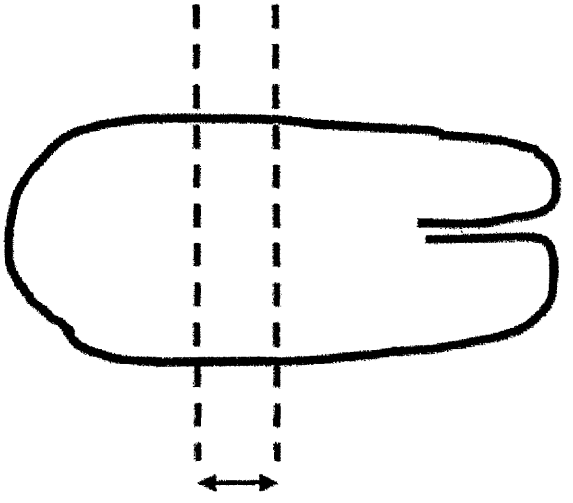

0.5-1 cm

Dr Colin Stewart
Consultant Pathologist
Royal Infirmary

Dr Ian Gibson
Consultant Pathologist
Victoria Infirmary

Dr Margaret Burgoyne
Consultant Pathologist
Southern General Hospital

Dr Rodney Burnett
Consultant Pathologist
Western Infirmary

Dr David Millen
Consultant Pathologist
Stobhill Hospital

Appendix.1 (continued)

Processing of Transverse Uterine Slice by Researchers

"Flattened Cavity"

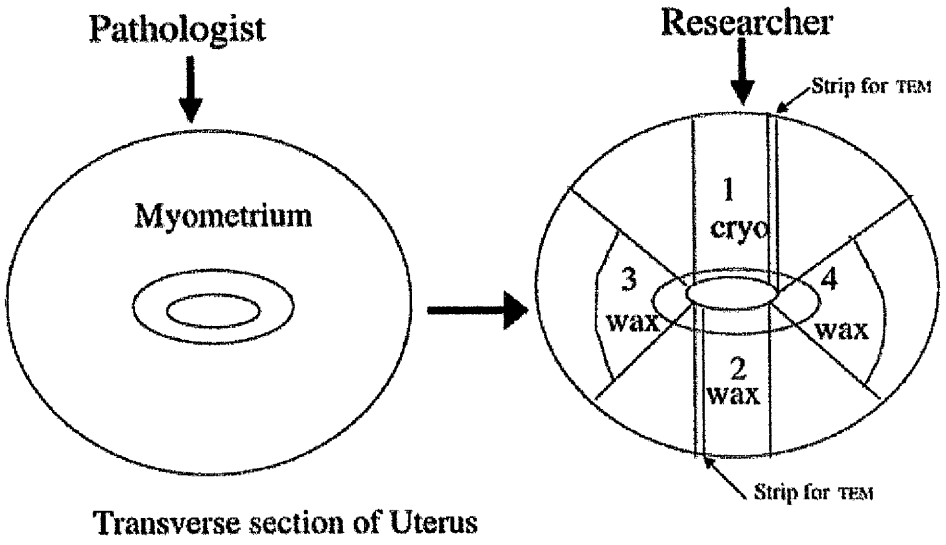

Transverse section of Uterus

"Round Cavity"

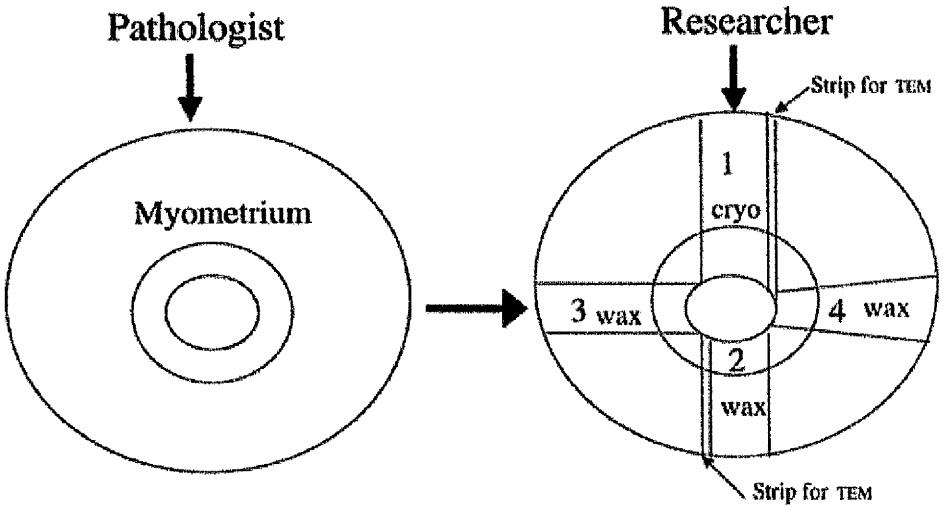

Transverse section of Uterus

Appendix.2

Collection of Human Endometrium for Research: Patient Information and Consent

The University Department of Obstetrics and Gynaecology at the Royal Infirmary has a specialist interest in the lining of the womb (endometrium). We are actively involved with research in this area in the hope of acquiring a better understanding of a variety of disorders related to the endometrium, including heavy periods (menorrhagia), painful periods (dysmenorrhoea), and early miscarriage.

Part of this research involves the study of tissue samples removed at the time of operation. At the time of your operation (hysterectomy) the tissue that is removed is sent to the Pathology Laboratory for analysis. Quite often not all the tissue is needed by the Pathologist and therefore some tissue left over and could be used for research. I would therefore like to ask your permission for us to keep a small piece of the tissue which is not required by the Pathologist so that we can use it for research purposes. The type of research to be carried out will usually involve examining the tissue under a microscope to detect the presence of molecules which may play a part in the control of the blood supply to the endometrium. In addition, some studies will involve culturing cells to observe the effects of hormones. Cells would normally be cultured for a few days but on occasion might be cultured for up to six weeks. The proposed research would not involve the long term culture or growth of living cells.

In making this request I would like to stress to you that the tissue that we would collect would be only that removed in the normal course of your operation and which was not subsequently needed by the Pathologist. Any tissue samples that we would store or use would be anonymous and would not be linked to your name in any way. I would also like to reassure you that there is no question of us removing any extra tissue above that which is necessary for your treatment.

If you are willing to participate in this study please sign the consent slip below. If you do so, your GP will be informed of this. Finally, I should point out that if you do not wish to allow some of your endometrium to be used for research you do not need to do so, and this decision will not affect your medical treatment in any way.

Professor I.A. Greer

I..... of.....

.....

have discussed this research project with .....
and have read and understood the above letter and hereby give my consent for the Department of Obstetrics and Gynaecology to obtain a small sample of tissue removed during the normal course of my operation for the purposes of research.

Signed..... Date.....

Witness ..... Date.....

Appendix.3

Tissue Collection Form

Rrecored No. .....

NAME .....

Collected by .....

Consultant .....

DOB .....

Parity .....

LMP .....

Cycle length .....

GRI or WIG

Reasons for surgery .....

Date of collection .....

Samples collected .....

Samples stored .....

Medication .....

PATHOLOGY

menstrual ( ) proliferative ( ) early secretory ( ) late secretory ( )

Other comments .....

Appendix.4

Qualitative analysis of the β2 laminin chain and collagen IV in 8 partial myometrial thickness cryosections

β2 laminin chain ***Collagen IV***

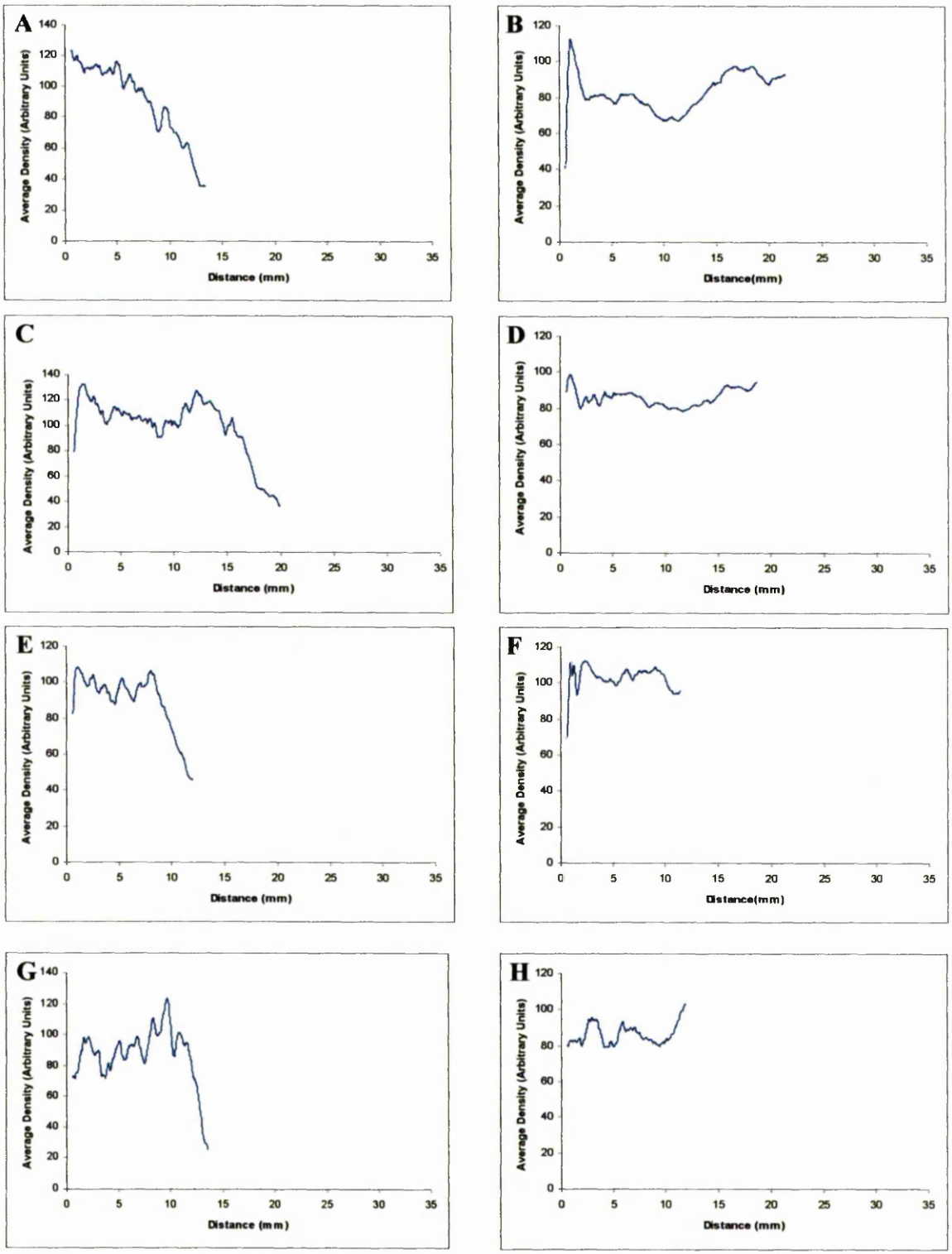

Appendix.4 (continued)

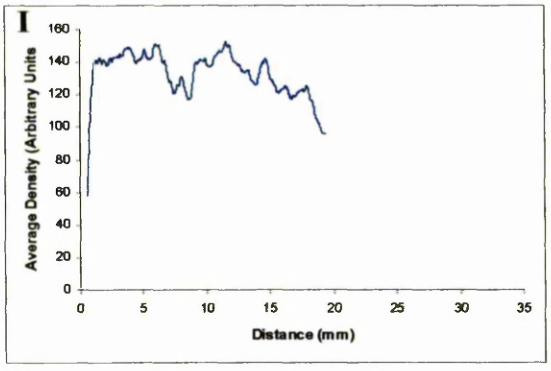

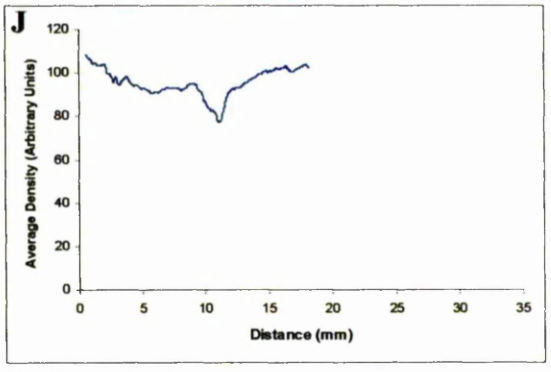

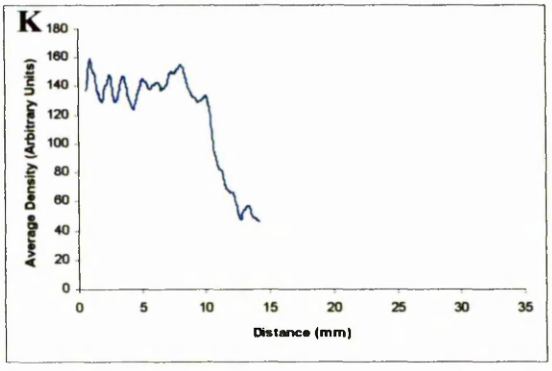

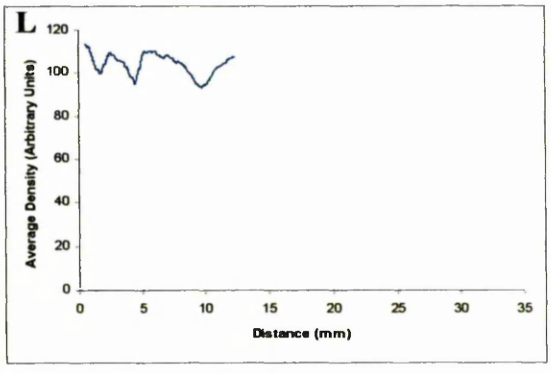

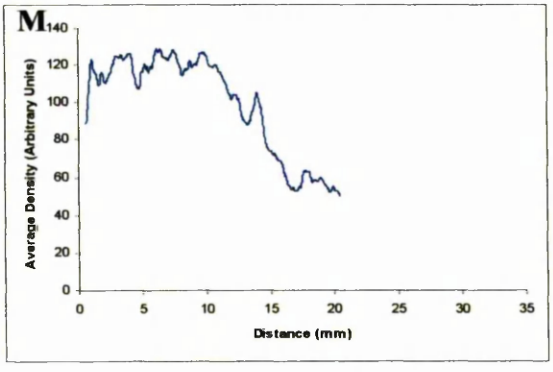

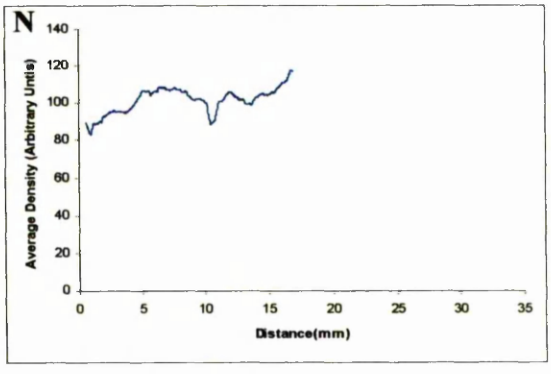

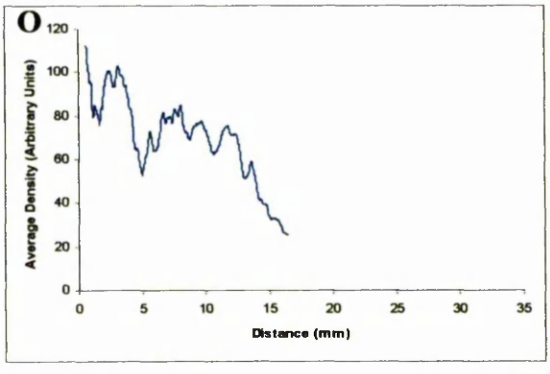

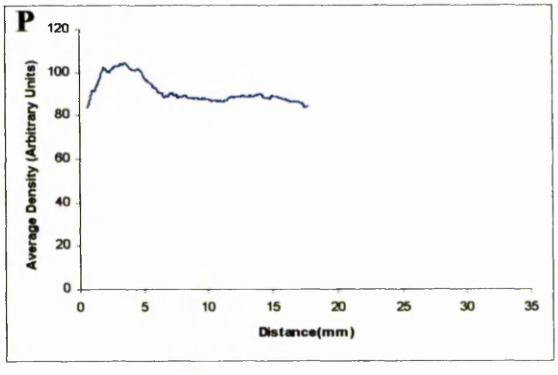

Appendix.1

ENDOMETRIAL BREAKTHROUGH BLEEDING

Uterine Sampling Protocol

If the pathologist feels the uterus is grossly normal, and that it does not need to be sampled otherwise, please trim the specimen as illustrated below:

- Please cut the uterus transversely and provide the researcher with a slice that is 0.5 - 1 cm thick
- The researcher will divide the slice into pieces for wax embedding and cryo-sectioning
- The researcher will ensure that relevant clinical details are provided on the request form

Mid Corpus Slice

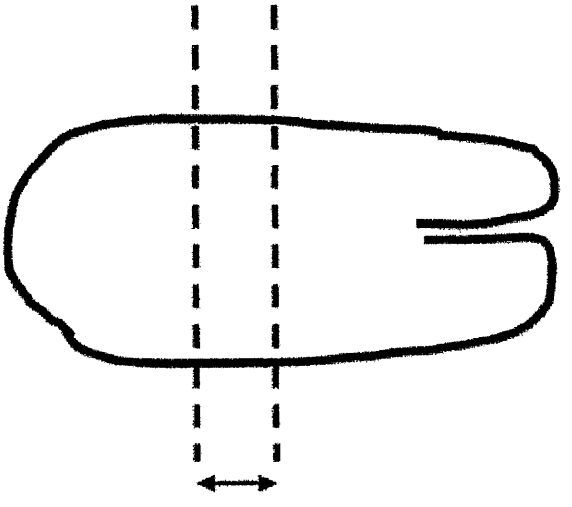

0.5-1 cm

Dr Colin Stewart
Consultant Pathologist
Royal Infirmary

Dr Ian Gibson
Consultant Pathologist
Victoria Infirmary

Dr Margaret Burgoyne
Consultant Pathologist
Southern General Hospital

Dr Rodney Burnett
Consultant Pathologist
Western Infirmary

Dr David Millen
Consultant Pathologist
Stobhill Hospital

Appendix.1 (continued)

Processing of Transverse Uterine Slice by Researchers

"Flattened Cavity"

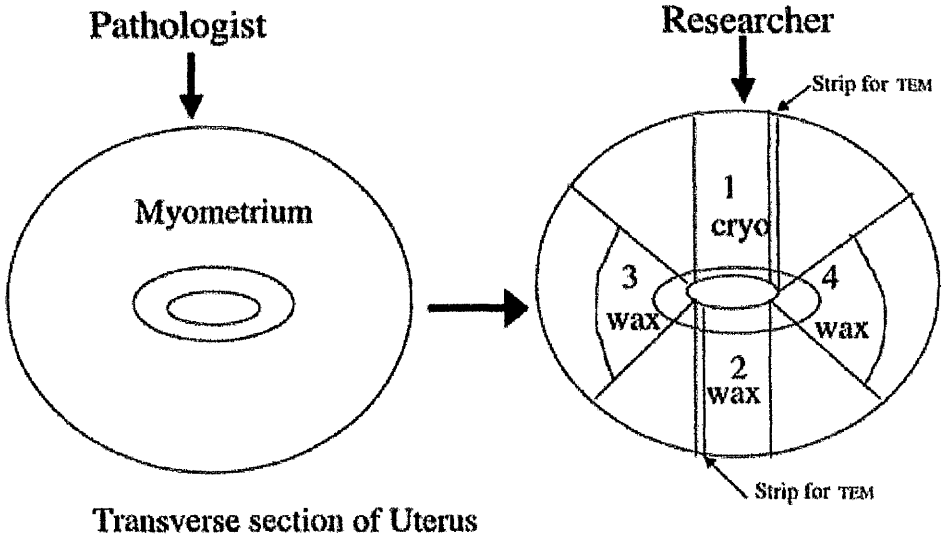

"Round Cavity"

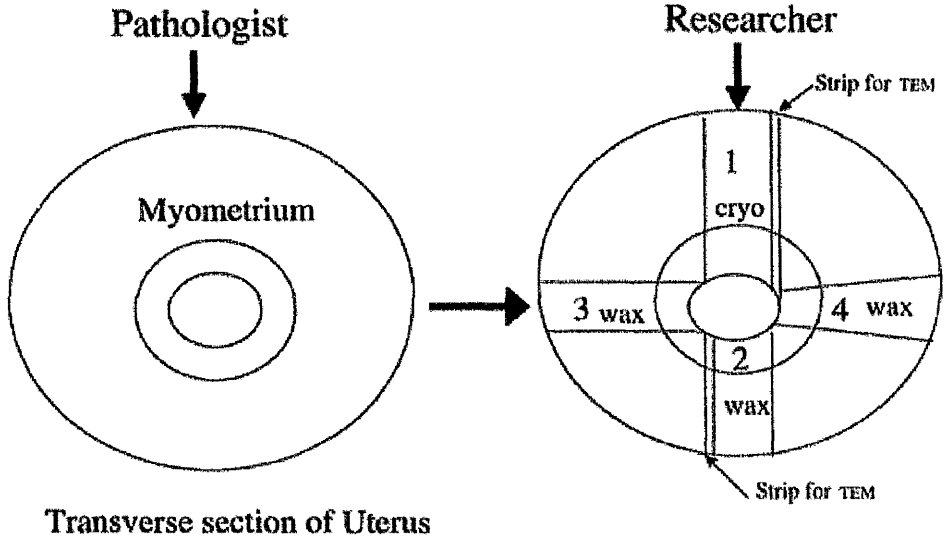

Appendix.2

Collection of Human Endometrium for Research: Patient Information and Consent

The University Department of Obstetrics and Gynaecology at the Royal Infirmary has a specialist interest in the lining of the womb (endometrium). We are actively involved with research in this area in the hope of acquiring a better understanding of a variety of disorders related to the endometrium, including heavy periods (menorrhagia), painful periods (dysmenorrhoea), and early miscarriage.

Part of this research involves the study of tissue samples removed at the time of operation. At the time of your operation (hysterectomy) the tissue that is removed is sent to the Pathology Laboratory for analysis. Quite often not all the tissue is needed by the Pathologist and therefore some tissue left over and could be used for research. I would therefore like to ask your permission for us to keep a small piece of the tissue which is not required by the Pathologist so that we can use it for research purposes. The type of research to be carried out will usually involve examining the tissue under a microscope to detect the presence of molecules which may play a part in the control of the blood supply to the endometrium. In addition, some studies will involve culturing cells to observe the effects of hormones. Cells would normally be cultured for a few days but on occasion might be cultured for up to six weeks. The proposed research would not involve the long term culture or growth of living cells.

In making this request I would like to stress to you that the tissue that we would collect would be only that removed in the normal course of your operation and which was not subsequently needed by the Pathologist. Any tissue samples that we would store or use would be anonymous and would not be linked to your name in any way. I would also like to reassure you that there is no question of us removing any extra tissue above that which is necessary for your treatment.

If you are willing to participate in this study please sign the consent slip below. If you do so, your GP will be informed of this. Finally, I should point out that if you do not wish to allow some of your endometrium to be used for research you do not need to do so, and this decision will not affect your medical treatment in any way.

Professor I.A. Greer

I..... of.....

.....

have discussed this research project with .....
and have read and understood the above letter and hereby give my consent for the Department of Obstetrics and Gynaecology to obtain a small sample of tissue removed during the normal course of my operation for the purposes of research.

Signed..... Date.....

Witness ..... Date.....

Appendix.3

Tissue Collection Form

Rrecored No. .....

NAME .....

Collected by .....

Consultant .....

DOB .....

Parity .....

LMP .....

Cycle length .....

GRI or WIG

Reasons for surgery .....

Date of collection .....

Samples collected .....

Samples stored .....

Medication .....

PATHOLOGY

menstrual ( ) proliferative ( ) early secretory ( ) late secretory ( )

Other comments .....

Appendix.4

Qualitative analysis of the β2 laminin chain and collagen IV in 8 partial myometrial thickness cryosections

β2 laminin chain ***Collagen IV***

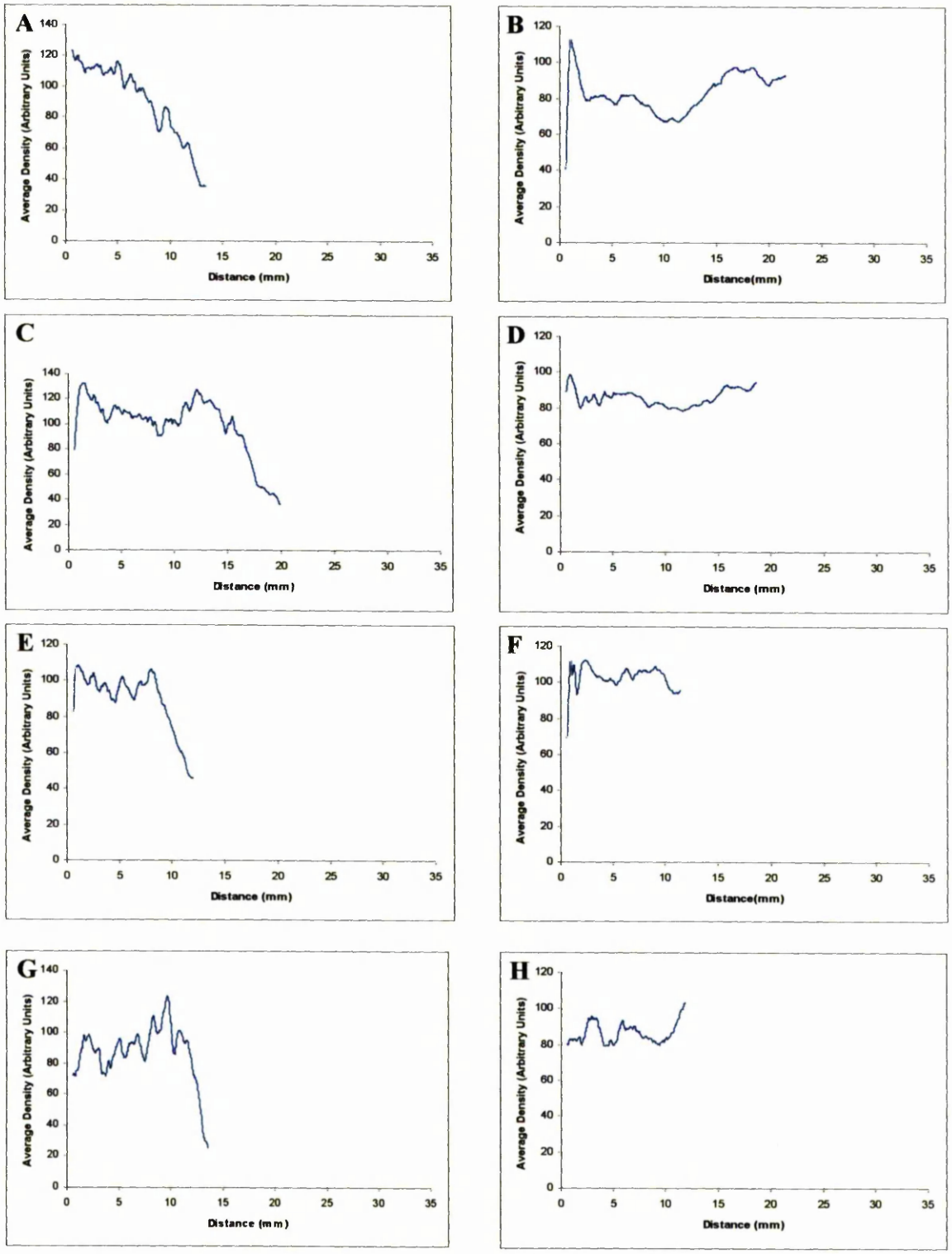

Appendix.4 (continued)

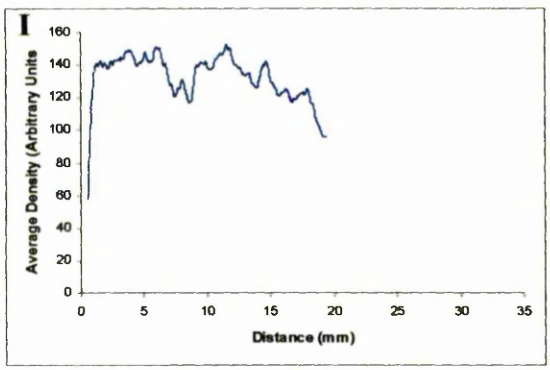

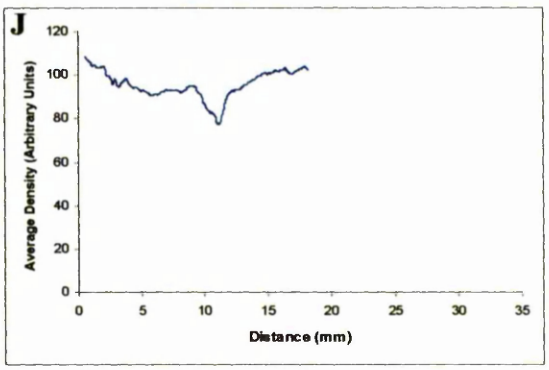

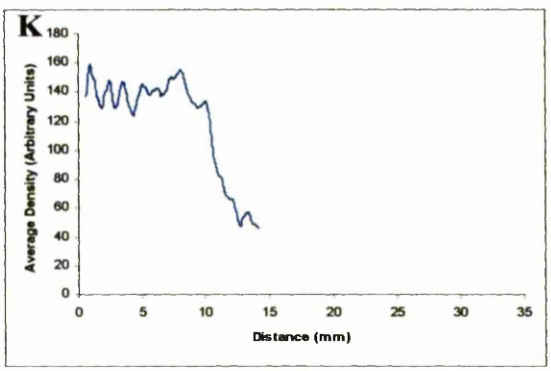

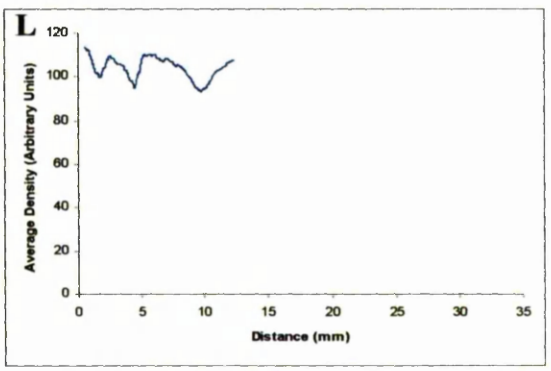

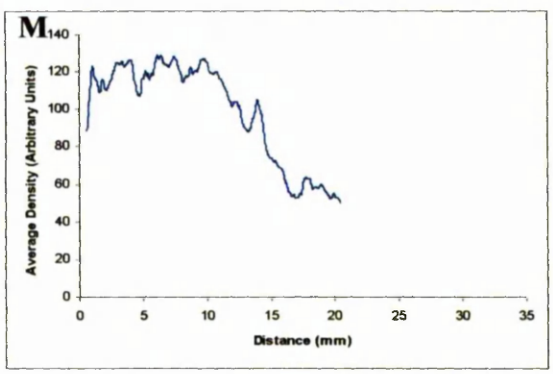

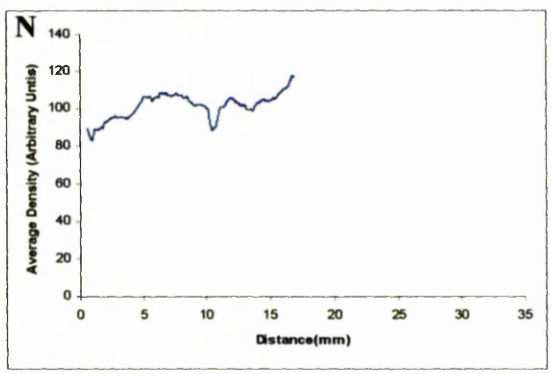

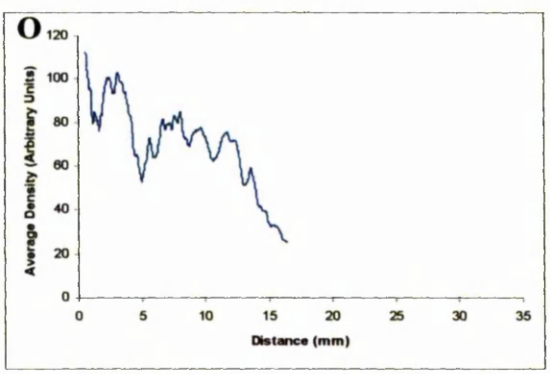

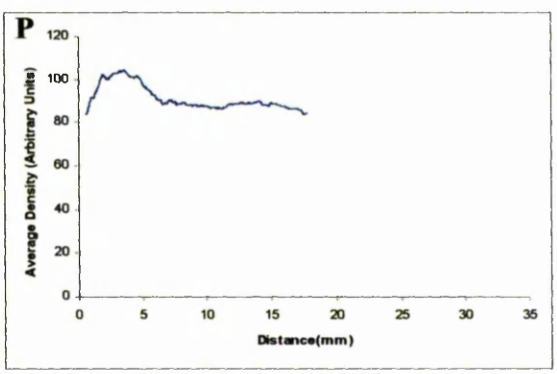

Appendix.4 Line profiles for the intensity of the β2 laminin chain and collagen IV from low magnification scans of partial myometrial thickness. A gradient is observed in the myometrial distribution of the β2 laminin chain in contrast to the more uniform distribution of collagen IV. No endometrial data are shown. (**A**) β2 laminin chain distribution in a menstrual phase section of 13mm length. (**B**) collagen IV distribution in a consecutive sections of 22 mm length. (**C**) β2 laminin chain distribution in a proliferative phase sections of 20 mm length. (**D**) collagen IV distribution in a consecutive section of 19 mm length. (**E**) β2 laminin chain distribution in a proliferative phase section of 12mm length. (**F**) collagen IV distribution in a consecutive section of 12 mm length. (**G**) β2 laminin chain distribution in a proliferative phase section of 14mm length. (**H**) collagen IV distribution in a consecutive section of 12mm length. (**I**) β2 laminin chain distribution in a secretory phase section of 19mm length. (**J**) collagen IV distribution in a consecutive section of 18mm length. (**K**) β2 laminin chain distribution after exposure to exogenous levonorgestrel for 10 months in a sections of 14mm length. (**L**) collagen IV distribution in a consecutive section of 12mm length. (**M**) β2 laminin chain distribution after exposure to exogenous levonorgestrel for 9 months in a section of 20mm length. (**N**) collagen IV distribution in a consecutive section of 17mm length. (**O**) β2 laminin chain distribution after exposure to exogenous levonorgestrel for 8 weeks in a section of 16mm length. (**P**) collagen IV distribution in a consecutive section of 18mm length.